UNIVERSITÀ
DEGLI STUDI
DI PADOVA

Sede amministrativa: Università degli Studi di Padova

Dipartimento di Principi e Impianti di Ingegneria Chimica “I. Sorgato”

SCUOLA DI DOTTORATO DI RICERCA IN INGEGNERIA INDUSTRIALE
INDIRIZZO INGEGNERIA CHIMICA
CICLO XXIV

LOW SHEAR WET AGGLOMERATION OF MINERAL AND METALLIC POWDERS

Direttore della Scuola: Ch.mo Prof. Paolo Bariani
Coordinatore dell’Indirizzo: Ch.mo Prof. Alberto Bertucco
Supervisore: Ch.mo Prof. Andrea Santomaso

Dottoranda: Laura Susana

Alla mia famiglia

Acknowledgements

While working on my PhD project I have benefit from the support and help of many people, few of them I would like to thank here.

First and foremost I would like to express my great thank to my project supervisor Prof. Andrea Santomaso whose insights, enthusiasm and constant support were essential to my success.
Thank you also to my colleagues and friends Dr.ssa Erica Franceschinis, Dr. Mauro Cavinato and Dr. Riccardo Artoni, I really enjoyed the time spent with you in many congresses.

I would like to thank Trafilerie di Cittadella - Fileur® for providing a financial support for all this PhD project. Thank you especially to Dr. Davide Rocco, Dr. Filippo Campaci, Ing. Andrea Ribaudo and Ing. Matteo Mason.

From the time I spent at the University of Leeds, I would like to express my gratitude to Prof. Mojtaba Ghadiri and Dr. Ali Hassanpour for giving me the opportunity to join their research group. I also would like to thank all my Leeds colleagues Afsheen, Colin, Graham, Massih and Umair for being so helpful.
Thanks also to my friends Ale, Teo, Maurizio, Arianna and Sanj for making my period abroad a great and fulfilling experience.

A particular thanks goes to my friend Monia for sharing with me this PhD experience, for her constant support and encouragement.

Last but by no means least my dearest thanks goes to my parents, Aldo and Maria and my sister Gabriella for their never-ending love and support.

My special thanks goes to Mattia for his unconditional love and support through the numerous ups and downs of my life.

Contents

Summary

Since the beginning of the 1960s, agglomeration process has been a commonly used and important unit-operation to convert fine powders to granular materials with controlled physical properties in many industrial sectors, from the pharmaceutical industry to fertilizer, food or detergents production and to the mineral processing industries (Iveson *et al*., 2001). Agglomeration and related process cover a wide range of application which handle particulate feeds, intermediates or products. This in itself is testimony to the value of this operation. However, in spite of its widespread use, economic importance and almost 50 years of research, agglomeration has in practice remained more of an art than a science.

Wet granulation process is a subset of size enlargement methods, which involves any process whereby small particles are formed into structural, larger and physically strong aggregates (granules) in which the original particles can still be identified. This is performed by adding a liquid binder onto the powder mass and by the agitation imposed through an impeller turning at moderate to high speed in a tumbling drum, fluidized bed, low and high shear mixer or similar device. A chopper, with the function as a breakage device is often situated inside the vessel. The liquids binds the single primary particles together by a combination of capillary and viscous forces until more permanent bonds are formed by subsequent drying.

Wet granulation process have been traditionally been considered an empirical art, with great problems in predicting and understanding observed behaviour. Industries dealt with a range of problems caused by improper granulation such as segregation, caking and poor product performances.

In the last decades, there have been significant advancements in understanding of the mechanisms of size enlargement. Quantitative prediction of granules attributes is difficult but we have a qualitative understanding of the effects of different variables on granulation behaviour.

However in the literature most reports on granulation process have focused on the agglomeration of pharmaceutical ingredients (microcrystalline cellulose powder, lactose, mannitol, calcium carbonate powder) with common polymeric binders for instance hydroxypropyl-cellulose (HPC), polyvinylpyrrolidone (PVP) and polyethylene glycol (PEG) in high - shear mixer.

No published work has been found in the literature on how the wet granulation is sensitive to changes in product properties (binder viscosity, powder wettability) and process variables (impeller rotational speed, mixing time) in the case of mineral and

metallic powders. Moreover there is a limited data available on wet granulation in low shear mixer.
The need of additional research is obvious and this forms the motivation of the main part of this work.
Since agglomeration process is often required to prevent segregation of critical components in a powder mixture, the present work deals also with this problem which is of particular interest to those industries where homogeneity is a critical requirement. In particular in the pharmaceutical industry demixing during handling and processing of such granules might give problems in meeting the demands on the content uniformity of the final dosage form. However not only the drug substance is susceptible to demixing. but also pharmaceutical filler materials tend to segregate. A good granulation process can therefore create designed structure agglomerates having similar size and composition, thus reducing segregation of materials.
The present research mainly focuses on the low shear wet agglomeration of mineral and metallic powders. Particularly, this experimental study is a practical framework of binder granulation which takes place in the process of manufacturing of welding rods.
The aim of this work is to better understand the effect of starting materials properties (e.g. formulation composition, primary particle size distribution) and operating parameters (e.g. mixing speed, agglomeration time) on the final granules attributes. The effect of binder properties such as viscosity, surface tension on the final granule characteristics were investigated as well.
Particular attention has also paid to the effect of particle size on the internal structure of granules and to investigate this effect the process of seeded granulation is simulated by the Discrete Element Method (DEM). Finally a new sampling device for assessing the composition of granulated powder mass and for finding evidence of segregation during agglomeration process is developed and characterized.

The research activities were mainly carried out in:

- Dipartimento di Principi e Impianti Ingegneria Chimica “I. Sorgato”, Università degli Studi di Padova, Padova (Italy);
- Trafilerie di Cittadella, Fileur®, R&D, Cittadella (Italy);
- Institute of Particle Science and Engineering, University of Leeds, Leeds (UK).

Results of research activities are here summarized in five chapters:

- Chapter 1 gives a brief overview on the main powder agglomeration process and on the techniques for measurement of contact angles on powder surface. A brief description of segregation mechanisms which can occur during agglomeration is also provided;

- in Chapter 2 wettability of mineral and metallic solids is characterized, particularly applicability and limitations of sessile drop method and Washburn technique on metallic surface are discussed;
- the experimental study of agglomeration of mineral and metallic powders in a low shear pilot plant is described by Chapter 3. The effects of physical properties of starting feed and the operative variables on the granule characteristics are analyzed as well in this chapter;
- Chapter 4 is about the application of Discrete Element Method (DEM) for simulation of seeded granulation;
- in Chapter 5 a new sampling device for evaluating the composition of bulk solids is presented;
- conclusions and proposals for future work can be found in Chapter 6.

Sommario

Sin dall'inizio degli anni '60, il processo di accrescimento delle dimensioni delle particelle attraverso l'agglomerazione ad umido è stato considerato una delle tecniche maggiormente impiegate per trasformare le polveri fini in granuli strutturati di determinate proprietà chimico-fisiche. L'agglomerazione è un processo comune in vari settori industriali come ad esempio in quello farmaceutico (propedeutico alla realizzazione di varie forme farmaceutiche), nel settore agricolo (fertilizzanti e diserbanti), in quello alimentare e nell'industria dei detergenti (Iveson *et al*., 2001).
L'importanza di tale processo è testimoniato dal largo impiego in diversi settori industriali e dalla presenza di materiali granulari sia nelle materie prime che nei prodotti intermedi e finiti. Tuttavia, nonostante l'uso diffuso, l'importanza dal punto di vista economico e i risultati di quasi cinquant'anni di ricerche, il processo di agglomerazione è rimasto nella pratica più un'arte che una scienza.

Il processo di agglomerazione ad umido permette di trasformare una miscela di polveri fini in un agglomerato strutturato avente dimensioni maggiori rispetto alle particelle di partenza (formulazione), migliori proprietà di scorrevolezza e potenzialmente meno soggetto al fenomeno della segregazione dei diversi costituenti. Tale operazione richiede l'aggiunta di un legante liquido e l'imposizione di un energico mescolamento attraverso l'impiego di un agitatore primario (*impeller*) e di un agitatore secondario (*chopper*). Il liquido bagnante consente di creare dei ponti di liquido tra le particelle primarie attraverso l'instaurarsi di forze viscose e capillari.
Nonostante l'importanza e l'utilizzo diffuso di questa tecnica in molteplici settori industriali non è ancora possibile correlare univocamente il processo di granulazione (con le sue variabili operative e formulative) alla struttura dei granuli finali. La granulazione umida ad alto shear non sempre garantisce le proprietà fisiche dei granuli desiderate e questo può costituire una limitazione importante in settori come quello farmaceutico, dove il controllo di qualità è un fattore di primaria importanza. Negli ultimi decenni tuttavia ci sono stati importanti progressi nella comprensione dei meccanismi di agglomerazione. Non è ancora possibile predire quantitativamente le caratteristiche finali del granulo, ma gli effetti qualitativi di numerosi parametri di processo sono noti.
La maggior parte della letteratura è incentrata sull'agglomerazione di polveri farmaceutiche (cellulosa microcristallina, lattosio, carbonato di calcio) con leganti polimerici, quali ad esempio l'idrossipropilcellulosa (HPC), il polivinilpirolidone (PVP) ed il polietilenglicole (PEG) in miscelatori ad alto *shear*.

Per quanto riguarda le polveri minerali e metalliche, allo stato attuale non ci sono studi che riescano a correlare relative le proprietà formulative (viscosità del legante, bagnabilità della polvere) e le variabili di processo (intensità dell'agitazione, tempo di granulazione) alle caratteristiche finali dell'agglomerato. Inoltre vi sono informazioni limitate sulla granulazione ad umido a basso *shear*.
In questo campo è quindi evidente la necessità di ulteriori ricerche e ciò rappresenta la motivazione per la parte principale del presente lavoro.
Un ulteriore tematica che viene affrontata in questo progetto di ricerca è la segregazione delle miscele multicomponente, essendo l'agglomerazione una tecnica in grado di ridurre e contrastare questo fenomeno. In particolare nell'industria farmaceutica la possibilità di impedire la segregazione dei diversi costituenti consente di ottenere un elevato grado di omogeneità spaziale del principio attivo incapsulato nella forma farmaceutica. Inoltre, non solo il principio attivo è potenzialmente soggetto al fenomeno della segregazione, ma anche i diversi eccipienti sono sensibili a tale fenomeno. Attraverso un processo di granulazione è possibile ottenere dei granuli che, presentando dimensioni e composizione chimica simili, sono meno soggetti alla segregazione.

La presente ricerca riguarda principalmente l'agglomerazione ad umido a basso *shear* di polveri metalliche a minerali. In particolare è presentato il processo di agglomerazione adottato nel processo industriale di produzione di fili animati per la saldatura ad arco.
Lo scopo principale è approfondire la conoscenza sul ruolo delle proprietà formulative (composizione della formulazione, distribuzione granulometrica, viscosità e tensione superficiale del legante) e dei parametri di processo (velocità di miscelazione, tempo di agglomerazione) nel determinare le caratteristiche del prodotto finale.
Con l'obiettivo di approfondire la struttura interna dei granuli, è' stato inoltre studiato un particolare tipo di granulazione detto *seeded granulation* attraverso un software dedicato alla simulazione di sistemi particellari e basato sul metodo agli elementi discreti (*Discrete Element Modelling*, DEM).
Infine, è stata sviluppata e caratterizzata una sonda in grado di campionare materiali granulari coesivi superando i limiti dei dispositivi attualmente impiegati. Attraverso questa sonda è stato possibile inoltre valutare la composizione dei granuli formati nel processo di agglomerazione delle polveri minerali e metalliche ed evidenziare la presenza di segregazione.

Le attività di ricerca si sono svolte principalmente presso:

- Dipartimento di Principi e Impianti Ingegneria Chimica "I. Sorgato", Università degli Studi di Padova, Padova (Italia);
- Trafilerie di Cittadella, Fileur®, R&D, Cittadella (Italia);

- Institute of Particle Science and Engineering, University of Leeds, Leeds (UK).

I risultati di tale ricerca sono riassunti nei seguenti quattro capitoli:

- nel Capitolo 1 si descrivono brevemente sia i meccanismi e le fasi di un processo di agglomerazione che le tecniche per valutare la bagnabilità delle polveri. Si introducono inoltre i diversi meccanismi di segregazione che caratterizzano i materiali granulari.
- Nel Capitolo 2 è proposto lo studio della bagnabilità delle polveri minerali e metalliche, ed in particolare vengono discussi l'applicabilità e i limiti del metodo della goccia sessile e della tecnica di Washburn.
- Lo studio sperimentale dell'agglomerazione di polveri minerali e metalliche in un impianto pilota a basso *shear* viene descritto nel Capitolo 3.
- Il Capitolo 4 riporta i risultati della simulazione della *seeded granulation* attraverso la tecnica agli elementi discreti (DEM).
- Nel Capitolo 5 viene caratterizzata infine una nuova sonda per la valutazione dell'uniformità di composizione in una miscela di polveri.
- Le conclusioni e le prospettive future sono esposte nel Capitolo 6.

Chapter 1

Introduction

Many raw materials, intermediates and final products are present in a wide range of industries as granular materials such as pharmaceuticals, food, detergents, agrochemicals, mineral and metallic powders. In the chemical industry alone it has been estimated that 60% of products are manufactured as particulates and a further 20% use powders as ingredients. The annual value of these products is estimated at US$1 trillion in the US alone (Bridgwater, 1995).

The reasons for this widespread use are various: powders are often easy to handle and process, they can be dissolved in liquids, compressed to form tablets or capsules and swallowed in order to transfer nourishment or medicines in the human body.

Granulation also known as agglomeration, pelletization or balling is one of the most important operations involving granular materials. This process converts fine powders to granular materials with controlled physical properties (Litster and Ennis, 2004). The primary powder particles are forced to adhere and form granules (or agglomerates) using a liquid binder.

Granulation is an example of particle design. The desired attributes of the product granules are controlled by a combination of formulation properties such as feed powder and liquid properties and process parameters like the type of granulator and operating parameters (Iveson *et al.*, 2001).

Recent research in wet granulation aims to quantify these effects in order to make granulation process a quantitative engineering than an empirical art (Hapgood *et al*., 2002). There are many reasons for granulating fine powders. Some of the desired attributes of final granules include for example the reduction of dustiness in order to minimize losses, inhalation and explosion risks. It is often required to prevent the segregation of critical components in a powder mixture by reducing the difference in size and density between different powders. A good granulation process can therefore improve flow ability and powder handling (Litster and Ennis, 1997; Ennis, 2005).

1.1 Granulation mechanisms

Wet granulation is complex: many phenomena occur simultaneously in the granulator which influence the granule attributes. According to the theory developed by Ennis and

Litster (1997), granulation can be considered as the combination of only three sets of rate processes (see Figure 1.1):

1. wetting and nucleation, where the liquid binder is distributed onto the powder mass giving a distribution of nuclei granules;
2. consolidation and growth, where collisions between granules and as well granules and initial powder particles lead to the granule compaction and growth;
3. attrition and breakage, where granules deform or break under the action of shearing and impact forces.

The first stage of granulation is the binder addition in order to form nuclei granules. The liquid binder is usually sprayed onto the powder mass. Litster and Ennis (2004) consider two different extremes in the wet granulation process: (i) if the liquid drop size is large compared to the primary particle size, nucleation occurs by immersion mechanism; and (ii) if the particle size is larger than the binder droplet, distribution mechanism occurs. In the former case, the binder droplet spread across the bed surface and nuclei formation depends on the dynamic of partially wet mass. In the latter case, the liquid coats the particles and nuclei are formed by coalescence of the wetted primary particles. Both the rate and extent of wetting are important for understanding nucleation and binder distribution (Iveson *et al*., 2001). If wetting and nucleation are effectively controlled, nuclei granules will increase in size (granule growth) and in density (granule consolidation).

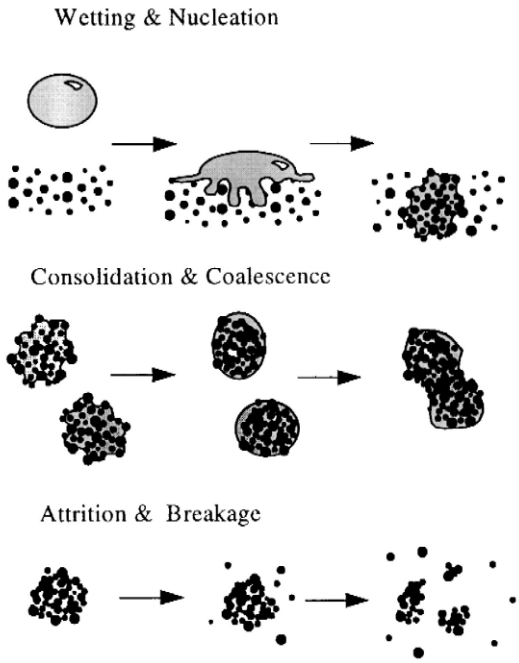

Figure 1.1 *Schematic of granulation processes (Iveson et al., 2001)*

Finale granule properties are affected by granule mechanics (Rumpf, 1962) and macroscopic properties that characterize the behaviour of a granule on the collisions with other particles and granulator.
The extent of consolidation depends on agitation intensity and the granule strength to deformation. Granules consolidation controls the finale porosity as well.
In the third class of granulation process that control the final properties of granules two different phenomena can occur: (1) the breakage of wet granules in the granulator and (2) the attrition of dried granules in subsequent handling. In the first case the finale granule size is determined by the extent of the wet agglomerates breakage. In the latter case, the fracture of dried granules leads to the generation of dusty fines and this a situation to be avoided.
Understanding, control and optimization of rate processes involved in granulation processes are therefore of strategic importance, but at the same time very challenging. It is very important to know which rate processes is dominant in any particular application in order to define the controlling formulation properties and process parameters for each rate process.

1.2 Granulation equipment

The variety of size enlargement equipment available in the market is enormous. The better approach to choice an equipment takes into account the finale desired granules properties (e.g. granules size, porosity, density) and some possible constraints such as the form of starting materials, handling aspects and economical reasons.
The most common granulation technologies are the mixer granulators as they find wide application for pharmaceuticals, minerals, ceramics, detergents and chemical products. Mixers can be divided into two classes according the agitation intensity of the impeller: low shear mixer (< 60 rpm) and high shear mixer (60 ÷ 800 rpm, up to 3500 rpm in terms of chopper speed) (Knight *et al*., 2001). There are a huge range of geometries and designs covering batch and continuous configurations.
The mixer bowl is usually fixed while powder motion is induced using a rotating impeller and/or chopper. Liquid binder can be poured or sprayed onto the moving powder mass. These mixers range in scale from 10 litres to 1200 litres and typical batch times are of the order of 5 minutes.

1.3 Introduction to mineral and metallic wet agglomeration

This PhD project deals with a particular industrial application where granulation is used to produce useful structural forms and co-mixing of particles which would otherwise segregate during handling and processing.

In the manufacturing of tubular welding wires a closed steel tube is filled with suitable blends of powders. The low shear wet granulation process includes the following steps:

1. according to specific end user requirements, a proper composition of mineral and metallic powder mixture is loaded into the mixer bowl;
2. mixing of dry powder mixtures at low impeller speed for a few minutes;
3. addition of aqueous solutions of potassium or sodium silicates (binder liquids) while the impeller is running;
4. wet agglomeration while both the impeller and chopper are running;
5. discharge of granules from the mixer and drying in a fluid dryer and oven;
6. sieving of dry agglomerates.

Liquid binder is poured onto the powder mass, therefore nucleation will occur by immersion of the smaller particles into the larger drop. This will produce nuclei with saturated pores.

Agglomeration process is carried out in a low shear Siome® mixer whose design is unique: both the impeller blades and chopper rotate on eccentrically mounted vertical shafts. In addition, the bowl rotates in the opposite direction. The whole process of manufacturing of welding wires is simplified in Figure 1.2.

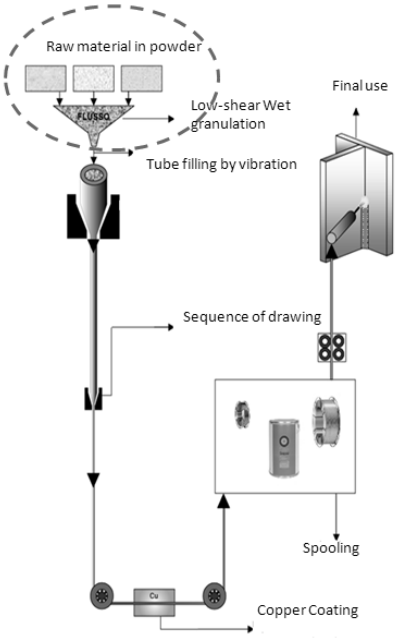

Figure 1.2 *Schematic of manufacturing of welding rods process*

The tube is thus filled through a sequence of wire drawing operations until the required size is achieved. It is then copper coated by the copper coating baths. Coating makes the welding wires high resistance to the surface oxidation. Moreover it allows reducing hydrogen contents and additionally improving current flow.

1.4 Methods of wettability measurements for mineral surfaces

The first stage in any wet granulation process is the distribution of the liquid binder through the feed powder. As the wetting process proceeds, the fluid penetrate into the pores of the powder surface, forms a nucleus and migrates outwards as the nucleus consolidates and grows. Both the wetting kinetics and thermodynamics define the nuclei size distributions. Poor wetting results in drop coalescence, and in fewer, larger nuclei with ungranulated powder, leading to broad nuclei distribution. Therefore knowledge of the wetting characteristics of powder surface is paramount in enhancing the understanding and optimization of agglomeration process.
The contact angle value is a useful indicator in providing data on the wettability characteristics of the solid surfaces (de Gennes, 1985).
Over the years, many different techniques have been developed for the measurements of contact angles. For mineral and metallic powders only a few of them can provide with meaningful and realistic contact angle values. Because of surface roughness and chemical heterogeneity, the contact angle may change from one point to another along the contact line. Generally the existing methods can be divided into two categories: direct methods and indirect ones (Lazghab *et al*., 2005; T.T. Chau *et al*., 2009). In Chapter 2 the sessile drop method (direct method) and Washburn's technique (indirect method) are compared and discussed.

1.4.1 Direct methods

All these method are based on the microscopic visualization of the solid/liquid interface. The apparent contact angle can be determined using a goniometer or image analysis. Two microscopic methods are reported in the literature, which are the sessile drop method and the captive-bubble method. In the sessile drop technique, a liquid droplet of controlled volume is placed on the powder substrate and contact angle can be measured by viewing the drop profile. The captive-bubble method is a variant of the profile method: a bubble is attached to the bottom side of the surface immersed in the test liquid. The advantages using these techniques are that only small quantities of liquid and powder are required However it is quite difficult to get reproducible results because of surface heterogeneity which may cause variation of contact angle along the three-phase line contact. If high

accuracy is not required these methods are considered the most convenient techniques for wettability measurements (T.T. Chau *et al*., 2009).

1.4.2 Indirect methods

Among the indirect methods the Washburn's technique is the best know method based on capillary rise wetting. The powder compact is placed into a tube whose bottom is permeable. The filled tube is suspended from an electronic balance just above the test liquid. The rate of liquid penetration thought the powder can be used to calculate the contact angle from the Washburn model (for more details see Chapter 2).
Lago and Araujo (2001) developed an alternative method to the conventional capillary rise test based on the equilibrium capillary height. In this method, the capillary suction is equal to the height of the penetrated liquid according to (1.1):

$$h_e = \frac{\gamma_{LV} \cos \vartheta_e}{c'} \rho g. \tag{1.1}$$

This approach is required with non Newtonian liquids which do not fulfill the Washburn's assumptions.
There are also methods based on immersional wetting such as the microcalorimetric method which studies the wettability from an energetically point of view. Because of the temperature dependence of contact angle wettability is related to the heat absorbed or released when the powder is immerse in the test liquid. It was demonstrated that the heat of immersion, ΔH_{im}, is correlated to the wettability by (1.2):

$$\Delta H_{im} = \frac{\gamma_{LV}}{\gamma_{LV} - T \dfrac{\partial \cos \vartheta}{\partial T}} \cdot T \cdot \frac{\partial \cos \vartheta}{\partial T} - \cos \vartheta. \tag{1.2}$$

Concerning the adsorptive techniques, the inverse gas chromatography (iGC) is the best method to characterize powder wettability. Calculation of the solid surface energy requires the measurement of the dynamic adsorption characteristics of known gases called probe gases. This technique is identical to conventional gas chromatography except that the analysis subject is the solid phase and rather that the gas one.

1.5 Agglomeration process to prevent particle segregation

Segregation of multi-component mixtures is a common problem, which is of particular interest to those industries where homogeneity is a critical requirement (Iveson *et al*., 2001). For example in pharmaceutical industry, when a mixture of drug and one or more

excipients is granulated, large differences in drug content of different granule size fraction can occur. This implies a lack of uniformity on terms of drug content of the final solid dosage form (tablet, capsule). Also in the mineral and metallic agglomeration, demixing during handling and processing of granules might give serious problems in meeting the demands on the content uniformity of the final formulation.

It should be noted that each industry or application has its own acceptable limit for the degree of segregation, i.e. the level of homogeneity in a pharmaceutical product does not necessary meet the demands of the content uniformity in the food industry.

However authorities tend to demand that intermediate products also meet the content uniformity specifications, forcing industries to pay more attention to the manufacturing process. The current code of federal regulations specified by the FDA (*Food Drug Administration*) contains the following guideline (CFR-21 Section 211.110): "To assure batch uniformity and integrity of drug products, written procedures shall be established and followed that describe the in-process controls and tests, or examinations to be conducted on appropriate samples of in-process materials of each batch. Such control procedures shall be established to monitor the output and to validate the performance of those manufacturing process that may be responsible for causing variability in the characteristics of in-process material and drug product."

This results in an increasing interest for these industries in the understanding of the segregation tendencies of particulate mixtures. In spite of a considerable amount of research done on the segregation of mixtures there is still no universally accepted method for quantifying segregation. Extensive work has been done on describing causes and mechanisms of segregation. Nonetheless the mechanisms of segregation are not fully understood. Many causes have been suggested including composition and particle size differences, binder fluid migration and particle solubility.

In Chapter 5 a new sampling thief probe for collecting granular material is described and characterized in terms of drag and sampling efficiency. A method based on image analysis to quantify segregation is proposed as well. In this experimental work sampling by thieves is used as a tool to assess the bulk solid composition during the granulation process in order to find evidence of segregation and investigate binder spreading homogeneity and nucleation/growth mechanisms.

1.5.1 Segregation mechanisms

The processes of segregation are complex and difficult to predict quantitatively. Segregation is caused by any physical differences between constituents in a mixture including: (i) size distribution, especially the presence of cohesive fines which are poorly flowing due to the strong influence of adhesive forces (Rosato *et al*., 1991), (ii) density

ratio (Ellenberg *et al*., 2006), cohesion intensity (Yang, 2006), particle shape (Johanson *et al*., 2005) and external factors such as vibrations (Williams and Richardson, 1981).
Several interdependent segregation mechanisms are described in the literature (Shulze, 2007). A brief description of the main segregation mechanisms are reported here:

- sifting effect is a mechanism whereby on any inclined surface of a particle bed larger particles predominantly roll down to the base of the surface, while small particles smaller particles have a higher probability to be caught by a sufficiently large cavity on the powder bed;
- percolation of fines is the process by which small particles migrate preferentially by filling voids which become available because of particles rearrangement when particle bed is deformed;
- trajectory segregation is a mechanism whereby particles become airborne: fine particles are more affected by air resistance than coarser particles and, therefore, fines do not travel as far as coarser particles;
- free surface segregation refers to the segregation that occurs upon pouring granular materials into a heap.

1.6 References

Bridgwater, J., 1995. Particle Technology, Chemical Engineering Science 50, pp. 4081-4089.

Chau, T.T., 2009. A review of techniques for measurement of contact angle and their applicability on mineral surface. Mineral Engineering 22, pp. 213-219.

de Gennes, P.G., 1985. Wetting: static and dynamics. Review of Modern Physics 57, pp. 827-863.

Ellenberg, J., Vandu, C.O, Krishna, R., 2006. Vibration-Induced Granular segregation in multi-component in a pseudo-2D column, Powder Technology 165, pp. 168-173.

Ennis, B.J., Litster, J.D.,1997. Particles size enlargement, in: R. Perry, D. Green (Eds.), Perry's Chemical Engineers Handbook, 7th edn., McGraw-Hill, New York.

Ennis, B.J., 2005. Solids-solids processing, in: R. Perry, D. Green (Eds.), Perry's Chemical Engineers Handbook, 8th edn., McGraw-Hill, New York.

Ennis, B.J., 2005. Theory of granulation: an engineering perspective, in: D.M. Parikh (Eds), Handbook of Pharmaceutical Granulation Technology, 2th edn, Taylor and Francis Group, New York.

Hapgood, K.P., Litster, J.D., Biggs, S.R., Howes, T., 2002. Drop Penetration into Porous Powder Beds. Journal of Colloid and Interface Science 253, pp. 353-366.

Iveson, S.M., Litster, J.D., Hapgood, K., Ennis, B.J., 2001. Nucleation, growth and breakage phenomena in agitated wet granulation processes: a review, Powder Technology 117, pp. 3-39.

Johansen, K., Eckert, C., Ghose, D., Djomlija, M., Hubert, M., 2005. quantitative measurement of particle segregation mechanisms, Powder Technology 159, pp. 1-12.

Kenningley, S.T., Knight, P.C., Marson, A.D., 1997. An investigation into the effects of binder viscosity on agglomeration behaviour, Powder Technology 91, pp. 95-103.

Knight, P.C, Seville, J.P.K., Wellm, A.B., Instone T., 2001. Prediction of impeller torque in high shear powder mixers, Chemical Engineering Science 56, pp. 4457-4471.

Lago, M., Araujo, M., 2001. Caplillary rise in porous media. Physica A: Statistical Mechanics in porous media 289, pp. 1-17.

Lazgab, M., Khashayar, S., Pezron, I., Guigon, P., Komunyer, L., 2005. Wettability assessment of finely divided solids. Powder Technology 157, pp. 79-91.

Litster, J.D., Ennis, B.J., 2004. The science and engineering of granulation process, Kluwer academic publishers, Dordrecht, The Netherlands.

Rosato, A.D, Lan, Y., Wang, D.T., 1991. Vibratory Particel Size Sorting in Multi-Component Systems, Powder Technology 66, pp. 149-160.

Rumpf, H., 1962. The strength of granules and agglomerates, in: Agglomeration, W.A. Knepper, ed. Interscience, New York, pp. 379-414.

Schulze, D., 2007. Powders and bulk solids, Springer.

Schaefer, T., Johnsen, D., Johansen, A., 2004. Effects of powder particle size heterogeneity during high shear granulation, European Journal of Pharmaceutical Sciences 21, pp. 525-531.

Williams, J.C., Richardson, R., 1981. The continuous mixing of segregating particles, Powder Technology 33, pp. 5-16.

Yang, S.C., 2006. Segregation of cohesive powders in a vibrated granular bed, Chemical Engineering, 61, pp. 6180-6188.

Chapter 2

Wettability of mineral and metallic powders

2.1 Summary

Characterization of powder wettability is a prerequisite to the understanding of many processes of industrial relevance such as agglomeration which spans from pharmaceutical and food applications to metallurgical ones. The choice of the wetting fluid is crucial: liquid must wet the powder in order for agglomeration to be successful. The solid-liquid contact angle of the system directly affects the characteristics of the granulated product. Different methods for wettability assessment of powders were reported in the literature, however the sessile drop method and capillary rise test remain among the most widely employed because they are easy to perform and inexpensive. Experimental literature data in this area were mostly limited to pharmaceutical solids (lactose, paracetamol powders) with water solutions of polymeric binders (HPMC, PVP, PEG). In this research work, the application and limitations of sessile drop method and capillary rise test on mineral and metallic surface were discussed. This work provides a collection of wettability measurements using several powders and binders which are involved in the manufacturing process of welding wires. Moreover a new reference liquid for the calibration of capillary rise method was proposed. Furthermore the theory of infiltration of liquid into porous media presented by Hilpert and Ben-David (2009) is applied for the all the powder tested.

2.2 Introduction

Agglomeration process converts fine powders to granular materials with controlled physical properties. Wet granulation of fine powders is carried out in many industries, from pharmaceutical and pharmaceutical and agrochemical industries to mineral and plastic ones, to improve physical and material properties of powders such as flowability, rate of dissolution and robustness to segregation (Pietsch, 1991; Litster and Ennis, 2004; Parick, 2005). Litster and his co-workers (2001) described granulation as a rate process where three types of simultaneous mechanisms occur: wetting and nucleation,

Submitted in:
Susana L., Campaci F., Santomaso A.C., Wettability of mineral and metallic powder: applicability and limitations of sessile drop method and Washburn's technique, Powder Technology.

consolidation and growth and breakage and attrition. These three mechanisms are affected by a combination of formulation parameters such as the physiochemical properties of powder and of liquid binder and process parameters like the type of granulator and its operating conditions. Knowledge of wetting and spreading of the liquid binder through the feed powder is a prerequisite for understanding and controlling the first stage in any wet granulation process since the binder is used to form liquid bridges between the solid particles. Experimental method for wettability assessment of powders have been recently reviewed (Lazghab *et al*., 2005; Chau, 2009). Wettability describes the ability of a surface to be wetted by the probing liquid and it can be characterized by different parameters. The wettability of solid surface is generally characterized in terms of the contact angle, θ, i.e. the angle comprised between the tangent to powder surface and the tangent to the liquid drop at the vapour-liquid-solid intersection (de Gennes, 1985). The contact angle is a useful and concise indicator of hydrophobic characteristics of solids. Wettability depends on several variable such as particle size, bulk density and porosity of the powder bed and the molecular interactions between the phases entering into contact (Hapgood and Khanmohammadi, 2009).

When a small drop of liquid is placed on solid substrate, it assumes a shape that minimizes the free energy of the system. Young's equation represents the equilibrium conditions between three interfacial tensions, the solid–vapour γ_{SV}, solid–liquid γ_{SL} and liquid–vapour γ_{LV}:

$$\gamma_{LV}\cos\vartheta = \gamma_{SV} - \gamma_{SL} \ . \tag{2.1}$$

Eq. (2.1) implies the existence of only one equilibrium contact angle and it is valid for ideal solid surface, which means a homogeneous and flat surface. The contact angle approach is conceptually easy to apply for a flat, smooth and chemically homogeneous surface. Unfortunately real surfaces detach from this assumption because of surface roughness and chemical heterogeneity. Furthermore wettability of finely divided solids depends on variables such as particle size and porosity of the powder bed beside the molecular interactions between the phases entering into contact (Hapgood and Khanmohammadi, 2009). Due to surface irregularities, molecular orientation and partial dissolution of the solid in the fluid, the contact angle may change along the contact line from one point to another. Three distinct contact angle can be assumed to exist: the intrinsic, the apparent and the actual one (Marmur, 1996). For an ideal surface the contact angle does not change along the contact line and it is called intrinsic contact angle (Figure 2.1a). The actual contact angle on a real surface is instead the angle between the tangent to the surface at a given point and the tangent to the liquid droplet in the same point (Figure 2.2b). Finally the apparent contact angle is measured between the tangent to the

liquid surface and the tangent to the powder surface if it is assumed to be ideal (Figure 2.2c). Moreover it has been known for a long time that a wide range of stable apparent angle can be measured on a real surface, this range is referred to as hysteresis (de Gennes, 1985). Figure 2.1 illustrates the three different definitions of the contact angles.

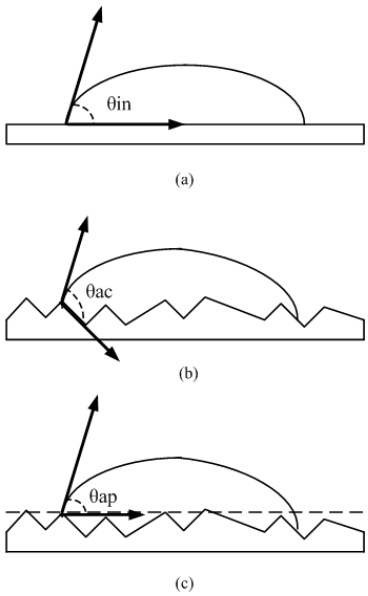

Figure 2.1 *Definition of the contact angles: (a) the intrinsic contact angle, (b) the actual contact angle and (c) the apparent contact angle*

In order to characterize the wetting behaviour of porous media such as powder systems, experimental methods require to form tablets or compacts by exerting a pressure before conducting contact angle measurements. In this case, imbibition of a single droplet into a porous media depends on powder bed porosity and the size and orientation of the pores. Kossen and Heertjes (1967) developed a method to relate the actual contact angle, θ, to the apparent contact angle, θ' and powder porosity, ε through (2.2):

$$(1-\varepsilon)\cos\vartheta = \cos\vartheta' - \varepsilon. \tag{2.2}$$

In general, methods for wettability assessment of finely divided solids can be divided into two categories: methods based on direct observation of the solid/liquid interface such as the sessile drop method (Heertjes and Kossen, 1967), the flotation technique (Fuerstenau *et al.*, 1991) and techniques based on wetting processes (adhesive, spreading, condensional and immersional wetting) such as the capillary rise test known also as Washburn test (Washburn, 1921), the equilibrium height method (Lago and Araujo, 2001) and inverse gas chromatography (Feeley *et al.*, 1998). The first category of method can be used if powder is homogeneous and for small particles (smaller than 500 μm) and they provide with the apparent contact angle measurement by the direct analysis of drop shape

(Lazghab *et al*., 2005). The other techniques are indirect measure of the apparent contact angle: for instance in Washburn method the contact angle between the liquid and the capillary surface is computed by measuring the liquid rising speed.

There are no models for the imbibition of drops into powders but a detailed theory for penetration of a single droplet into a porous surface was presented by Hilpert and Ben-David (2009). This approach applies the Washburn equation where flow is driven by the capillary pressure and resisted by viscous dissipation. The theory shows that infiltration of droplets into dry porous media involves three phases due to contact angle hysteresis: (1) an increasing drawing area (IDA) phase during which the interface between the droplet and the porous medium increases, (2) a constant drawing area (CDA) phase during which the contact line of the droplet remains pinned, and finally (3) a decreasing drawing area (DDA) phase. The theory is based on the following assumptions: (i) the droplet has the shape of a spherical cap, (ii) the porous medium consists of a bundle of vertical tubes of same size, and (iii) the pressure within the droplet is uniform.

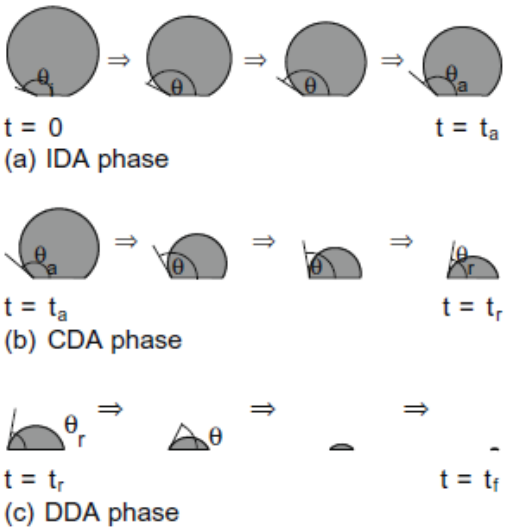

Figure 2.2 *Infiltration occurs in three phases: (a) during the IDA phase, the drawing radius increases while the contact angle of the droplet decreases until it assumes the advancing contact angle* θ_a. *(b) During the CDA phase,* θ *decreases from* θ_a *until it assumes the receding contact angle* θ_r *while drawing radius keeps constant. (c) During the DDA phase, the drawing radius decreases until the droplet is depleted*

It was found that infiltration always consists of a cascade process formed by the IDA, CDA, and DDA phases, where the overall process may begin or end in any of the three phases (see Figure 2.2). This theory also takes into account the contact angle hysteresis, which is defined as the difference between advancing, θ_a and receding θ_r contact angles.

Most of the reports in the literature have focused on wetting and agglomeration phenomena concerning pharmaceutical powders like lactose and salicylic acid powders with water and PVP and PEG solutions. (Krycer, 1983; Waldie, 1991, Shaafsma *et al*., 1998; Hapgood *et al*., 2002; Zhang, 2002). A few studies deal with the capillary rise experiments on silica flour, calcium carbonate and glass (Siebold *et al*., 1997; Labajos-Broncano *et al*., 1999; Siebold *et al*., 2000). Nonetheless, less attention has been paid so far to the wettability of mineral and metallic powders (Ivenson *et al*., 2000) even though they are involved in many important processes such as the manufacture of ceramics, welding wires, rods and electrodes and powder metallurgy.

The goal of our study was to examine use and limit of Washburn technique and of sessile drop method for mineral and metallic solids (mainly involved in the welding wire production) and in particular to find an appropriate reference liquid for Washburn method calibration.

Moreover we attempt to provide with an experimental verification of drop penetration theory proposed by Hilpert and Ben-David (2009).

2.3 Theory

In a typical Washburn test, a cylindrical tube with a permeable filter at the bottom is filled with the powder sample. The bottom of the tube is brought into contact with the wetting liquid so that the fluid can rise into the tube because of capillary forces and the liquid front rising in the vertical tube is observed.

An equation that describes the penetration of a liquid into a cylindrical capillary is the Hagen–Poiseuille's law:

$$v = \frac{dh}{dt} = \frac{{r_C}^2}{8\mu h}\Delta P, \tag{2.3}$$

where v is the liquid rising speed, h denotes the distance penetrated by the liquid, t is the time of infiltration, r_C is the radius of the capillary, η is viscosity of the probing liquid and ΔP is the pressure difference across the invading liquid meniscus.

The driving pressure is given by the sum of a capillary pressure described by Laplace equation and a hydrostatic pressure:

$$\Delta P = \frac{2\gamma_{LV}\cos\vartheta}{r_C} + \rho g h \tag{2.4}$$

g is the gravitational force, ρ is the liquid density and γ_{LV} is the liquid–air interfacial tension. If the liquid weight can be neglected, integration of (2.3) for the boundary condition $h = 0$ when $t = 0$ leads to the well-know Washburn's equation for one capillary:

$$\frac{h^2}{t} = \frac{r_C \gamma_{LV}\cos\vartheta}{2\eta}. \tag{2.5}$$

According to this model, a bed of powder can be modelled as an array of parallel capillaries with constant radius where penetration into the substrate is driven just by capillarity and the following conditions are applied: (i) steady–state laminar flow, (ii) no slip of the fluid along the porous wall, (iii) no externally applied pressure. Under these conditions and with a Newtonian fluid the Washburn's equation predicts that a plot of h^2 vs. t is a straight line.

Using the Kozeny approach the radius r_C is replaced by the equivalent or effective radius, r_{eff} which accounts for the non – ideality of the system, particularly the variation in bed porosity and tortuosity of a porous substrate.

The equivalent radius is defined as:

$$r_{eff} = 2R_h \tag{2.6}$$

where R_h is the hydraulic radius defined as the ratio between the cross section available for flow and the wetted perimeter. In terms of unit volume of powder bed the hydraulic radius can be expressed as:

$$R_h = \frac{\varepsilon}{a} = \frac{\varepsilon}{a_S(1-\varepsilon)} \tag{2.7}$$

where ε is the bed porosity, a is the ratio of the wetted surface and the bed volume and a_S is the particle specific surface area which for spherical particle is $6/d$.

In order to account for non-sphericity of the particles a shape factor φ (Wadell's sphericity) is introduced and (2.7) becomes:

$$R_h = \frac{\varphi d_V \varepsilon}{6(1-\varepsilon)} = \frac{d_{32}\varepsilon}{6(1-\varepsilon)}, \tag{2.8}$$

where d_V is the spherical equivalent diameter by volume, d_{32} is the Sauter's mean diameter of the particles. In our experiments particle size was determined by sieving so that the proper spherical equivalent diameter should be equivalent by mesh size (i.e. sieving opening size) d_L. Taking the approximation that for isotropic particles $d_L \approx d_V$ the sieve diameter has been used. In this work Washburn's equation was expressed in terms of liquid weight in order to overcome some limitations of the original optical method. Particularly the visual observation of the liquid front is not always clear and the observed front may not reflect liquid rising can be non-homogeneous in the whole powder bed, moreover the measurements can be affected by the subjectivity introduced by operator observation.

The weight w of the penetrated liquid is given by (2.9):

$$w = \varepsilon \rho \pi r_{eff}^2 h. \tag{2.9}$$

After modification, combining (2.5) with (2.6) and (2.9) Washburn's equation in terms of liquid weight can be derived:

$$\frac{w^2}{t} = C \frac{\rho^2 \gamma_{LV} \cos\vartheta}{\eta}, \tag{2.10}$$

where C is a geometric constant which accounts for the properties of particles arrangement in the packed bed. This constant cannot be know a priori and its determination is essential for a precise and accurate application of Washburn's equation. To calculate C a completely wetting liquid is required ($\theta = 0$, then $\cos\theta = 1$). From the measurement curve slope $\Delta w^2/\Delta t$ and knowing the liquid properties (η, γ_{LV}, ρ), the value of the constant C is determined. The choice of the reference liquid is a crucial step of this method. Most of the reported studies in the literature focus on the choice of a completely wetting liquid for powders and reference liquids which are mainly used are alkenes such as ciclohexane, heptane and octane (Litster and Ennis, 2004; Ennis, B.J., 2006, Siebold *et al*., 2000, Tampy *et al*., 1988, Iveson *et al*., 2000).

2.4 Experimental

2.4.1 Materials

Several mineral and metallic powders were selected in order to cover a range of material properties and collect information on wettability as a function of different bulk density (or bed porosity), particle size and chemical nature. Powders used in this experimental work are the raw materials used in the production of welding wires and they were supplied by Fileur®, Cittadella, Italy.

Particle size distributions were measured by sieving; the true density of the particles was determined by liquid pycnometer. Poured density was measured following the standard procedure ISO 3923/1 (International Organization for standardization, 1976) which prescribes filling a 25 ml cup from a hopper, 2.5 cm above it. The procedure ISO 3953 was followed for measuring tap density: it requires vertically tapping a graduated container until the powder bed stabilizes at a minimum volume. These measurements were performed in triplicate and the average result is given in Table 2.1. Fe^a and Fe^b powders are both iron ores but they differ in terms of particle size distribution. All powders used in this work have not undergone any preparation or surface cleaning and were used 'as received'.

Table 2.1 *Summary of the main physical powder properties*

Powder properties	d_{32} (µm)	True particle density (g/cm^3)	Poured density (g/cm^3)	Tap density (g/cm^3)
Fe^a	42.24	7.684	2.483	2.840
Mn	14.08	6.969	2.887	3.558
Fe – Mn (C < 1%)	65.12	6.917	3.212	3.696
Fe – Mn (C < 8%)	86.24	9.742	3.106	3.509
Fe – Si	110.88	5.122	2.963	3.057
Fe^b	129.36	7.812	2.884	3.003
TiO_2	95.04	4.063	2.324	2.549

Potassium and sodium silicate is specifically recommended as a binder in the wet granulation process for the manufactory of consumable electrodes. Both of them are available in aqueous solutions. Potassium (K_2SiO_3) and Sodium Silicate (Na_2SiO_3) liquids are prepared by dissolving Potassium Silicate glass and Sodium Silicate glass in hot water respectively. By varying the silica to Potassium/Sodium Oxide (K_2O/Na_2O) ratio, products of definite but widely different properties are produced. Aqueous solutions of these polymeric binders at different concentrations in terms of water are selected to provide a range of interfacial chemistries. Liquid viscosity was determined using a Haake RV3 rheometer, surface tension was measured using a KRUSS K6 tensiometer.

Table 2.2 *Physico-chemical properties of binder solutions at 20° C*

Binder liquid	Density ρ_L (g/mL)	Surface tension γ_{LV} (mN/m)	Viscosity η (Pa·s)
85.7 wt% sodium silicate	1.303	59.2	0.031
50 wt% sodium silicate	1.159	62.2	0.009
28.6 wt% sodium silicate	1.086	65.3	0.006
85.7 wt% potassium silicate	1.315	61.3	0.029
50 wt% potassium silicate	1.163	63.3	0.007
28.6 wt% potassium silicate	1.090	66.3	0.005

The viscosity of these binders spanned a range of two orders of magnitude. Table 2.2 presents the physico-chemical properties of binder solutions.

2.4.2 Sessile drop experiments

The experimental apparatus for sessile drop method consisted of a Petri dish containing about 80 g of powder corresponding to layer of 20 mm deep . A powder bed was formed by sieving the powder through a 150 μm sieve into the Petri dish and scraping the level with a metal spatula to make the powder surface smooth.

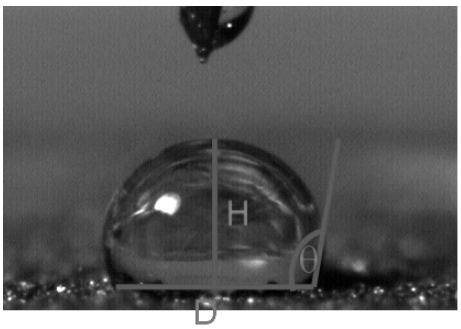

Figure 2.3 *Photograph of a potassium silicate droplet on Fe-Mn surface using the Photron Fastcam-Pci® video recorder. The apparent contact angle θ, the diameter, D and the height, H of the droplet after the impact on powder are visualized*

A 5 μL micro syringe was positioned 20 mm above the bed surface and sessile drop penetration was filmed by Photron Fastcam-Pci® video recorder operating at different frame rate: from 25 to 1000 frames/s. The drop sizes varied by 0.05 – 0.15 μL.
In order to investigate the wetting behaviour, the apparent contact angle θ was measured by drawing a tangent to the drop profile at the point of three-phase contact using the image analysis open–source software *ImageJ* (for general information see Abramoff *et*

al., 2004). Other parameters which were measured included the radius of the drop before and immediately after the impact on the compact and the maximum radius that the drop reached during the spreading process. Three replicates were performed only for the less dilute binder solutions. Figure 2.3 shows the sessile drop spread wetting for a metallic powder.

2.4.3 Drop penetration time

The same experimental apparatus and procedure described in §3.2 were used to measure the drop penetration time which was defined as the time taken by the drop to penetrate completely into the bed powder. Moreover for each powder the fluid rate penetration was determined as the ratio between the initial height of droplet and the drop penetration time. Results are reported in Table 2.3.

2.4.4 Washburn's experiments (weight based)

The experimental setup for weight measurement consisted of an aluminium cylindrical tube of 10 mm inner diameter and 60 mm height which had a nylon membrane placed at the bottom to sustain powder sample. A fixed quantity of powder has been weighted and placed in the capillary with a standard procedure that requires to fill the tube by pouring powder through a 150 μm sieve. The tube was linked to an electronic balance and weight data versus time were recorded with a frequency of 2 Hz as the imbibition proceeded. The data acquisition started when tube entered in contact with the probing liquid. Tree replicates were performed for each system powder-binder.

The experimental set up for capillary rise measurements and a typical output from Washburn method are provided respectively in Figures 2.4 and 2.5.

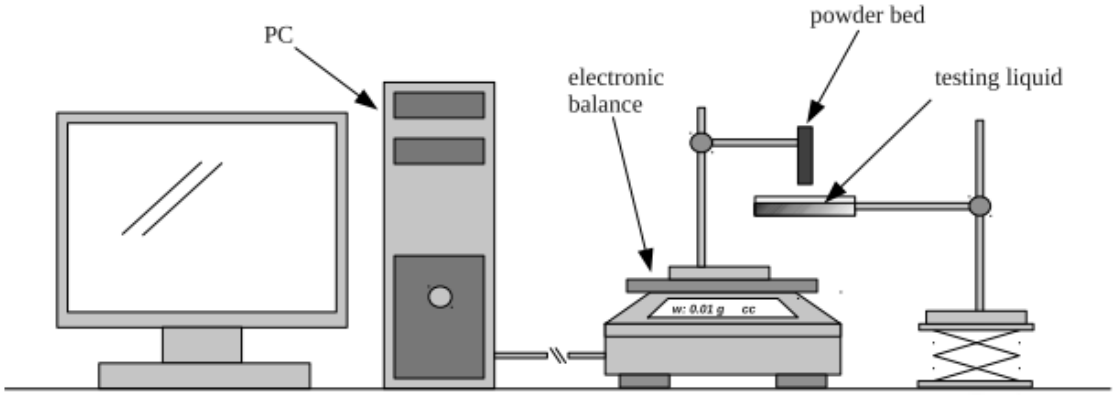

Figure 2.4 *Schematic diagram of experimental set up for Washburn's method*

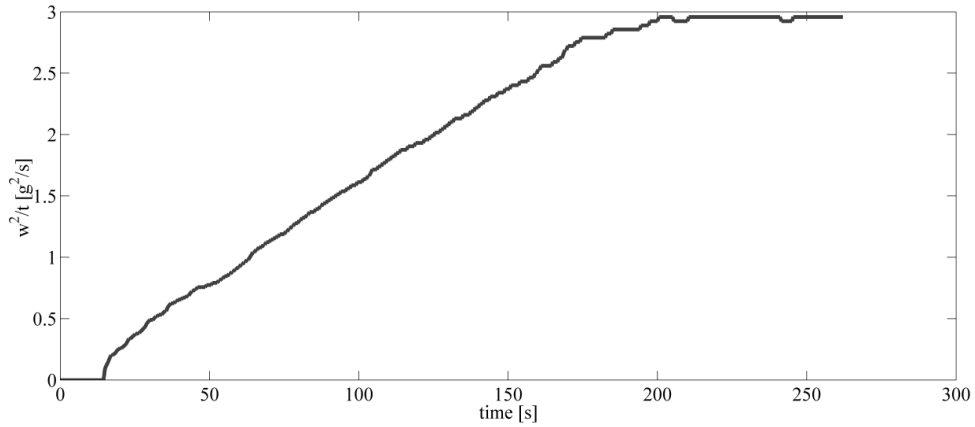

Figure 2.5 *Squared of weight gained by iron powder, w^2,versus penetration time of potassium silicate*

Particular attention was paid in pouring the powders into the tube and in handling the tube after filling in order to have a strict powder packing control and get reproducible results. The results from all the experiments are discussed below.

2.5 Results and discussion

2.5.1 Sessile drop experiments

Figures from 2.6 to 2.8 illustrate a series of images taken with the high speed video camera of typical drop penetration experiments for potassium silicate-water solution on iron ore Fe[a], manganese and Fe – Mn (C < 1%) powders respectively. After the impact on the powder surface the liquid drop spread out and stretched quickly on the surface. At the same time it was drawn into the powder bed. The same behaviour has been observed for all the powders employed in the experiments. The infiltration of the fluids into the powders can be described as a balance of thermodynamic and kinetic contributions. The thermodynamic definition of contact angle according to Young-Duprè implies a force balance which allows to reach a final equilibrium shape of the droplet only if the liquid drawing kinetics into the powder is low enough. So it is generally difficult to obtain contact angle measurements un-biased by the kinetic contribution.

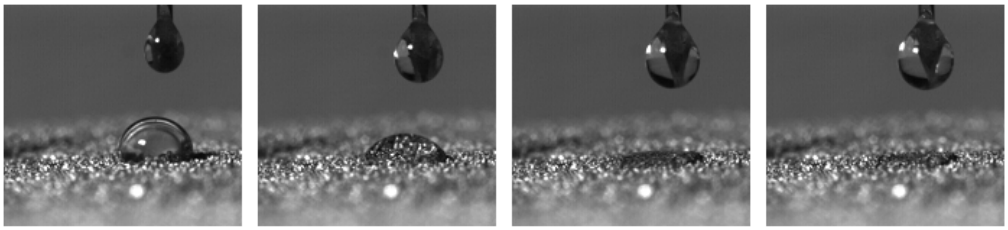

Figure 2.6 *Penetration of 85.7 wt% potassium silicate solution on iron. The picture are taken at (a) after the impact on powder compact, (b) 0.02 s, (c) 0.10 s, (b) 0.20 s and (d) 0.30 s after the impact*

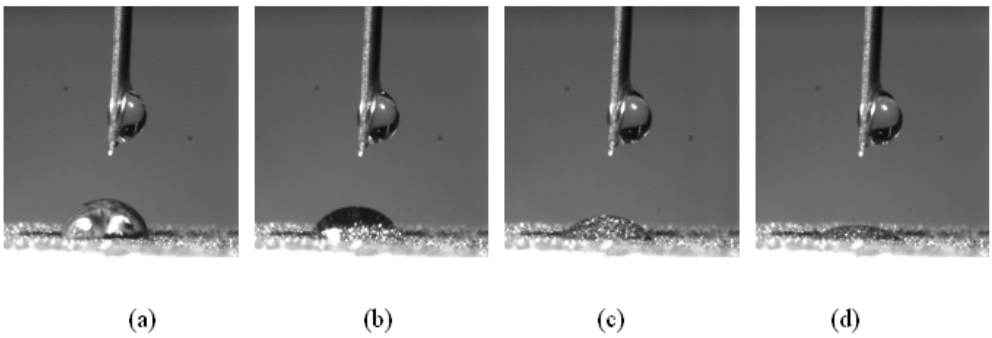

Figure 2.7 *Penetration of a 85.7 wt% potassium silicate drop on Mn powder. The picture are taken at (a) after the impact on powder compact, (b) 0.20 s, (c) 0.70 s and (d) 0.65 after the impact*

Table 2.3 shows the experimental mean drop penetration time and the standard error of the mean for each powder varying liquid binder. Table 2.3 also provides the fluid rate penetration and the contact angle for the two different binders.

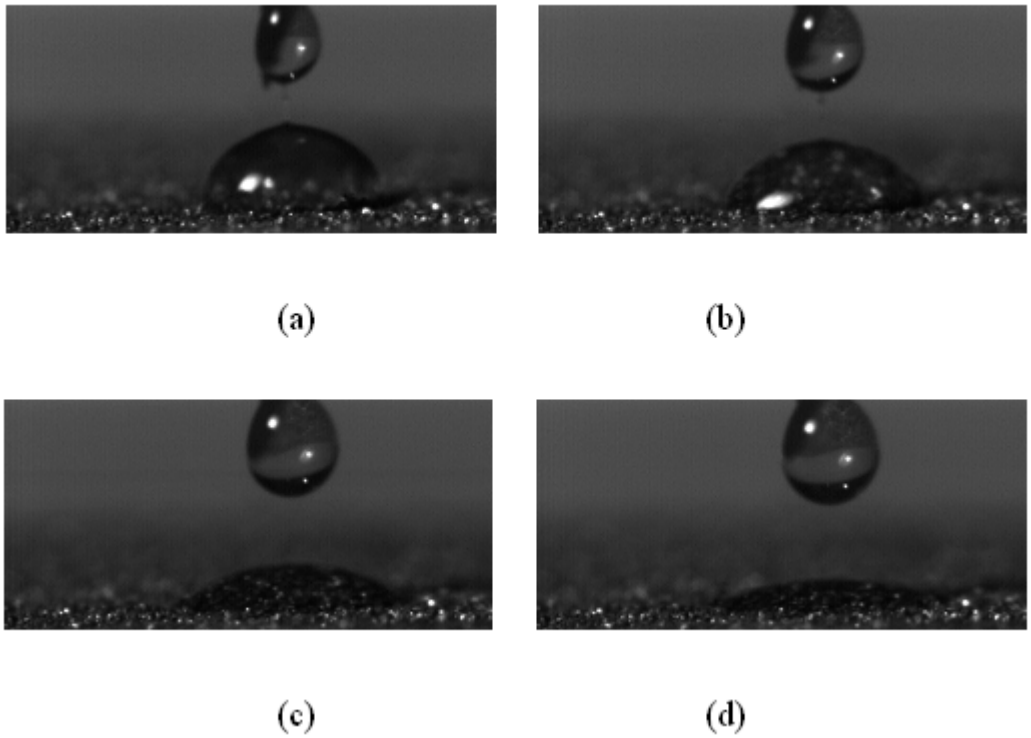

Figure 2.8 *Penetration of a 85.7 wt% potassium silicate drop on Fe - Mn powder. The picture are taken at (a) after the impact on powder compact, (b) 0.15 s, (c) 0.30s and (d) 0.45 after the impact*

The mean penetration rate is a more representative wettability index than the penetration time since it does not depend on the volume of the droplet. Because of the rough and irregular surface of the powders the measurements of the apparent contact angle by the image analysis was not straightforward (see Figures 2.6 ÷ 2.8). It has been very difficult to identify the solid/liquid interface since the surface was not uniform. Therefore data are affected by operator error and they present relatively large standard errors as can be seen from Table 2.4. Nonetheless some general evidence can be collected.

All of the apparent contact angles measured are high and fall between 70 and 90 degrees. For the same powder the apparent contact angles are always greater for the sodium silicate excepted for the Fe–Si powder. Even if sodium and potassium silicate have similar physical properties fluid rate penetration can vary widely: from a minimum of 598.81 μm/s for sodium silicate on manganese powder to 7112.66 μm/s for the same binder on iron powder (Fe^b). We can observe that the same powder interacts differently with the binder: for example for manganese powder the fluid rate penetration can triplicate by varying the kind of binder. Moreover there is not a general trend between the fluid rate penetration and the contact angle values for the powder–liquid systems examined.

Table 2.3 *Drop penetration results*

Powder	Binder Fluid	Penetration time, t_p (s)	Penetration rate v_p (µm/s)	Contact angle, Θ (°)
Fe[a]	85.7 wt% sodium silicate	0.42 ± 0.02	3741.97 ± 517.27	87.50 ± 0.77
	85.7 wt% potassium silicate	0.49 ± 0.09	3606.30 ± 225.26	83.00 ± 1.13
Mn	85.7 wt% sodium silicate	3.95 ± 0.11	598.81 ± 74.82	89.50 ± 4.64
	85.7 wt% potassium silicate	0.75 ± 0.16	2088.24 ± 434.15	74.75 ± 1.27
Fe – Mn (C < 1%)	85.7 wt% sodium silicate	0.79 ± 0.05	3097.00 ± 78.88	86.50 ± 2.12
	85.7 wt% potassium silicate	0.35 ± 0.10	6638.13 ± 673.38	83.30 ± 3.89
Fe – Mn (C < 8%)	85.7 wt% sodium silicate	0.65 ± 0.15	3905.08 ± 722.81	83.00 ± 1.41
	85.7 wt% potassium silicate	0.53 ± 0.03	3036.20 ± 298.16	78.85 ± 0.63
Fe – Si	85.7 wt% sodium silicate	0.86 ± 0.02	1171.02 ± 264.28	87.58 ± 4.80
	85.7 wt% potassium silicate	1.08 ± 0.09	2553.63 ± 222.64	89.80 ± 2.40
Fe[b]	85.7 wt% sodium silicate	0.31 ± 0.01	7112.66 ± 123.51	85.15 ± 1.62
	85.7 wt% potassium silicate	0.36 ± 0.03	7323.77 ± 17.91	80.70 ± 2.89
TiO_2	85.7 wt% sodium silicate	0.96 ± 0.05	2464.46 ± 402.28	85.92 ± 3.39
	85.7 wt% potassium silicate	0.58 ± 0.13	3241.18 ± 138.97	69.80 ± 1.76

Only for a subset of materials, iron (Fe[b]), manganese, Fe–Mn (C < 1%) and rutile powders, results where as expected, i.e. the larger the penetration velocity, the lower the contact angle.

2.5.2 Comparison to the theory

Figures 2.9 and Figure 2.10 show the values of drawing area versus penetration time for a droplet of 85.7 wt% potassium and 85.7 wt% sodium silicate obtained by placing drops

of silicate on the same porous substrate of iron and manganese powders. We can observe that the imbibition of potassium silicate is described by only two limiting cases: the increasing drawing area (IDA) and constant drawing area (CDA) for iron and the IDA and DDA phases for rutile powder. This experimental finding can be explained if we consider that the time taken for the potassium droplet to penetrate completely into the porous substrate is lower than that for the sodium one for the most of the powders tested. All the three phases identified by Hilpert and Ben-David's theory (2009) described the behaviour for complete drop penetration of sodium silicate.

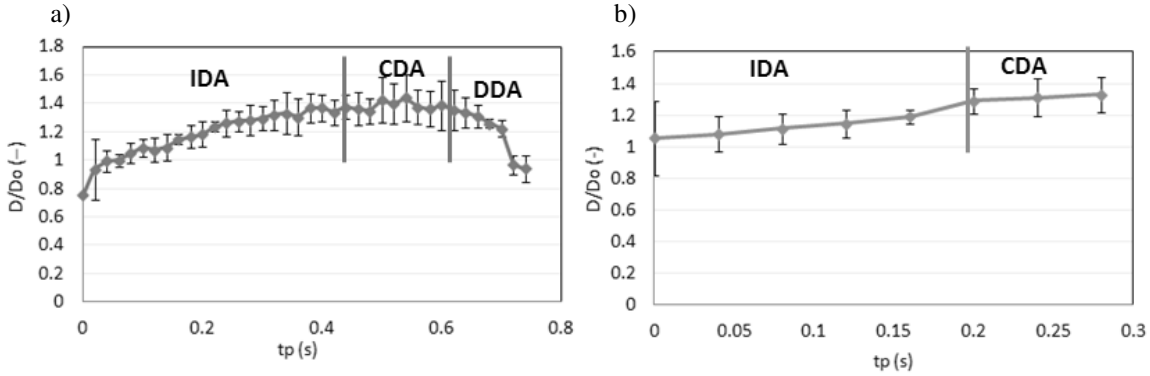

Figure 2.9 *The imbibition of sodium (a) and potassium (b) silicate onto iron powder compact*

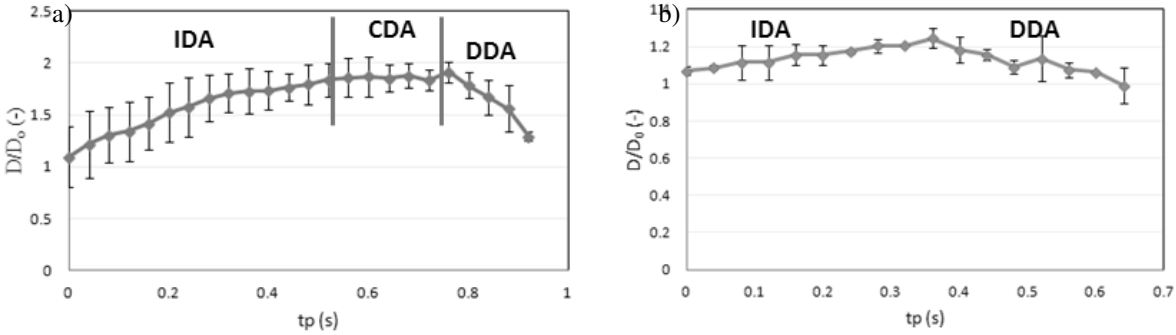

Figure 2.10 *The imbibition of sodium (a) and potassium (b) silicate onto rutile powder compact*

The types of the penetration we have recorded are not in agreement with the theory proposed by Hilpert and Ben-David since for some powders only two phases are required to describe the imbibition of sodium silicate into porous media. The experimental data suggest that imbibition of a single droplet into a porous substrate also depends on the surface chemistry within the bed but not a clear relationship was found.

2.5.3 Washburn experiments results

Table 2.4 summarizes Washburn's results for all the combination of powders and binders used to investigate the wettability behaviour. It is interesting to note that binder solution's viscosity plays an important role: for the various fluids the ranking of parameter w^2/t matches with that of fluid viscosity. The value of w^2 versus time vary by one order of magnitude for lower viscosity for the same kind of binder. For instance for potassium silicate solution which is more diluite the slope w^2/t value is 17.5 10^{-8} kg^2/s on iron Fe^a powder, for the same binder most concentrated the value is reduced by 90%. The same trend is shown for the sodium silicate. Differently from the results of sessile drop experiments, Washburn data exhibited a clear trend with respect to the powder- liquid binder systems: all the powders showed more affinity (i.e. higher slope of the curve) for the potassium silicate solutions, independently of the dilution of the liquid binder.
To determine the apparent contact angle between the liquid binders and the powders, the calculation of the constant term *C* is required. However, as mentioned in the Introduction, finding a total wetting liquid can be an issue for this kind of analysis. It has been indeed very difficult to find a total wetting liquid for our mineral and metallic powders, also because of a lack of information on this aspect in the literature. Therefore a dedicated study, addressed to the investigation of the best wetting liquid, has been carried out. The first reference liquid used in the method calibration was n-heptane which is largely employed as total wetting liquid in literature (Litster and Ennis, 2004; Ennis, B.J., 2006, Siebold *et al*., 2000, Tampy *et al*., 1988, Iveson *et al*., 2000). This preliminary step was carried out for the most concentrated potassium and sodium silicates solutions as liquid binders since highly concentrated potassium and sodium silicate solutions are employed in the wet granulation process for manufacturing of welding rods.

Table 2.4 *Values of the slope w^2/t (10^{-8} kg^2/s) obtained from capillary rise experiments*

Powder	Binder Fluid	Binder composition	w^2/t (10^{-8} kg^2/s)
Fe[a]	potassium silicate	85.7 wt% 50 wt% 28.6 wt%	1.650 ± 0.001 13.420 ± 0.012 17.500 ± 0.006
	sodium silicate	85.7 wt% 50 wt% 28.6 wt%	1.270 ± 0.002 10.350 ± 0.003 17.100 ± 0.011
Mn	potassium silicate	85.7 wt% 50 wt% 28.6 wt%	0.380 ± 0.001 2.770 ± 0.002 3.810 ± 0.005
	sodium silicate	85.7 wt% 50 wt% 28.6 wt%	0.300 ± 0.001 2.610 ± 0.002 4.020 ± 0.004
Fe – Mn (C < 1%)	potassium silicate	85.7 wt% 50 wt% 28.6 wt%	0.670 ± 0.001 3.590 ± 0.002 6.810 ± 0.007
	sodium silicate	85.7 wt% 50 wt% 28.6 wt%	0.450 ± 0.001 3.780 ± 0.001 5.840 ± 0.005
Fe – Mn (C < 8%)	potassium silicate	85.7 wt% 50 wt% 28.6 wt%	0.320 ± 0.001 3.540 ± 0.002 4.480 ± 0.008
	sodium silicate	85.7 wt% 50 wt% 28.6 wt%	0.400 ± 0.001 2.640 ± 0.004 4.660 ± 0.007
Fe – Si	potassium silicate	85.7 wt% 50 wt% 28.6 wt%	0.400 ± 0.001 3.320 ± 0.012 5.220 ± 0.007
	sodium silicate	85.7 wt% 50 wt% 28.6 wt%	0.360 ± 0.002 3.330 ± 0.003 4.060 ± 0.010
Fe[b]	potassium silicate	85.7 wt% 50 wt% 28.6 wt%	4.220 ± 0.006 23.760 ± 0.024 34.690 ± 0.082
	sodium silicate	85.7 wt% 50 wt% 28.6 wt%	2.420 ± 0.001 20.910 ± 0.023 34.600 ± 0.020
TiO_2	potassium silicate	85.7 wt% 50 wt% 28.6 wt%	0.560 ± 0.001 6.140 ± 0.007 10.590 ± 0.001
	sodium silicate	85.7 wt% 50 wt% 28.6 wt%	0.410 ± 0.001 5.730 ± 0.002 9.800 ± 0.008

The values of constant C and $cos\theta$ determined in this way are reported in Table 2.5. Three replicates were performed for each powder-liquid binder system.

Table 2.5 *Washburn's results assuming n-heptane as total wetting liquid*

Powder	w^2/t (10^{-8} kg^2/s)	C (m^5)	87.5% wt potassium silicate		87.5% wt sodium silicate	
			$cos\theta$ (-)	θ (°)	$cos\theta$ (-)	θ (°)
Fe[a]	7.890 ± 0.007	3.21E-15	>1	-	>1	-
Mn	1.980 ± 0.001	8.07E-16	>1	-	0.89	27.12
Fe – Mn (C < 1%)	2.910 ± 0.002	1.18E-15	>1	-	>1	-
Fe – Mn (C < 8%)	3.600 ± 0.001	1.52E-15	0.76	40.53	0.82	34.91
Fe – Si	3.40 ± 0.006	1.38E-15	0.79	37.81	0.67	47.93
Fe[b]	11.97 ± 0.007	4.87E-15	>1	-	>1	-
TiO_2	4.510 ± 0.006	1.83E-15	0.83	33.90	0.62	51.68

Unfortunately we can see in Table 2.5 that for most of the powders the value of $cos\theta$ exceeds unity meaning that the tested liquid wets the powder bed better than the reference liquid. Using an apolar reference liquid it is therefore possible to determine the contact angle only for few powders. Particularly n-heptane works well for Fe–Mn (C < 8%), Fe–Si and rutile powders.

For the choice of an appropriate liquid, hopefully working for all the powders of this study, it can be useful to characterize powders in terms of affinity to apolar and polar liquid. Yang and Chang (2008) did an extensive study on the wettability of filter media using capillary tests. The wastewater treatment filters used were anthracite, manganese ore and quartz with size fraction in the range of 0.9–1.2 mm. The lipophilic to hydrophilic ratio (LHR) was employed to compare the selectivity of filter media towards oil and water in terms of wettability.

In the present work the LHR index was used to compare the difference of selectivity, in terms of wettability, between apolar and polar liquid for a specific powder. LHR was defined as:

$$LHR = \frac{\cos \vartheta_A}{\cos \vartheta_P}, \tag{2.11}$$

where θ_A and θ_P are respectively the apparent contact angle of an apolar liquid and a polar liquid for a powder.

Combining (2.10) with (2.11) this index can be written in terms of Washburn's equation:

$$LHR = \frac{(w_2/t)_A \eta_A}{(w_2/t)_P \eta_P} \cdot \frac{\rho_P^2 \gamma_P}{\rho_A^2 \gamma_A}. \qquad (2.12)$$

For measuring the LHR value, apolar n-heptane and polar water representing the oil phase and the water phase respectively were used in Washburn's experiments. Their properties are presented in Table 2.6.

Table 2.6 *Properties of reference liquids at 20° C*

Reference liquid	Density ρ_L (g/mL)	Surface tension γ_{LV} (mN/m)	Viscosity η (mPa·s)
n-heptane	0.684	21.00	0.400
Water	1.000	72.10	1.002
Surfactant solution (a)	1.000	17.20	1.002
Surfactant solution (b)	1.000	21.50	1.002
Surfactant solution (c)	1.000	22.15	1.002

The slope of the lines w^2 versus time for the apolar phase (n-heptane) and for the polar phase (water) and the calculated LHR values are collected in Table 2.7.

Table 2.7 *Wetting parameters and LHR values for all the powders*

Powder	n-heptane w^2/t (10^{-8} kg^2/s)	Water w^2/t (10^{-8} kg^2/s)	LHR (-)	Powder characteristic
Fe[a]	7.89	28.55	0.80	Hydrophilic
Mn	1.98	5.50	1.05	Lipophilic
Fe – Mn (C < 1%)	2.91	6.14	1.38	Lipophilic
Fe – Mn (C < 8%)	3.60	6.12	1.72	Lipophilic
Fe – Si	3.40	8.53	1.16	Lipophilic
Fe[b]	11.97	49.14	0.71	Hydrophilic
TiO_2	4.51	15.27	0.86	Hydrophilic

Among the powders used, LHR values for iron powders are lower than one meaning that both of them are hydrophilic. The other powders have a LHR values larger than one so that they show a lipophilic behaviour. Manganese powder does not show a clear behaviour.

An apolar fluid like n-heptane was expected to be the best reference liquid for powders which exhibit a lipophilic behaviour. Comparison with data from Table 2.5 however shows that for Fe–Mn (C < 1%) and Mn powders it is not possible to calculate the apparent contact angle by assuming n-heptane as total wetting liquid. It is also interesting to note that for rutile powder we can calculate the apparent contact angle even if rutile shows more affinity to polar fluids (LHR < 1).
At this point it can be interesting to perform a test on the same set of powders using water as total wetting liquid instead of n-heptane in order to verify how LHR behave with respect to the powders previously identified as hydrophilic in Table 2.7.
Results are presented in Table 2.8.

Table 2.8 *Washburn's results assuming water as total wetting liquid*

Powder	w^2/t (10^{-8} kg^2/s)	C (m^5)	87.5% wt potassium silicate		87.5% wt sodium silicate	
			$cos\theta$ (-)	θ (°)	$cos\theta$ (-)	θ (°)
Fe[a]	0.286 ± 0.007	3.91E-15	>1	-	0.97	14.07
Mn	0.055± 0.003	7.53E-16	>1	-	0.96	16.26
Fe–Mn (C < 1%)	0.061 ± 0.005	8.41E-16	>1	-	>1	-
Fe–Mn (C < 8%)	0.061 ± 0.001	5.11E-16	>1	-	>1	-
Fe–Si	0.085 ± 0.025	1.17E-15	0.94	19.94	0.79	37.81
Fe[b]	0.491 ± 0.053	6.73E-15	>1	-	>1	-
TiO_2	0.153 ± 0.025	2.02E-15	0.75	41.40	0.56	55.94

Assuming water as the reference fluid, it is possible to determine a value of contact angle for the two iron powders and the sodium silicate (but not the potassium silicate). Some values of contact angle are obtained for manganese powder and Fe–Si powder but they are different (lower) than those obtained using n–heptane. This is due to the fact that these powders having a lipophilic behaviour exhibit an higher affinity to apolar liquid. On the contrary, the contact angle calculated for rutile and water are larger because of the hydrophilic behaviour of this powder. All these results suggest that the LHR can give only limited information on the affinity of the wetting medium with the powder and cannot be used as a general guide for the selection of the proper wetting fluid. They also confirm that Washburn's method is extremely sensitive to the choice of the reference liquid used. For instance the rutile – potassium silicate system has an apparent contact angle ranging from 33° to 41° by changing the total wetting liquid.

2.5.4 Towards a total wetting liquid for metallic and mineral powders

Notwithstanding the difficulties in finding a total wetting liquid a further effort was made using surfactant aqueous solutions. It is known that partially or fully fluorinated hydrocarbon compounds exhibit outstanding chemical and thermal stability, low solubility in water and excellent lubricating properties because of their very low interfacial energy (Zaggia *et al*., 2010). So three wetting media were prepared using different fluorinated compounds. Surfactant solution (a) was prepared by slowly dissolving 1 g of N diethyl – 3 heptadecafluorine – 2 hydroxypropane – 1 ammonium iodide in 999 g of cold water. Surfactant solution (b) had a concentration of 0.5 g/l of 1 – perfluorotooctyl – 3 propan – 2 ol and finally surfactant solution (c) contained 0.5 g/l of N – benzyl – N, N – propyl – 3 – heptadecafluorine – 2 – hydroxypropane – 1 – ammonium bromide. These three solutions were expected to have the same physical properties of water in terms of density and viscosity because of their high dilution. Surface tension was the only physical property markedly different from that of water. Their characteristics are reported in Table 2.6.

A preliminary study was conducted for iron and Fe–Mn powders. These two powders have been chosen because their opposite behaviour in terms of LHR value. In Figure 2.11, Washburn's experiments for iron Fe[a] powder were plotted. These three curves describe the wetting behaviour of the different surfactant solutions.

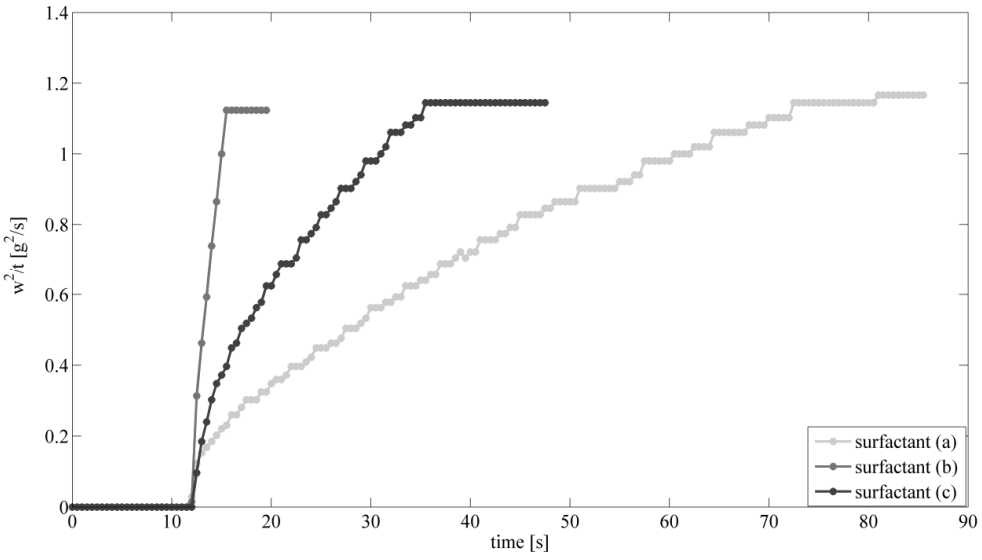

Figure 2.11 *The slope w_2 versus time for three different surfactant solutions on iron powder*

It can be observed that the rate of imbibition is clearly higher for the surfactant solution (b).

The other powder exhibited the same behaviour as summarized in Table 2.9.

Table 2.9 *Washburn's results assuming surfactant solutions as total wetting liquids*

Powder	Surfactant (a) w^2/t (10^{-8} kg^2/s)	Surfactant (b) w^2/t (10^{-8} kg^2/s)	Surfactant (c) w^2/t (10^{-8} kg^2/s)
Fe[a]	0.98	25.19	8.70
Fe[b]	1.68	29.07	1.49
Fe – Mn (C < 1%)	1.23	3.97	1.96
Fe – Mn (C < 8%)	1.61	5.22	3.60

Table 2.9 demonstrates that for the same powder the slope w^2 versus time is at least one order of magnitude larger in the case of surfactant (b). For this reason, the 1 – perfluorotooctyl – 3 propan – 2 ol solution can be considered as the best wetting liquid for the powders tested. The measured slopes for the fluorinated surfactant (b) leads to the constants *C* given in Table 2.10.

Table 2.10 *Washburn's results assuming surfactant solutions (b) as total wetting liquids and relative values of contact angles for 87.5% wt potassium and 87.5% wt sodium solutions*

Powder	w^2/t (10^{-8} kg^2/s)	C (m^5)	87.5% wt potassium silicate		87.5% wt sodium silicate	
			$cos\theta$ (-)	θ (°)	$cos\theta$ (-)	θ (°)
Fe[a]	25.19 ± 0.01	1.17E-14	0.385	67.35	0.325	71.03
Mn	5.25 ± 0.01	2.44E-15	0.424	64.91	0.296	72.78
Fe – Mn (C < 1%)	3.97 ± 0.01	2.02E-15	0.901	25.71	0.614	52.12
Fe – Mn (C < 8%)	5.13 ± 0.01	2.39E-15	0.484	61.05	0.981	11.19
Fe – Si	7.08 ± 0.01	3.73E-15	0.334	70.49	0.249	75.58
Fe[b]	29.07 ± 0.07	1.64E-14	0.702	45.41	0.452	63.13
TiO_2	11.08 ± 0.01	5.15E-15	0.296	72.78	0.220	77.29

The values of the constant *C* determined using surfactant solution (b), allow us to determine the contact angles for all the tested powders according to (2.10). This means that the fluorinated solution (b) can be considered among the wetting liquid tested here the best total wetting liquid for the mineral and metallic powders examined.

2.5.5 Further comparisons

As final remark a comparison between capillary rise technique (Washburn) and sessile drop method is reported. In Table 2.11 the apparent contact angles obtained using the two methods are compared. It can be observed that it does not exist a clear correlation between the contact angles measured by the two different approaches. The apparent contact angles measured by sessile drop technique are larger than those calculated using Washburn's method but at a first sight it is difficult to identify which of the two methods provide with the most meaningful and realistic contact angle values. However if we consider the uncertainties introduced by the sessile drop measurement and summarized in §2.5.1 (difficulty in the assessment of droplet equilibrium after the impact on powder compact, difficulty to isolate the droplet equilibrium position because of contemporary sinking in the compact, difficulty to have a perfectly flat surface for the compact, collapse of the compact because of the droplet weight and capillary forces), the capillary rise method should be expected to perform better. This hypothesis is confirmed by plotting data of Table 2.13 separately.

Table 2.11 *Comparison between the contact angles calculated by sessile drop and Washburn's method*

Powder	87.5% wt potassium silicate		87.5% wt sodium silicate	
	Sessile drop method θ (°)	**Washburn's method θ (°)**	**Sessile drop method θ (°)**	**Washburn's method θ (°)**
Fe[a]	83.00	67.35	87.5	71.00
Mn	74.75	64.91	89.50	72.80
Fe–Mn (C < 1%)	83.30	25.71	86.50	52.13
Fe–Mn (C < 8%)	78.85	61.06	83.00	58.45
Fe–Si	89.80	70.49	87.58	75.58
Fe[b]	80.70	45.41	85.15	63.09
TiO_2	69.80	72.78	85.92	77.29

Figure 2.12 and Figure 2.13 compare the apparent contact angle value estimated by the sessile drop method and Washburn technique respectively. The binders uses are the two liquid binders of industrial relevance, i.e the solutions at 87.5% in weight of potassium and sodium silicate in water. Sodium and potassium silicate are both used industrially because they have very similar physical properties (see Table 2.2). We can observe that in

the case of the sessile drop method there is not a simple correlation between experimental data for the same powder. Washburn method instead exhibits a clear correlation between the apparent contact angle values reflecting the similarity of the two liquid binders.

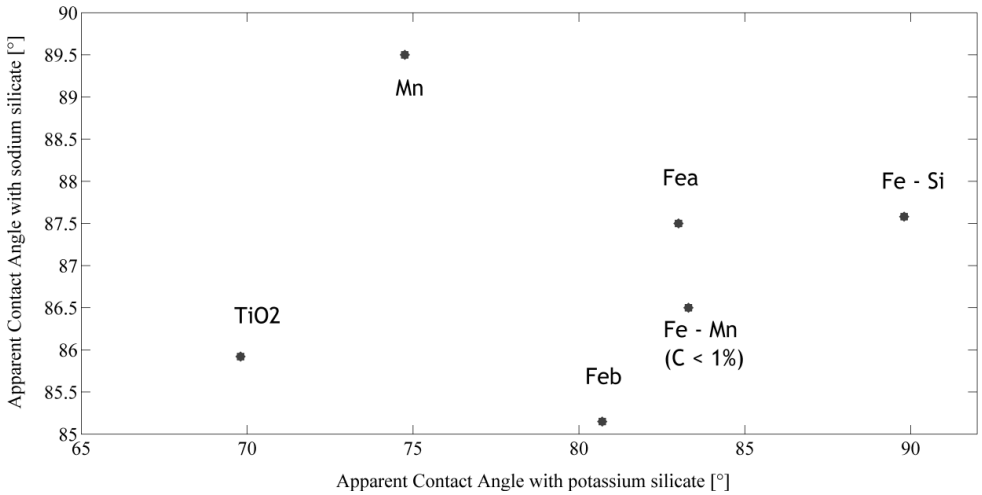

Figure 2.12 *Comparison of the apparent contact angles values using sessile drop method for the two binder liquids of industrial relevance*

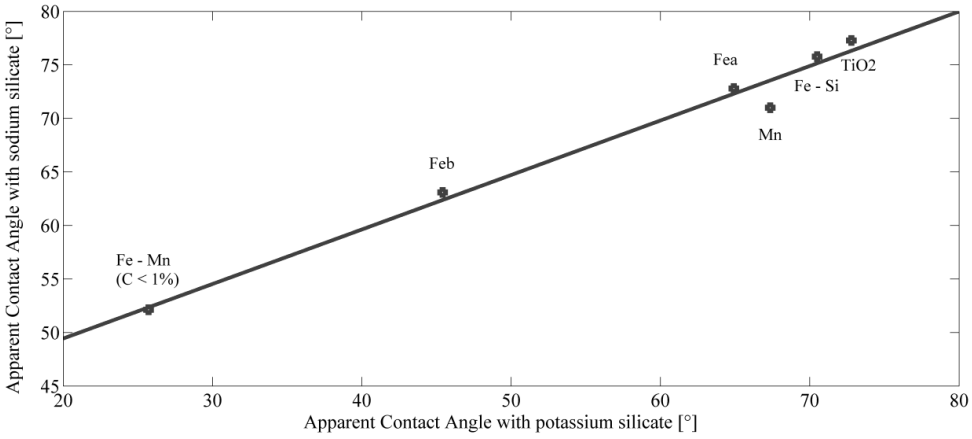

Figure 2.13 *Comparison of the apparent contact angles values using Washburn method for the two binder liquids of industrial relevance*

Moreover Washburn technique spans over a larger range of angles for both binders. This finding suggests that Washburn method has a higher sensitivity than the sessile drop one.

2.6 Conclusions

Investigation of wettability of mineral and metallic powders using the sessile drop technique and Washburn test was carried out. The objective was to collect information on

wetting behaviour of powders which are widely used in the powder metallurgy, particularly in the manufacture of welding rods.

For the drop penetration experiments, this work confirms that the drop penetration behaviour is quite complex and highly dependent on the structure of powder bed. For non-ideal surfaces such as mineral and metallic powder kinetics plays a more important role than thermodynamics in dictating wettability. Variables linked to kinetics such as binder viscosity seem to have the major role. For this reason fluid rate penetration is a more significant wetting index than the apparent contact angle in the sessile drop approach. The main weakness in the sessile drop method is that is very difficult to get reproducible data as the results are very sensitive to how the powder compact is prepared, particularly the porosity at the surface. Moreover it is not easy to recognize the correct instant when the drop penetration starts and this aspect can also affect the measurements of penetration time and rate.

Concerning Washburn's experiments, it is important to note that the choice of the best wetting liquid is a critical step because it affects the calculation of the material constant C and then the measurements of the apparent contact angle. This work showed that for mineral and metallic powders the reference liquids so far most commonly used in the literature (alkenes) are not suitable. The data demonstrate that a surfactant solution containing fluorinated ethers was the most appropriate total wetting liquid because it wetted better than the test liquid and the value of $\cos\theta$ never exceed unity for all the powders tested. On the whole Washburn's method performed much better then sessile drop method for the several powders tested in this work. However in general there is not an universal reference liquid for all the possible powders and the determination of the constant C remains a major limitation of this approach. As a future work it is therefore advisable to develop methods which does not require a calibration step with a total wetting liquid and improve our ability to evaluate C on the base of basic physical properties of powder packed bed (porosity, tortuosity, particle size).

2.7 References

Abramoff, M.D., Magalhaes, P.J., Ram, S.J., 2004. Image Processing with ImageJ. Biophotonics International 11, pp. 36-42.

Byron Bird, R., Stewart, W.E., Lightfoot, E.N., 2005. Transport Phenomena , 2nd ed. Wiley, New York (U.S.A.).

Chau, T.T., 2009. A review of techniques for measurement of contact angle and their applicability on mineral surface. Mineral Engineering 22, pp. 213-219.

de Gennes, P.G., 1985. Wetting: static and dynamics. Review of Modern Physics 57, pp. 827-863.

Ennis, B.J., 2006. Theory of granulation: an engineering perspective. In: Parikh, D.M. (Ed.), Handbook of Pharmaceutical Granulation Technology, 2nd ed. Taylor and Francis Group, New York (U.S.A.).

Ennis, B.J., Litster, J., 1997. Principles of size enlargement, in: D. Green, R. Perry (Eds.), Perry's Chemical Engineers, Mc Graw Hill, New York, Handbook-7th Edition.

Feeley, J.C., York, P., Sumby, B.S., Dicks, H., 1998. Determination of surface properties and flow characteristic of salbutamol sulphate, before and after micronisation. International Journal of Pharmaceutics 172, pp. 89-96.

Fuerstenau, D.W., Diao, J., Williams, M.C., 1991. Characterization of the wettability of solids particles by film flotation 1. Experimental investigation. Colloids and Surface 60, pp. 127-144.

Grassi, M., Grassi, G., Lapasin, R., Colombo, I., 2007. Understanding Drug Release and Absorption Mechanism. CRC Press (U.S.A.), pp. 256-266.

Hapgood, K.P., Litster, J.D., Biggs, S.R., Howes, T., 2002. Drop Penetration into Porous Powder Beds. Journal of Colloid and Interface Science 253, pp. 353-366.

Hapgood, K.P., Khanmohammadi, B., 2009. Granulation of hydrophobic powders. Powdert Technology 189, pp. 253-262.

Heertjes, P.M., Kossen, N.W.F., 1967. Measuring the contact angle of powder-liquid system. Powder Technology 1, pp. 33-42.

Hilpert, M., Ben-David, A., 2009. Infiltration of liquid droplets into porous media: effects of dynamic contact angle and contact angle hysteresis. International Journal of Multiphase Flow 35, pp. 205-218.

Holman, R.K., Cima, M.J., Uhland, S.A., Sachs, E., 2002. Spreading and infiltration of inkjet-printed polymer solutions droplets on a porous substrate. Journal of Colloid and Interface Science 249, pp. 432-440.

Iveson, S.M., Susana, H., Biggs, S., 2000. Contact angle measurements of iron powders. Journal of Colloid and Surface A: Physicochemical and Engineering Aspects 166, pp. 203-214.

Kossen, N.W.F., Heertjes, P.M. (1967). The determination of the contact angle for systems with a powder. Chemical Engineering Science 20, pp. 593-599.

Krycer, I., Pope D.G., Hersey, J. A., 1983. An evaluation of tablet binding agents part I. Solution binders. Powder Technology 34, pp. 39-51.

Labajos-Broncano, L., Gonzales-Martin, M.L., Bruque, J.M., Gonzalez-Garcia, C.M., Janwzuk, B., 1999. On the Use of Washburn's Equation in the Analysis of Weight-Time Measurements Obtained from Imbibition Experiments. Journal of Colloid and Interface Science 219, pp. 275-281.

Lago, M., Araujo, M., 2001. Caplillary rise in porous media. Physica A: Statistical Mechanics in porous media 289, pp. 1-17.

Lazgab, M., Khashayar, S., Pezron, I., Guigon, P., Komunyer, L., 2005. Wettability assessment of finely divided solids. Powder Technology 157, pp. 79-91.

Litster, J.D., Ennis, B.J., Iveson, S.M., Hapgood, K., 2001. Nucleation, growth and breakage phenomena in agitated wet granulation processes: a review. Powder Technology 117, pp. 3-39.

Litster, J., Ennis, B.J., 2004. The science and engineering of granulation process, Kluwer academic publishers, Dordrecht, The Netherlands.

Marmur, A., 1995. Equilibrium contact angles: theory and measurement. Colloids and Surface A: Physicochemical and engineering Aspects 116 (1-2), pp. 55-61.

Parikh, D. M., 2005. Handbook of pharmaceutical granulation technology, 2nd ed., Taylor and Francis Informa Publications, pp. 191–228.

Pietsch, W., 1991. Size enlargement by agglomeration. Wiley; Aarau; Salle and Sauerländer, Chichester.

Shaafsma, S.H., Vonk, P., Kossen, N.W.F., 1998. Proc. World Congress on Particle on Particle Technology 3, Brighton, UK, July 6-9, IChemE

Siebold, A., Walliser, A., Nardin, M., Oppliger, M., Schultz, J., 1997. Capillary Rise for Thermodynamic Characterization of Solid Particle Surface. Journal of Colloid and Interface Science 186, pp. 60-70.

Siebold, A., Nardin, M., Walliser, A., Schultz, J., Oppliger, 2000. Effect of dynamic contact angle on capillary rise phenomena. Colloid and Surface in A: Physochemical and Enginnering Aspects 161, pp. 81-87.

Tampy, G.K., Chen, W., Prudich, M.E., Savage, R.L., 1988. Wettability Measurements of Coal Using a Modified Washburn Technique. Energy & Fuels 2, pp. 782-786.

Waldie, B., 1991. Growth mechanism and the dependence of granule size on drop size in fluidized-bed granulation. Chemical Engineering Science 46, pp. 2781-2785.

Washburn, E.W., 1921. The dynamic of capillary flow. Physical Review 17, p. 273.

Yang, B.W., Chang, Q., 2007. Wettability studies of filter media using capillary rise test. Separation purification technology 60, pp. 335-340.

Zaggia, A., Conte, L., Padoan, G., Ceretta, F., 2010. Synthesis and characterization of partially of fluorinated ethers. Journal of Fluorine Chemistry 131, pp. 844-851.

Zhang, D., Flory, J.H., Panmai, S., Batra, U., Kaufman, M.J., 2002. Wettability of pharmaceutical solids: its measurement and influence on wet granulation. Colloids and Surfaces A: Physicochemical and Engineering Aspects 206, pp. 547–554.

Chapter 3

Wet granulation of mineral and metallic powder in low shear mixer

3.1 Summary

Wet granulation is a particle size enlargement process which is frequently required in many industries, from pharmaceuticals and agrochemicals industries to minerals and plastic ones, to improve physical and material properties of powders such as flow ability, rate of dissolution and robustness to segregation.

This experimental work deals with the study of wet granulation of mineral and metallic powders by aqueous solutions of silicate using a laboratory scale low shear mixer.

The aim of this study is to investigate the effect of physicochemical properties of liquid binder and feed powders and the operating parameters on the properties of finale granules. The granulation experiments are carried out using three different blends of metallic and mineral powders as feed materials and aqueous solutions of potassium and sodium silicate concentrations as binder. It was found that there is a critical ratio of the amount of silicate beyond which the mean size increased abruptly from about 80 mm to 160 mm.

The effect of the physicochemical properties is also evaluated using a modified capillary viscous number, Ca, which is defined as the ratio between the viscous forces ($\mu_L U$) and the work of adhesion ($W_a = \gamma_L(1+cos\vartheta)$). For $Ca < 1$ the granule growth is not affected by an increase of the solution viscosity. For $Ca \geq 1$ the viscous forces predominate and control the granule growth. Granule growth is investigated by using Stokes criterion in order to define the condition for coalescence between granules for all the binder/powder blends systems.

Concerning the process variables the experimental results show that an increase in agitation intensity of impeller reduces the final granule mean size. Moreover the higher impeller speed, the higher values of Stokes number and crumb behaviour occurs.

3.2 Introduction

Granulation, also known as agglomeration, balling and pelletization, is one of the key unit operation in many industrial sectors for manufacturing a wide range of intermediates and

final products such as food, chemicals, pharmaceuticals, iron ore and metalliferous ores, plastics, pesticides, ceramics and detergents.

As already mentioned in Chapter 1 wet granulation converts fine powders to granular materials using a liquid binder to form larger granules with specific attributes. It is used to formulate compounds, improve flow and handling properties, reduce dustiness and segregation of critical components in a powder formulation. (Litster et al., 2001; Litster and Ennis, 2004; Parick, 2005).

Granulation is an example of *particle design* (Ennis *et al*.,1997). The different mechanisms by which size enlargement occur are clearly identified and classified (Iveson *et al*., 2001):

1. granule nucleation and binder distribution;
2. granule consolidation and growth;
3. granule attrition and breakage.

These rate processes combine to control properties of final granules (size, porosity, surface structure etc…) and they can be affected by materials variables such as binder viscosity and surface tension, feed particle size distributions, particle shape and operating conditions like granulation technique and equipment.

Granulation can be performed either by tumbling, mechanical agitation (low and high shear mixer) or fluidization. This study is concerned with low shear mixer.

Many problems in choosing the right formulation and the appropriate process conditions as well as difficulties in understanding and controlling the process arise because of variation in physical properties of the system feed powders – binders. In the last decades considerable progress has been made in the knowledge of the mechanisms of size enlargement. However quantitative prediction of granules attributes is difficult and this is a particular problem in those industries where many different feed formulations are required. One of the major challenges is to predict in advance the effect of variations in formulation properties and operating conditions on the outcome of the process (Knight, 2004).

Wet granulation is strongly dominated by liquid forces between particles, particularly static capillary forces and dynamic viscosity forces. Nucleation and binder distribution are the most important steps in agglomeration process as they affect the process kinetics, consequently granules properties (Knight *et al*., 1998; van den Dries and Vromans, 2009).

Many researchers have focused on the effect of binder content and binder viscosity on properties of granular flows (Iveson *et al*., 1996; Kenningley *et al*., 1997; Johansen and Schaefer, 2001; Yang and Hsiau, 2006; Chitu *et al*., 2011;)

The importance of the viscosity of the added liquid has also been investigated by Ennis et al. (1990, 1991) and Tardos et al. (1997). Rajniak *et al*. (2007) found a clear correlation between the granule porosity and the binder concentrations for different pharmaceuticals

excipients. Cheng and Hsiau (2010) discussed how the binder viscosity influence the agglomeration mechanism. It has been found that the agglomeration growth rate increased with increasing the liquid viscosity during the nucleation stage, but the exact opposite phenomena occurred in the consolidation stage. All the studies mentioned above deal with agglomeration of pharmaceutical ingredients (microcrystalline cellulose powder, mannitol, calcium carbonate powder) with common polymeric binders for instance hydroxypropyl-cellulose (HPC), polyvinylpyrrolidone (PVP) and polyethylene glycol (PEG).

However no report has been found in the literature on how the wet granulation is sensitive to changes in product properties (viscosity, wettability) and process variables (impeller rotational speed, mixing time) in the case of mineral and metallic powders. The need of additional research is obvious and this forms the motivation of this work.

This study presents a practical framework of binder granulation that takes place in the process of manufacturing of welding rods. The aim of this study is to better understand the effect of the operating conditions and the liquid binder physicochemical properties on the granules properties in the wet agglomeration of metallic formulations in a low-shear mixer.

3.3 Materials and methods

Three different powder mixtures of mineral and metallic powders were used as starting materials. These formulations are the feed powder in the manufacture of welding wires and they are supplied by the company Fileur – Trafilerie di Cittadella Spa (Cittadella, Italy).

Blend A is a formulation of mainly iron and iron-silica powders. Formulation B contains mainly fluorspar powder, while Blend C is a formulation of rutile powder. Other minor components can be iron-manganese ,iron- silica, silica-manganese and iron-boron powders. Particle size distribution of the three different powder formulations on the mass basis are reported in Table 3.1. Poured and tap density are also listed in Table 3.1.

Table 3.1 *Physical properties of the starting materials*

Powder	d_{50} (μm)	Span (-)	Poured density (g/cm^3)	Tapped density (g/cm^3)
Formulation A	118.52	1.49	2.58	3.53
Formulation B	74.33	2.15	1.10	2.59
Formulation C	75.94	1.37	1.39	2.86

It is seen from Table 3.1 that formulation B and C contain a larger amount of fine particles compared to formulation A. Table 3.1 also shows that there is a significant

difference in the span of the size distributions. Formulation B has the widest size distribution, where the size distribution of formulation A and C are almost identical and narrower. The poured and tap density (Table 3.1) show a looser packing of formulation B and C compared with the packing of formulation A.

Potassium and sodium silicate is specifically recommended as a binder in the wet granulation process for the manufactory of consumable electrodes. Both of them are available in aqueous solutions. Potassium (K_2SiO_3) and Sodium Silicate (Na_2SiO_3) liquids are prepared by dissolving Potassium Silicate glass and Sodium Silicate glass in hot water respectively. These binders are defined by the formulation and for this particular industrial process binder selection is practically reduced to adjusting the properties of the binder using different amounts of water. By varying the silica to Potassium/Sodium Oxide (K_2O/Na_2O) ratio, products of definite but widely different properties are produced. Silicate aqueous solutions were used as binders so that binder viscosity could be varied among a quite wide range. Solution percentages are calculated on weight basis. Binders were characterized in terms of density, viscosity and surface tension. Solution density was measured by precisely weighting 10 cm^3 of aqueous solution. In these granulation trials liquid binder is poured onto the moving powder mass.

Table 3.2 Physicochemical properties of binder solutions at 25 °C

Binder fluid	Density ρ_L (g/mL)	Surface tension γ_{LV} (mN/m)	Viscosity η (Pa·s)
90 wt.% sodium silicate	1.314	59.2	0.078
85.7 wt % sodium silicate	1.303	59.2	0.031
50 wt % sodium silicate	1.159	62.2	0.009
28.6 wt % sodium silicate	1.086	65.3	0.006
90 wt % potassium silicate	1.329	61.2	0.071
85.7 wt.% potassium silicate	1.315	61.3	0.029
50 wt.% potassium silicate	1.163	63.3	0.007
28.6 wt.% potassium silicate	1.090	66.3	0.005

The dynamic viscosity was obtained by the automated rheometer Rotovisco RV3 (Haake, Karlsuhe, Germany) and the surface tension was measured using the plate method (Tensiometer KRUSS K6, Kruss GmbH, Hamburg, Germany). Some relevant properties of these binders are presented in Table 3.2.

3.4 Wettability measurements

Our work on wettability of the pure components contained within the three different formulations has been already reported in Chapter 2 (Susana *et al.*, 2010) and is

summarized here. The wettability of the solutions on the powder blends are characterized by the contact angle which was determined by Washburn technique. According to this method, the value of contact angle can be calculate using the following relation:

$$\cos\theta = \frac{\eta}{C\rho_L^2\gamma_{LV}}\frac{w^2}{t}. \tag{3.1}$$

In order to estimate the contact angle for the powder blends a weighted averaged method based on the composition of the different formulation has been used. In Table 3.3 the contact angle for the three formulations are listed. The binder solutions employed for wettability measurements are those used in the industrial process for manufacturing of consumable electrodes (sodium and potassium silicate solutions).
Formulation B contains about 50% of fluorspar powder which was found to be hydrophobic. For this reason the contact angles of formulation B/potassium silicate solutions systems are greater than 90°.

Table 3.3 *Wettability of starting materials with different binder solutions*

Powder Mixture	**Binder solution**	**cosθ** (°)
Formulation A	90 wt.% sodium silicate	86.10
	87.5 wt.% sodium silicate	84.49
	50 wt.% sodium silicate	83.90
	28.6 wt.% sodium silicate	68.78
Formulation B	90 wt.% potassium silicate	109.00
	87.5 wt.% potassium silicate	107.66
	50 wt.% potassium silicate	105.89
	28.6 wt.% potassium silicate	104.63
Formulation C	90 wt.% potassium silicate	82.57
	87.5 wt.% potassium silicate	82.30
	50 wt.% potassium silicate	81.00
	28.6 wt.% potassium silicate	59.13

3.5 Photographs

Photographs of these formulations were taken by a scanning electron microscope (SEM), (JSM Jeol 6490, Japan).

a)

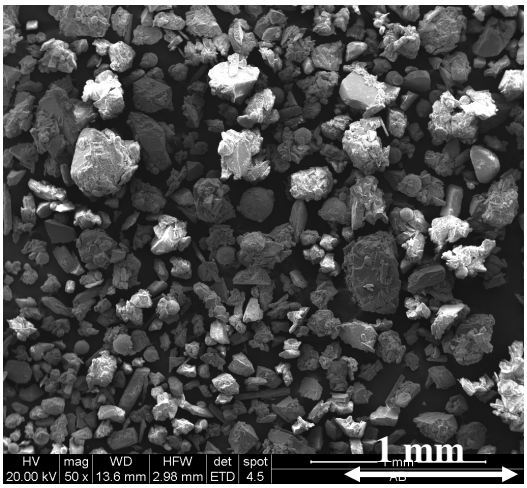

b)

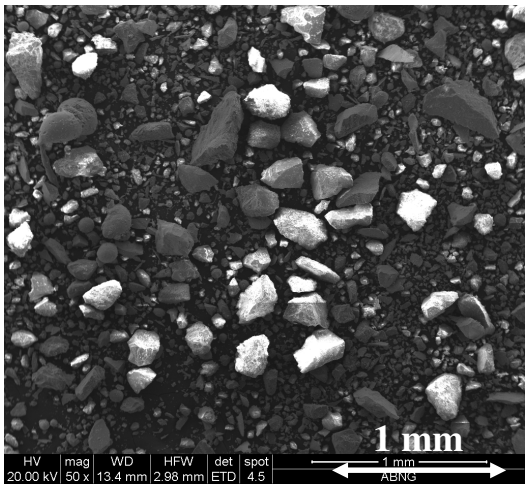

c)

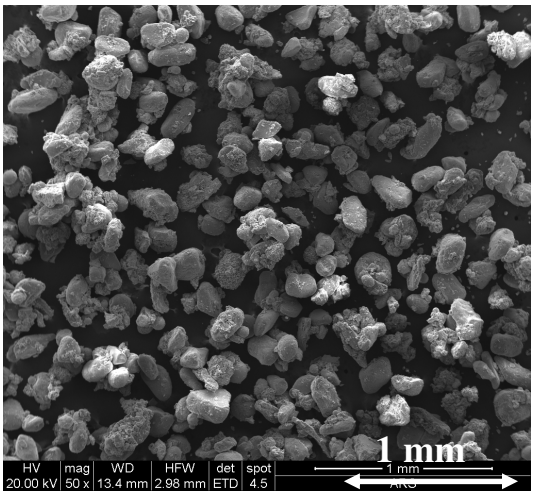

Figure 3.1 *SEM photographs of the starting materials: (a) Formulation A, 50x, (b) Formulation B, 50x and (c) Formulation C, 50x*

3.6 Experimental apparatus and procedures

Batch wet granulations were performed with a pilot plant low shear granulator. Its design is similar to the industrial horizontal pan mixer, which is commonly used for granulation of ceramics, clays and metals. The stainless steel mixer-granulator consists of a nominal volume of 55 L bowl. It was 52 cm in internal diameter and 28 cm in height. It is equipped with two agitators: a three-bladed impeller and a chopper. Both the impeller

blades and chopper rotate on eccentrically mounted vertical shaft. In addition the bowl rotate in the opposite direction.
The pilot plant is shown in Figure 3.2.

a) b)

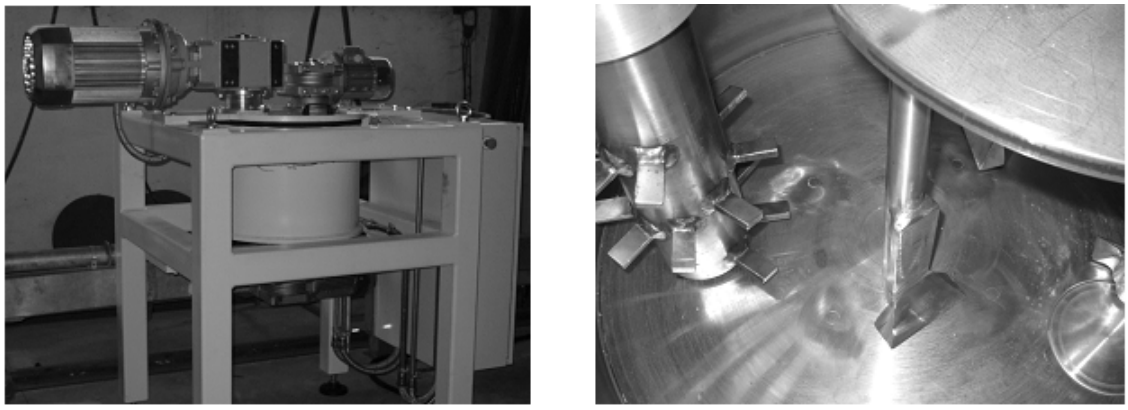

Figure 3.2 *Pilot Plant Low shear granulator: (a) view of 55 L bowl, (b) details of impeller blades (dx) and chopper (sx)*

Impeller speed can be varied from 30 to 60 rpm while chopper speed can be adjusted within the range of 160 – 320 rpm. The bowl can rotate up to 20 rpm.
To begin an experiment approximately 10 kg of feed formulation was charged into the vessel.
Granulation time was of about 7 min during which the powder bed was pre-homogenized by dry mixing for 2 min before a known amount of liquid binder was poured at a constant rate of 0.5 L/min directly onto the rotating powder mass. The start of pouring was also the starting time for the granulation experiments. During the pre-mixing stage impeller speed, chopper speed and bowl rotation were kept constant respectively at the rate of 30, 32, 7 rpm. After binder addition, impeller speed was increased to 40 rpm. These operating conditions were chosen as they gave a good mixing without generating excessive dust.
When the experiments were finished 20 – 50 gr samples were taken from the granulator in 9 different positions to assess particle size distribution, liquid content and granule friability as well. Powder samples were collected by using the thief probes which have been described and charcterized in Chapter 5. These samples of wet solid removed from the granulator were stored on plates, which were covered with plastic to prevent water evaporation. Then they were dried at 120 °C 90 minutes.

In Figure 3.3 a schematic view of sampling positions is given.

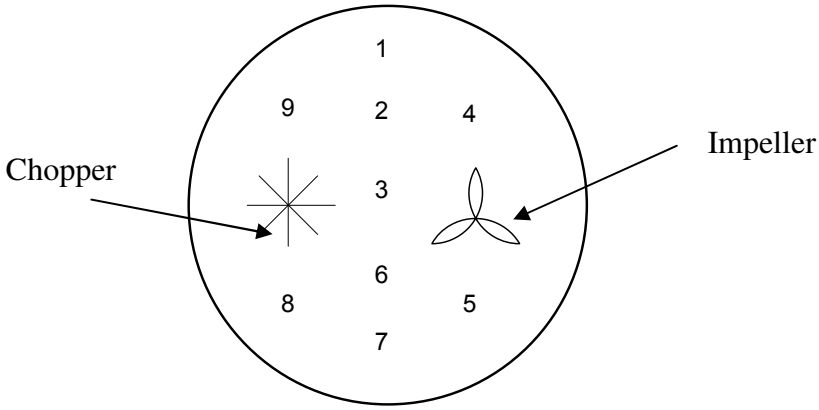

Figure 3.3 *Schematic view of sampling positions of wet granules*

3.7 Analysis of liquid dispersion

Binder content for water – bound granules were measured by mass difference before and after drying in oven at 120°C for 90 minutes. Water content was determined for all the 9 samples taken inside the vessel. This measure help to quantify binder distribution as the binder used are aqueous solutions of silicate. The degree of binder distribution affect the size distribution of the nucleated granules.

3.8 Analysis of granule size distribution

The granule size distribution was obtained by a sieve analysis of a sample of about 100 g. A series of 7 ASTM (American Society for Testing and Materials) standard sieves were used and vibrated for 10 minutes by a vibrator with amplitude of 0.7 mm. Seven different mesh sizes were used in this work: 45 µm, 100 µm, 160 µm, 200 µm, 300 µm, 400 µm and 500 µm. An electronic balance was used to weight the granules after sieving. The sieve analysis allows to determine the particle size distribution of granules and the weight mean diameter as well. This was calculated according to:

$$d_{pm} = \frac{\sum_i f_i d_{pi}}{\sum_i f_i}, \tag{3.2}$$

where f_i is the particle mass fraction of size interval i and d_{pi} is the mean diameter of size interval i. Kinetic results are expressed in terms of silicate mass percentage added to the sum of initial dry powder mass and silicate amount:

w_{solid} = Added Silicate Mass [kg] / (Initial Powder Mass [kg] + Added Silicate Mass [kg])

3.9 Analysis of granule friability

The granule strength has been characterized by batch grinding test experiments using a tumbling ball mill. About 40 gr sample of dried granules were charged into the mill of a capacity of 0.5 L.
Ceramic balls of 2 mm in diameter were used as the grinding medium. They occupied about the 40% of the mill volume. Powder samples were grinded at 25 rpm for 120 seconds.
The granules were then sieved. The following index was used to give a measurement of granule strength, i.e. the attrition resistance:

$$Friability = \frac{\left|d_{90} - d_{10}\right|_{post}}{\left|d_{90} - d_{10}\right|_{pre}} \tag{3.3}$$

It is defined as the ratio between the span of particle size distributions measured after and before the grinding test.

3.10 Results and discussion

A set of 30 experiments was performed to analyse the effect of formulation variables such as binder content and properties on the particle size distributions and the mechanical strength of the granules produced. The effect of operating conditions on final properties of agglomerates is also studied. In this work the process variables which were investigated are impeller rotational speed, chopper rotational speed and granulation time. The comparison criteria are the mean diameter of granules, the binder dispersion and granule friability. In this study all data on the granulation experiments are mean value of two experiments.

3.10.1 Effect of binder content on particle size

It is intuitively obvious that a critical amount of silicate in the binder solution is required before enough strong and sticky nuclei combine to form a granule. This critical value of binder is an important characteristic of the system and must be determined beforehand.
In this section this critical minimum amount of binder was determined for each powder-binder system.

The composition of binder solutions employed for the experimental trials discussed in this section are reported in Table 3.4

Table 3.4 *Composition of binder solutions carried out in granulation experiments*

Experiments	Binder Content	Powder
1	90 wt.% sodium silicate	Formulation A
2	85.7 wt.% sodium silicate	Formulation A
3	50 wt.% sodium silicate	Formulation A
4	28.6 wt.% sodium silicate	Formulation A
5	90 wt.% potassium silicate	Formulation B
6	85.7 wt.% potassium silicate	Formulation B
7	50 wt.% potassium silicate	Formulation B
8	28.6 wt.% potassium silicate	Formulation B
9	90 wt.% potassium silicate	Formulation C
10	85.7 wt.% potassium silicate	Formulation C
11	50 wt.% potassium silicate	Formulation C
12	28.6 wt.% potassium silicate	Formulation C

All the experiments were carried out using 10 kg of formulation and the amount of binder solution was kept constant at 0.5 kg. The operating conditions are listed in Table 3.5.

Table 3.5 *Operating conditions for granulation experiments described in this study*

	Pre-mixing (2 min)	Granulation (5 min)
Impeller speed (rpm)	30	40
Chopper speed (rpm)	32	32
Bowl speed (rpm)	7	9

Figure 3.4 shows the effect of silicate content (ω_{solid}) of particle size distributions of granule formed.

For each powder formulations we attempted in this study to determine the suitable amount of silicate addition by analysis of the particle size distributions and friability of the finale granules.

In Figure 3.4 we can observe that regardless of the nature of powder blend the fraction of fine particles with diameter less than 150 µm decreased with the increase of the amount of silicate in the binder aqueous solutions.

a)

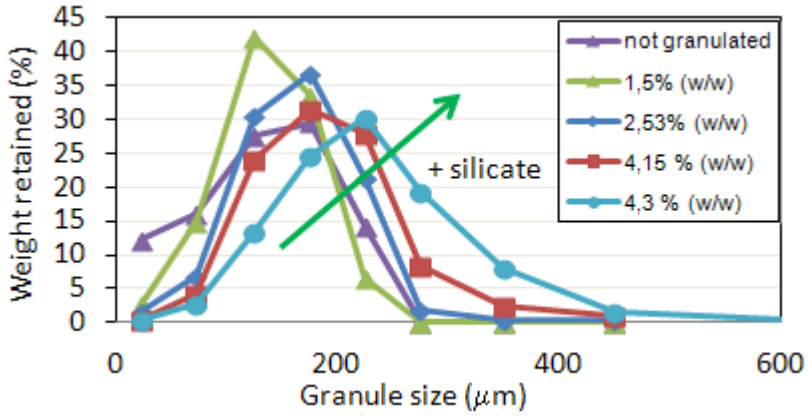

b)

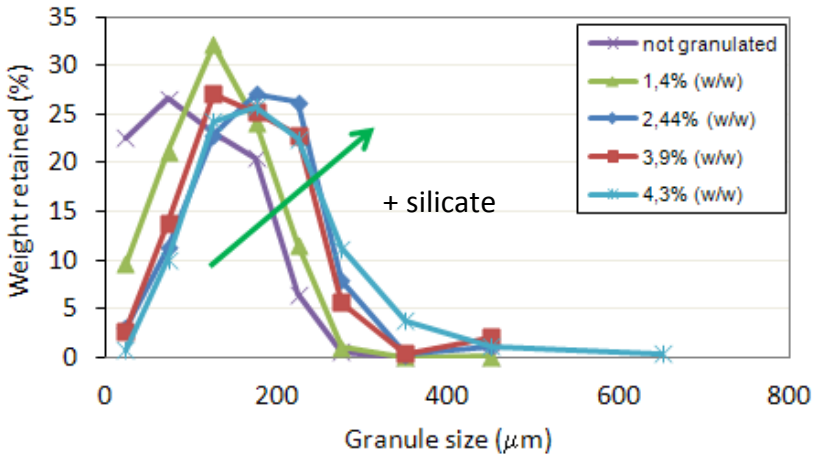

c)

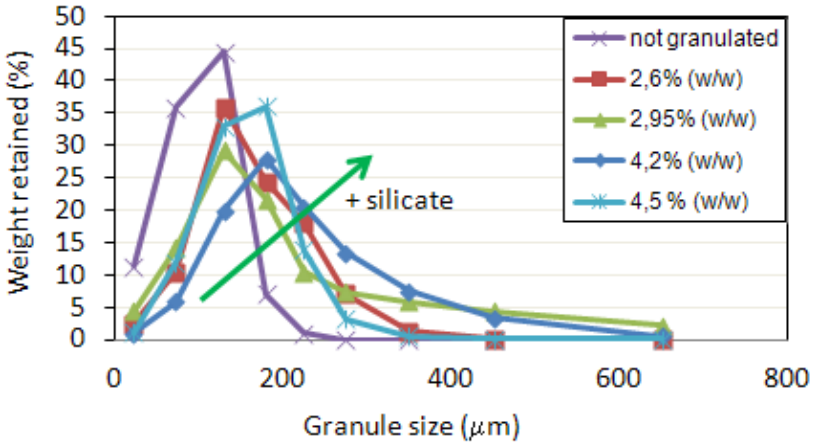

Figure 3.4 *PSDs of granules produced at different compositions of binder solutions for formulation A (a), formulation B (b) and formulation C (c)*

For all the experiments by increasing the silicate content particles easily formed liquid bridges and consequently coarser granules.

For the more concentrated binder solution (4.3 ÷ 4.5 wt.%) the fines fraction tends to zero. We can also see that formulation A was more sensitive to the silicate mass percentage as the means size grew relatively quickly compared to the other powder blends. In Figure 3.4 it is also shown the PSD of the feed powder formulation before adding liquid binder.

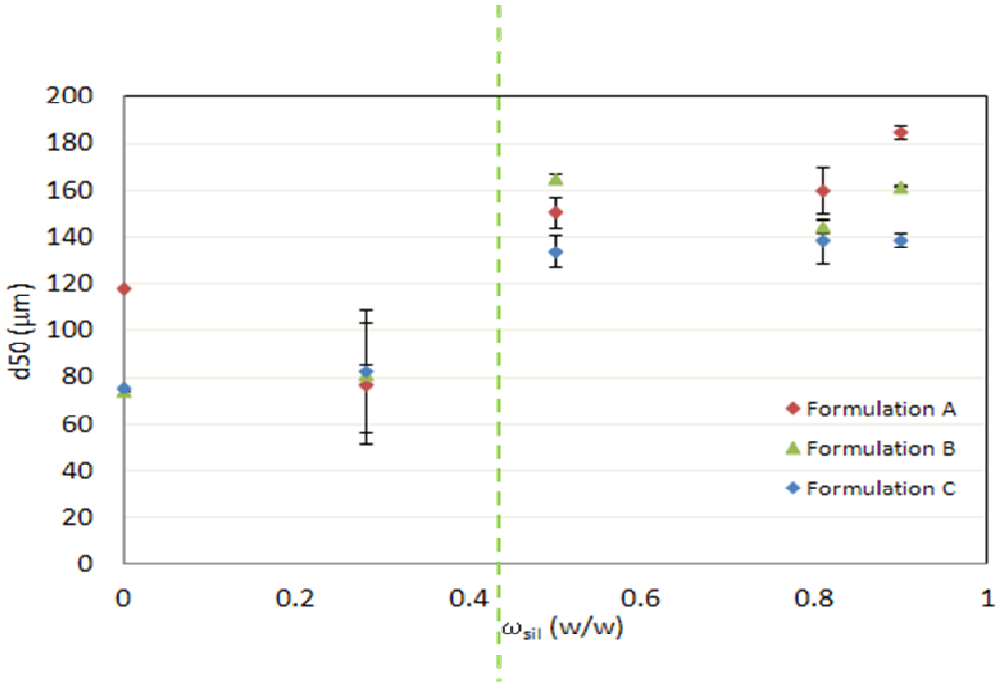

Figure 3.5 *Evolution of mean size of granules produced for the wet granulation runs with different amount of silicate*

Figure 3.5 shows the mean size diameter of granules products as a function of binder composition in terms of silicate content. The same trend has been found that for all the raw powders: there is a critical ratio of the amount of silicate beyond which the mean size increased abruptly from about 80 µm to 160 µm. Beyond the amount of silicate of about 0.4 the value of means size seems to remain constant. This finding can be explained if we consider that it exists a minimum amount of silicate (binder) required to start granule growth. A high silicate content caused increased granules deformation. During wetting stage different states of liquid bridges formation occur as the ratio of binder to powder increases and as the volume available for binder filling is reduced by granule consolidation: from the pendular to funicular and then to capillary state (Iveson *et al.*, 2001). For these powder blends the capillary state is probably yielded for the amount of silicate of about 0.4: for this critical silicate/powder ratio liquid binder is distributed over the surface of granules and particles growth was dominated by coalescence mechanism.

3.10.2 Effect of binder content on granule friability

Attrition of dried granule in the subsequent handling during the process leads to the generation of fine particles and this is a undesirable situation to be avoid for making the whole granulation process successful. Attrition resistance has been evaluated by batch crush strength tests. In Figure 3.6 the dry granule strength as a function of silicate content in binder solution is reported. We can note that regardless the formulations tested there is a critical value of silicate amount which results in weaker granules. For values of silicate amount less than 0.4 the dry granule strength increases just because the binder introduced is not enough to form solid bridge and create granules.

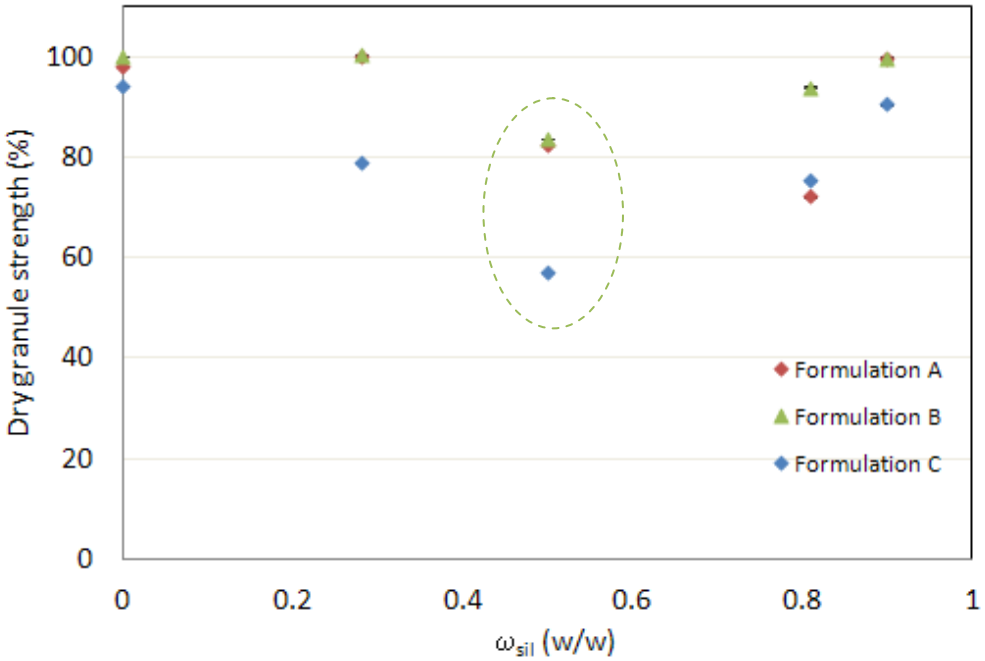

Figure 3.6. *Dry granule friability as a function of binder composition for all the three formulation studied*

In this case the size distribution of powder sample before and after the friability test are similar as there are no liquid bridge to break up and the index defined by (3.3) is close to 1.

3.10.3 Effect of particle size on granule friability

The influence of the primary particle size of formulation A, B and C on granule breakage for different amount of silicate in binders solution is shown in Figure 3.7.

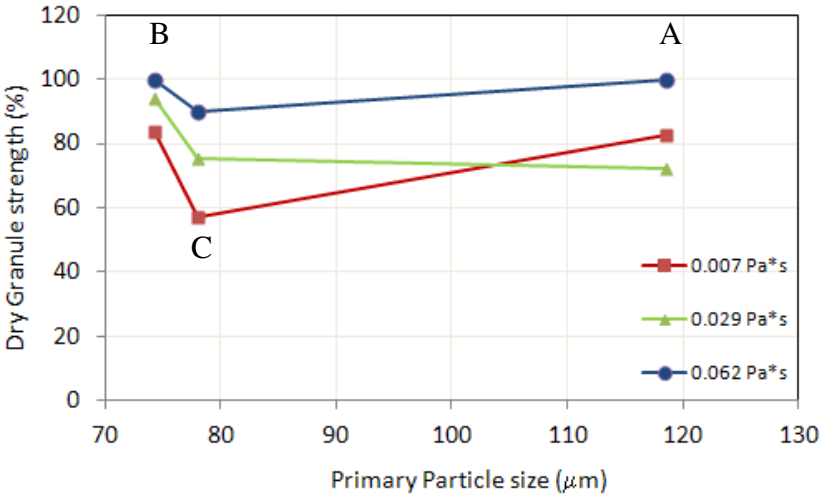

Figure 3.7 *Dry granule friability as a function of primary particle size*

We can observe that the breakage strength for formulation B and C show a similar behaviour: the greater the silicate content, the lower the dry granule friability. The binder viscosity is therefore an important factor for breakage to occur, because an increasing viscosity results in stronger solid bridge and consequently in less breakage. Moreover the formulation C was found to be the most sensitive to the grinding tests as its granule strength is lower than that of formulation A and C for all the binder used in granulation trials. In this analysis the formulation effect is not taken into account.

3.10.4 Effect of binder content on liquid dispersion

The degree of binder dispersion influence the quality of mixing between powder mass and binder fluid. Good binder distribution gives uniform wetting that means controlled nucleation. The degree of binder distribution is reflected in the particle size distribution of products. If all particles contain the same amount of binder their physical properties should be the same. If the binder is unevenly distributed some nuclei will be more saturated than others and growth will be preferential (Iveson *et al.*, 2001). Liquid distribution was measured by taking samples of material (about 50 g) from different positions within the bowl and by heating them at 120°C in order to remove the water contained in the binder solution by evaporation

Variation of water binder content with position within the vessel for three different powder blends as a function of solid content ω_s is given in Figure 3.8.

a)

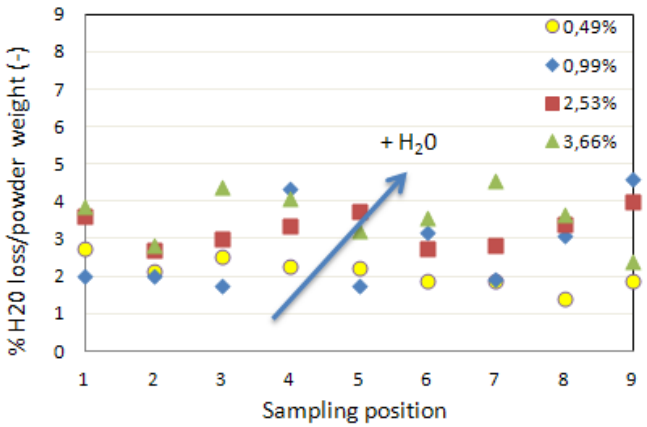

b)

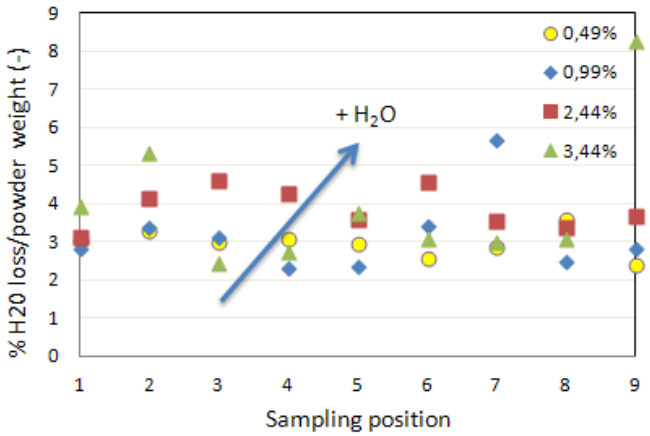

c)

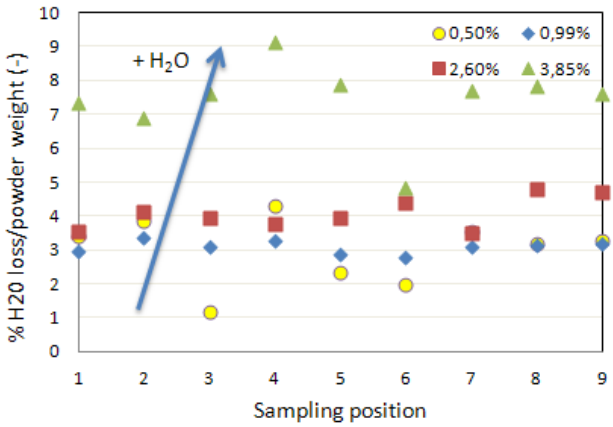

Figure 3.8 *Variation of water content with sampling position within the batch granulator for formulation A (a), formulation B (b) and formulation C*

In Figure 3.8 we can observe that water loss is clearly affected by binder composition. The observed experimental trend was expected: the greater the percentage of water in binder solution, the greater the water mass percentage evaporated in the oven.
Moreover we can see that formulation C has a greater ability to release water than formulation A and B. Figure 3.9 also shows the effect of binder dispersion on product size distribution for formulation C using the most diluted binder solutions.

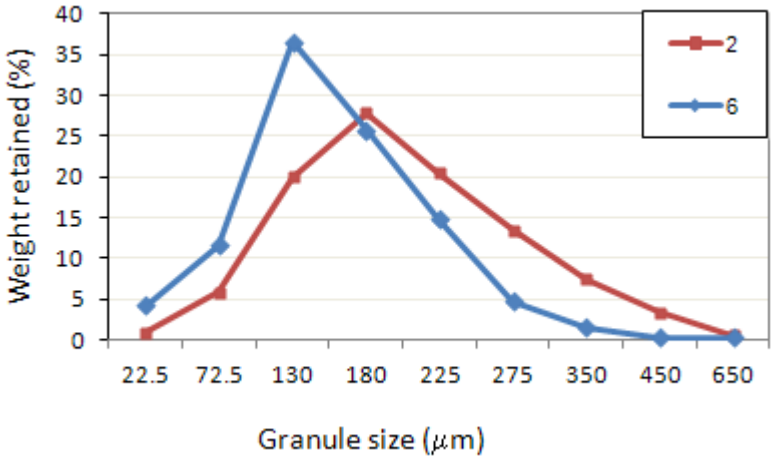

Figure 3.9 *Comparison of particles size distributions in two different sampling position*

As we can see in Figure 3.8c, powder samples in position 2 and 6 contain different amount of water and consequently different amount of silicate available to consolidate the granule growth. This is confirmed by different particle size distributions of granules produced: the grater the silicate amount in binder solutions, the greater mean particles size of product.

3.10.5 Effect of process variables

When liquid is added by pouring, the dispersion of liquid depend solely on mechanical mixing. Effective powder mixing is fundamental to binder distribution in the powder mass. In this study we varied the impeller speed from 22 to 56 rpm in order to find a relationship between operating conditions and granule properties. Operating conditions for this set of granulation experiments are given in Table 3.6.
The effect of the impeller speed is investigated for the binder composition which is carried out in the industrial process of welding rods, i.e 85.7 wt.% sodium or potassium silicate.

Granulation time, chopper and bowl speed are the same listed in Table 3.5.

Table 3.6 *Operating conditions for granulation experiments*

Experiments	Powder	Binder Content	Impeller speed (rpm)
13	Formulation A	85.7 wt.% sodium silicate	22
14	Formulation A	85.7 wt.% sodium silicate	40
15	Formulation A	85.7 wt.% sodium silicate	56
16	Formulation B	85.7 wt.% potassium silicate	22
17	Formulation B	85.7 wt.% potassium silicate	40
18	Formulation B	85.7 wt.% potassium silicate	56
19	Formulation C	85.7 wt.% potassium silicate	22
20	Formulation C	85.7 wt.% potassium silicate	40
21	Formulation C	85.7 wt.% potassium silicate	56

The dispersion of binder liquid as a function of impeller speed is reported in Figure 3.10.

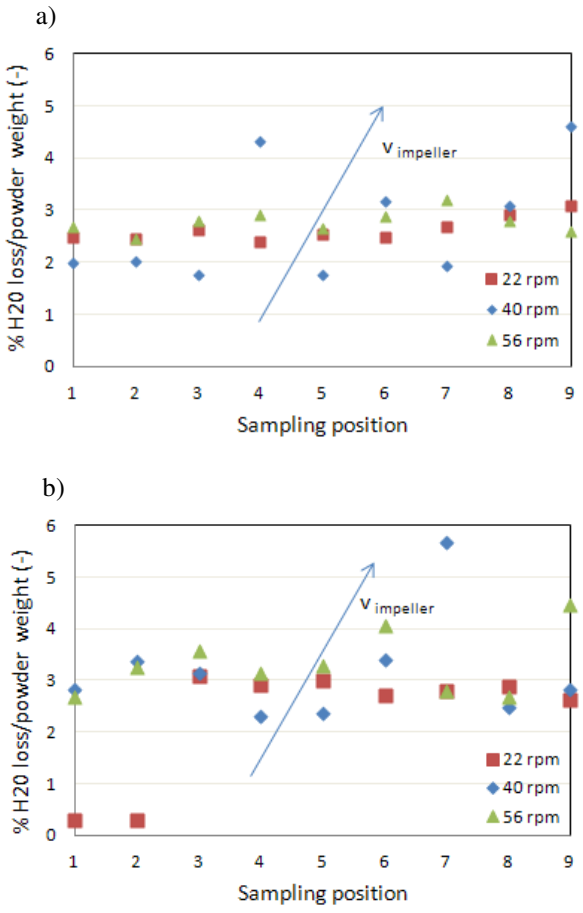

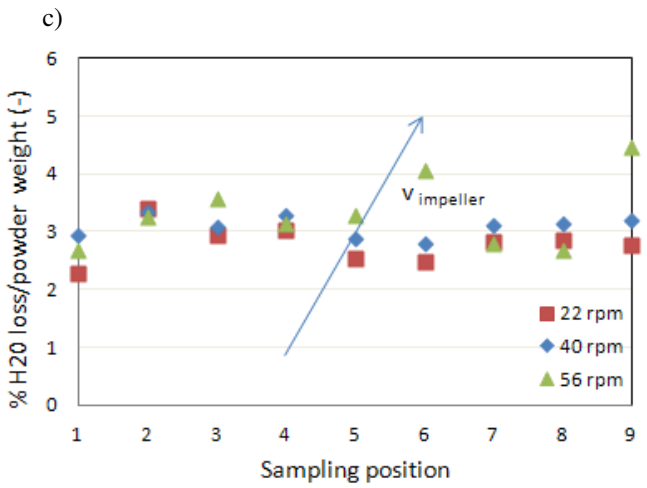

Figure 3.10 *Variation of water content with sampling position within the batch granulator for formulation A (a), formulation B (b) and formulation C (c) at different impeller speeds*

Unfortunately results are difficult to interpret. It was expected that an increase in impeller speed resulted in more effective binder dispersion. However there is a no clear trend. This can be explained if we consider that in these granulation experiments chopper is kept on. To investigate the effect of impeller speed on the granule properties a set of experiments with chopper off is carried out and it is discussed in the following paragraph. Nonetheless only for formulation B the higher impeller speed, the lower the standard deviation of binder distribution. With regard to the effect of impeller speed on granule size Figure 3.11 shows the particle size distribution of formulation B as a function of powder mixing.

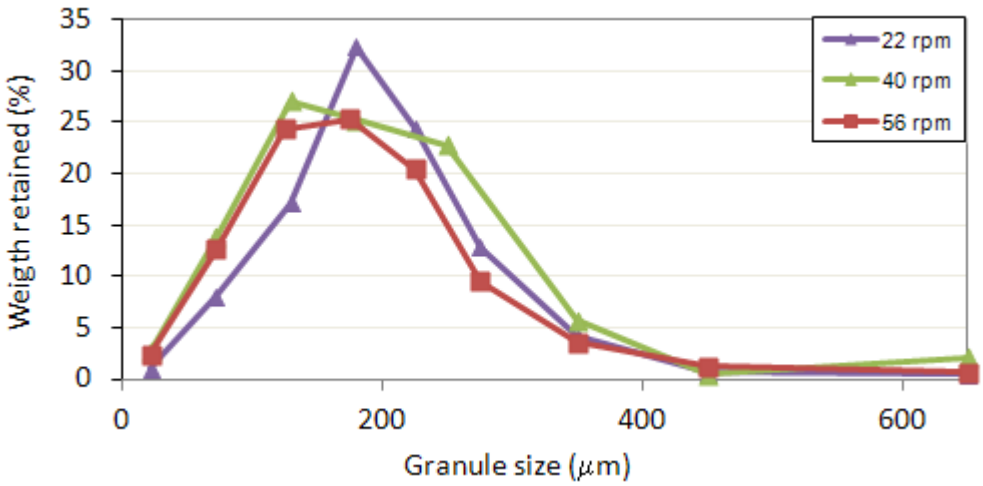

Figure 3.11 *PSDs of formulation B at different impeller speeds: 22, 40 and 56 rpm*

We can observe that increasing impeller speed, breakage may occurs and particle size distributions shift towards lower size. The influence of chopper speed was studied by the

granulation of formulation C with 85.7 wt.% potassium silicate. In the industrial process chopper is kept off during the whole granulation.

We varied the chopper speed from 32 to 316 rpm, impeller speed was fixed at 40 rpm (see Table 3.7). The chopper rotational speed seems to play a larger role than the impeller speed in the binder dispersion.

Table 3.7 *Operating conditions for granulation experiments*

Experiments	Powder	Binder Content	Impeller speed (rpm)	Chopper speed (rpm)
22	Formulation C	85.7 wt.% potassium silicate	40	32
23	Formulation C	85.7 wt.% potassium silicate	40	56
24	Formulation C	85.7 wt.% potassium silicate	40	158
25	Formulation C	85.7 wt.% potassium silicate	40	316

Figure 3.12 presents the standard deviation of binder distributions versus chopper speeds. Increasing the chopper speed leads to a more uniform liquid distribution which impacts controlled nucleation.

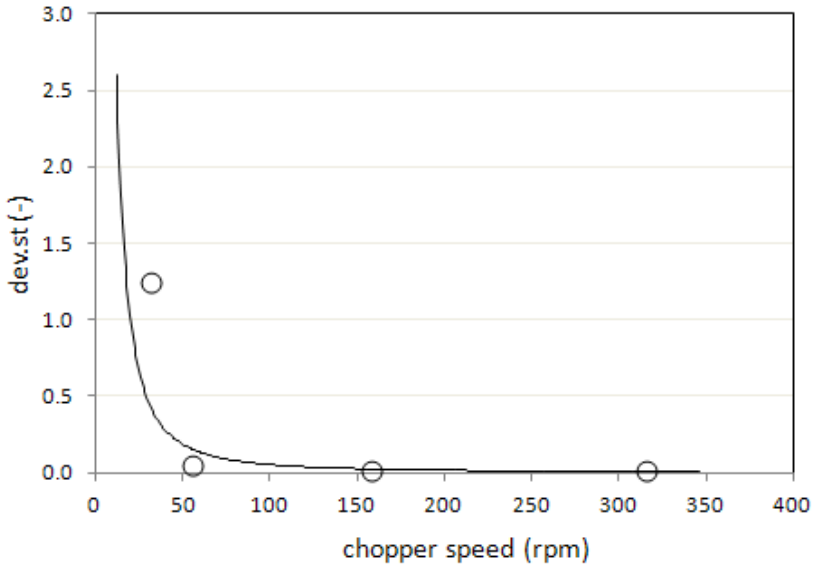

Figure 3.12 *Standard deviation of liquid distribution versus chopper speeds*

The increase of the shear induces a good mixing between liquid binder by reducing the localised over-wetting and powder and leads to granule compaction and densification as we can see in Figure 3.13.

On the contrary if chopper is not used in order to have a good dispersion of binder, high values of impeller speed are required as shown in Figure 3.14. We can conclude that in a low-shear process in order to have an effective mixing chopper should be on.

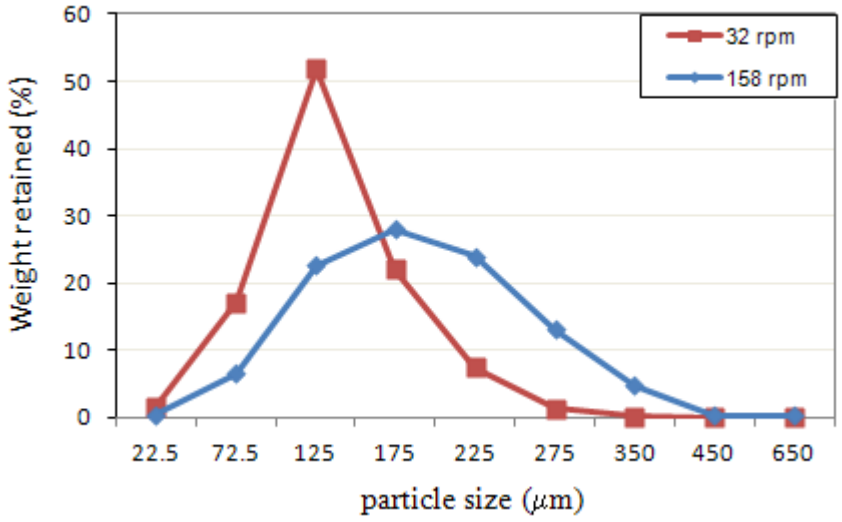

The effect of granulation time is investigated for the formulation C/85.7 wt.% potassium silicate system varying impeller speed from 22 to 60 rpm.

Figure 3.13 *PSDs of formulation C for different chopper speeds*

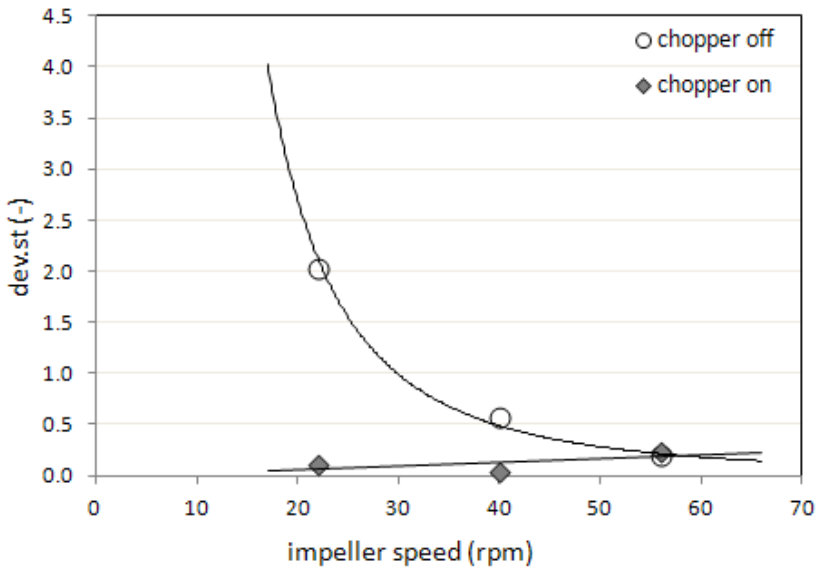

Figure 3.14 *Standard deviation of liquid distribution versus impeller speed with and without chopper*

Figure 3.15 represents the particle size distributions by halving granulation time for different impeller speeds. Chopper speed was fixed at 32 rpm. The observed experimental trends are difficult to interpret. By increasing granulation time, the proportion of agglomerates increases only at 40 rpm.

In the case of 22 rpm and 56 rpm instead higher granulation time increases the fine particle mass percentage.

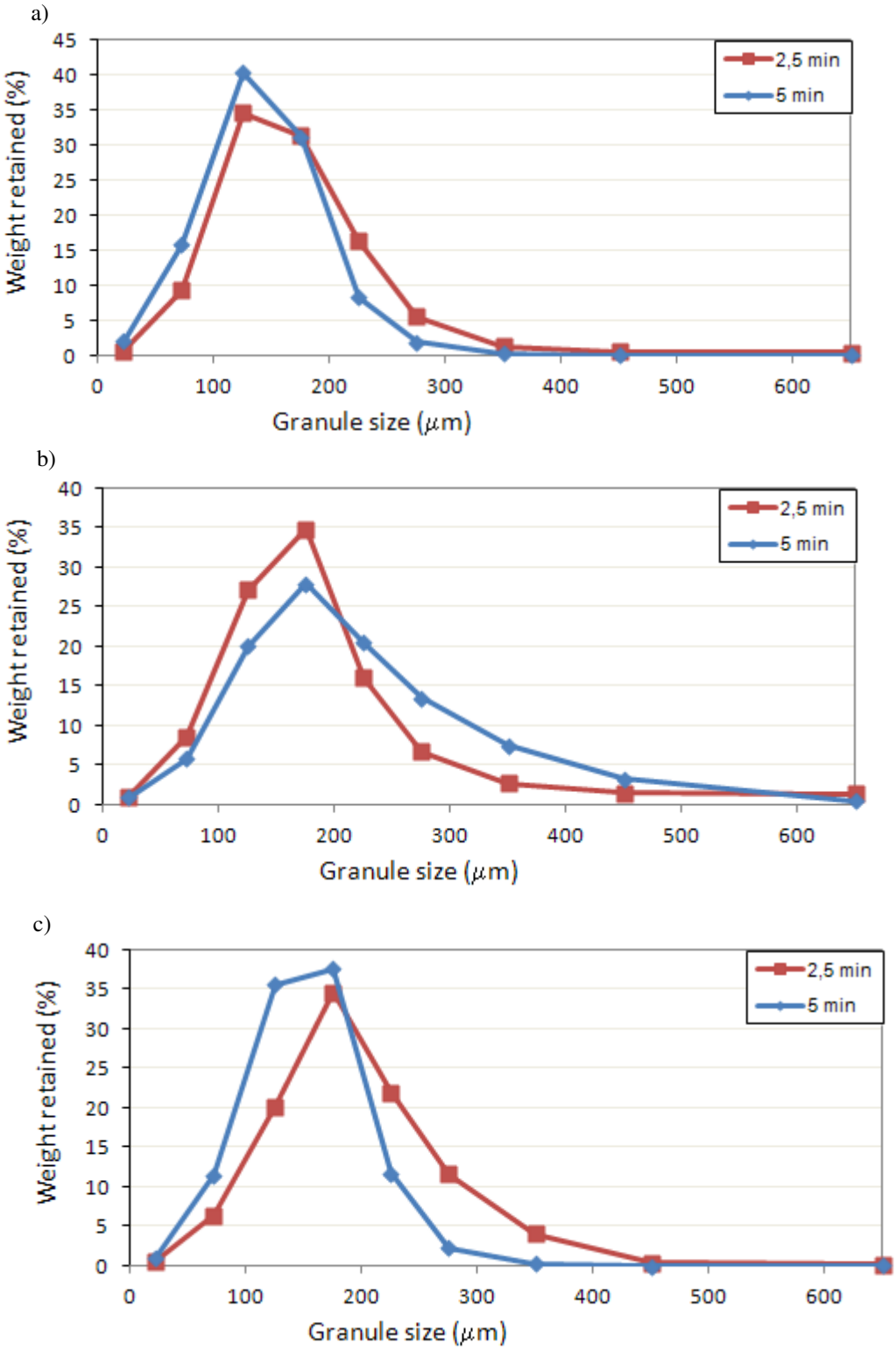

Figure 3.15 *PSDs of formulation C by halving granulation time at 22 (a), 40 and (b) and 56 rpm (c)*

3.10.6 Granule growth – Capillary criterion

During the wet agglomeration, wetting, mixing and coalescence occur simultaneously. Ennis *et al*. (1991) found that the agglomeration mechanisms are strongly affected by the competition between the capillary and viscous forces. They defined a viscous capillary number to express the importance of the viscous force in comparison with the capillary one:

$$Ca_{vis} = \frac{\mu_L U}{\gamma_L}, \tag{3.4}$$

where U is the speed of the particle (in mixing process $U = \pi ND$, where N is the impeller speed and D the impeller diameter), γ_l and μ_l are the binder surface tension and viscosity respectively. They found that for $Ca_{vis} < 1$ the energy dissipation due to the viscosity can be neglected compared to the capillary force. If $Ca_{vis} > 1$ the cohesion of dynamic liquid bridge is greater than that of static liquid bridge. In order to stress the importance of wettability of binder on particles in the agglomeration process, Benali et *al*. (2008) defined a modified capillary number where the binder surface tension is replaced by the work of adhesion, W_a:

$$Ca^* = \frac{\mu_l U}{\gamma_l (1+\cos\theta)}. \tag{3.5}$$

In this experimental work the influence of physicochemical properties was investigated using the modified capillary number.

Table 3.8 *Capillary viscous number, Stokes viscous number and Stokes deformation number values for different binder/powder blends couples described in this study*

Experiments	Powder	Binder solution	Ca (-)	St_{vis} (-)	St_{def} (-)
1	Formulation A	90 wt.% sodium silicate	8.422	1.291	0.012
2	Formulation A	85.7 wt.% sodium silicate	3.267	3.249	0.031
3	Formulation A	50 wt.% sodium silicate	0.894	6.980	0.106
4	Formulation A	28.6 wt.% sodium silicate	0.461	16.786	0.159
5	Formulation B	90 wt.% potassium silicate	11.763	0.494	0.005
6	Formulation B	85.7 wt.% potassium silicate	4.644	1.210	0.013
7	Formulation B	50 wt.% potassium silicate	1.041	5.015	0.055
8	Formulation B	28.6 wt.% potassium silicate	0.690	7.020	0.077
9	Formulation C	90 wt.% potassium silicate	7.025	0.618	0.006
10	Formulation C	85.7 wt.% potassium silicate	2.865	1.512	0.015
11	Formulation C	50 wt.% potassium silicate	0.954	6.264	0.064
12	Formulation C	28.6 wt.% potassium silicate	0.341	8.770	0.089

The values of modified capillary viscous number determined for different couple binder/powder blends are given in Table 3.8.

As we can see in Table 3.8 varying binder solutions in granulation experiments a wide range of Capillarity viscous number is obtained (for instance between 0.461 and 8.422 for formulation A). This analysis is an attempt to investigate the granule growth by using the capillary criterion. If we compare the evolution of the median size diameter for the different binder/powder blends system with the corresponding values of the capillary number calculated we can observe in Figure 3.16 that the granule growth is not affected by an increase of silicate amount in binder solution (i.e an increase of solution viscosity) for low values of Capillary number (Ca < 1). This result shows that granule growth takes place just when the silicate content is sufficient to create a minimum number of liquid bridges to ensure a non elastic collision between particles.

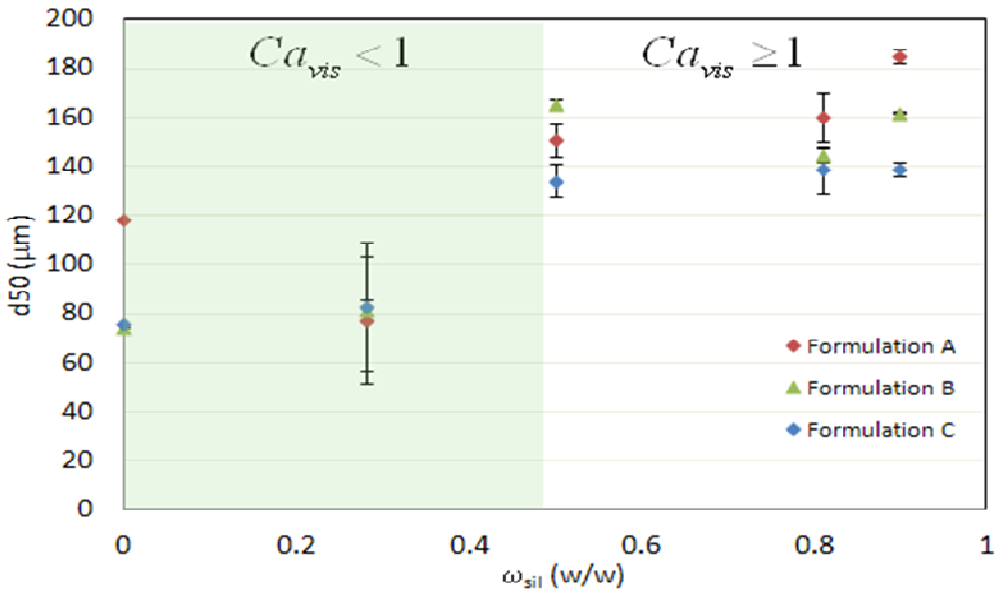

Figure 3.16 *Granule growth according to modified Capillary viscous number*

Granule growth occurs when viscous forces become dominant (Ca > 1). In this latter case, a sticky binder layer at the powder surface can be formed and agglomeration is controlled by viscous dissipation forces. In the following paragraph an alternative nucleation/growth criterion is investigated by using the Stokes viscous number which takes into account both the binder property (liquid viscosity) and the process parameter (collision velocity).

3.10.7 Granule growth – Stokes criterion for viscous dissipation

Growth processes are typically modelled using an energy balance that relates the applied force to a material property. Among the large number of theoretical models available in

the literature to predict whether or not two colliding particles will coalesce, the Stokes criterion is expressed in terms of a viscous Stoke number which is defined as the ratio between the collision energy and the energy of viscous dissipation:

$$St_{vis} = \frac{8\rho r v_C}{9\mu}, \tag{3.6}$$

where r is the harmonic mean granule radius of the two spheres ($1/r = 1/r_1 + 1/r_2$), v_c is the collision velocity, ρ and μ are the particle density and binder viscosity respectively. The collision velocity is assumed to be the 10% of the tip impeller speed (Liu *et al.*, 2009).
Successful coalescence is assumed to occur if the kinetic energy of impact is entirely dissipated by viscous dissipation in the liquid bridge.
The model predicts that collisions will result in coalescence when the viscous Stokes number (St_{vis}) is less than a critical viscous Stokes number (St^*_{vis}) which is defined by the following equation:

$$St^*_{vis} = \left(1 + \frac{1}{e}\right) \ln\left(\frac{h}{h_a}\right), \tag{3.7}$$

in which e is the coefficient of restitution, h is the thickness of the liquid surface layer and h_a is the characteristic height of surface asperities. For $St > St^*_{vis}$, viscous dissipation is insufficient and rebound occurs. The parameters for determining the critical Stokes number are difficult to measure. Literature data suggest for mineral powder a coefficient of restitution of 0.8 and a value of the ratio h/h_a of 20 (Iveson *et al.*, 2001). For these values the critical viscous Stokes number (St^*_{vis}) was about 7.
In an attempt to explain when two granules which collide in the granulator coalesce, the Stokes deformation numbers were estimated for each granulation experiment and they were compared to the value of critical Stokes viscous number. The Stokes deformation numbers calculated are given in Table 3.8.
Regardless of the formulations studied, the experimental trend of the mean size diameter shows that coalescence and therefore granule growth occur when $St_{vis} < 7$ ($= St^*_{vis}$). We found that if $St_{vis} > 7$ viscous dissipation in the bridge is not sufficient to absorb the elastic rebound energy of the collision, on the contrary for $St_{vis} \leq 7$ the initial kinetic energy is dissipated through viscous friction in the liquid layer during the collision and granules stick together.

Both the Capillary and the Stokes viscous criterion for granule growth suggest that agglomeration of mineral and metallic powders is promoted except when the most diluite binder solution is used (28.6 wt.% sodium or potassium silicate).

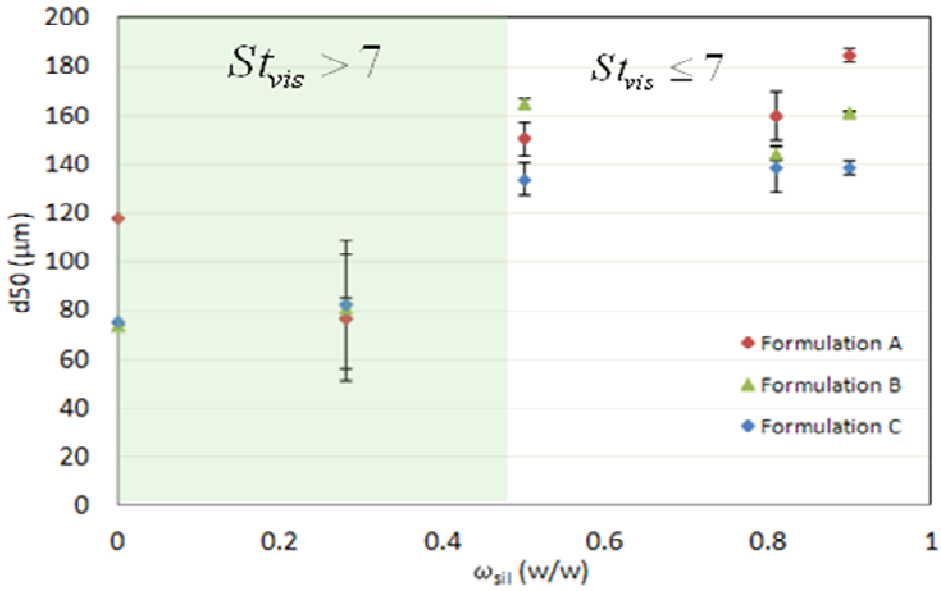

Figure 3.17 *Granule growth according to Stokes viscous number*

For this type of binder the kinetic energy in most or all the collisions exceeds viscous dissipation in the thin liquid layer formed and there is no coalesce.

3.10.8 Stokes deformation number and growth limitation

In the previous analysis we found that agglomerate growth is promoted by a Capillary viscous number higher than 1 and a Stokes viscous number lower than 7. Except for experiments number 4, 8 and 12, the range of viscous Capillary and Stokes number related to the experimental granulation trials leads to granule growth. Nonetheless the evolution of the mean granule diameter versus the silicate composition shows that the increase of granule particle size is moderate for all the three formulations studied. The mean size of granules have just doubled in value in comparison to the particle size of feed materials (see Figure 3.5).

This observed experimental trend may be explained by considering the theory and modelling available to predict conditions for wet breakage.

The granule breakage behaviour is a key parameter in the understanding of the granule growth mechanism. Several studies used the model proposed by Rumpf (1958) to calculate the tensile strength of a granule and predict granule breakage.

According to this model the granule strength is given by (3.8):

$$\sigma = \frac{9}{8}\frac{(1-\varepsilon)}{\varepsilon}\frac{F_{bond}}{d_{32}^2}, \tag{3.8}$$

in which ε is the granule porosity, F_{bond} is the bonding force between particle and d_{32} is the surface mean diameter of the primary particle size. the bonding forces include van der Walls, electrostatic or liquid bridge forces. In wet granulation the most important binding forces are the liquid bridges between particles which can generate both capillary and viscous forces, i.e static and dynamic, respectively. In order to stress the effect of viscous forces of liquid bridge Van den Dried and Vromans (2002) proposed a modified model to predict breakage behaviour of granules after impact under dynamic conditions.
The granules strength is linked to the viscous force of a liquid bridge instead of static one with the following equation:

$$\sigma = \frac{9}{8}\frac{(1-\varepsilon)^2}{\varepsilon^2}\frac{9\pi\mu v_P}{16 d_{32}^2}, \tag{3.9}$$

where μ is the liquid binder viscosity and v_p is the relative velocity of moving particles inside the granulator after the impact. Because it is difficult to determine this velocity, it is assumed that this velocity equals the tip speed. When the granule strength exceeds the impact forces granules will not break.
Another approach to predict the granules breakage is to calculate the Stokes deformation number, St_{def}, which compare the external applied kinetic energy with the energy required for deformation of the granule (Tardos *et al*., 1997; Iveson and Litster, 1998):

$$St_{def} = \frac{\rho_g v_C^2}{2\sigma}, \tag{3.10}$$

where v_c is the representative collision velocity in the granulator and it is assumed to be 12% of the impeller tip speed and ρ_g and σ are the granule density and dynamic yield stress, respectively. Therefore the Stokes number takes into account both the process agitation intensity and the granule mechanical properties.
According to Tardos *et al*., (1997), the theory to predict conditions for breakage leads to a Stokes deformation number criteria:

$$St_{def} > St_{def}^{*}, \tag{3.11}$$

where St^*_{def} is the critical value of Stokes number that must be exceeded for breakage to occur. The boundary between breakage behaviour and no breakage behaviour (i.e. steady growth - crumb regime boundary) was experimentally established by Tardos *et al*. (1997) and resulted to be St_{def} ~ 0.2. Iveson *et al*. (2001) found that this boundary occurred at St_{def} ~ 0.04. The boundary between steady and induction growth occurred at St_{def} between 0.001 and 0.003. Figure 3.18 shows the Stokes deformation number as a function of the maximum pore saturation which is defined as:

$$S_{\max} = \frac{w\rho_S(1-\varepsilon_{\min})}{\rho_l \varepsilon_{\min}}, \tag{3.12}$$

where w is the ratio between liquid and solid masses, ρ_s and ρ_l are solid particles and liquid density, respectively, ε_{min} is minimum porosity for the particular set of operating conditions.

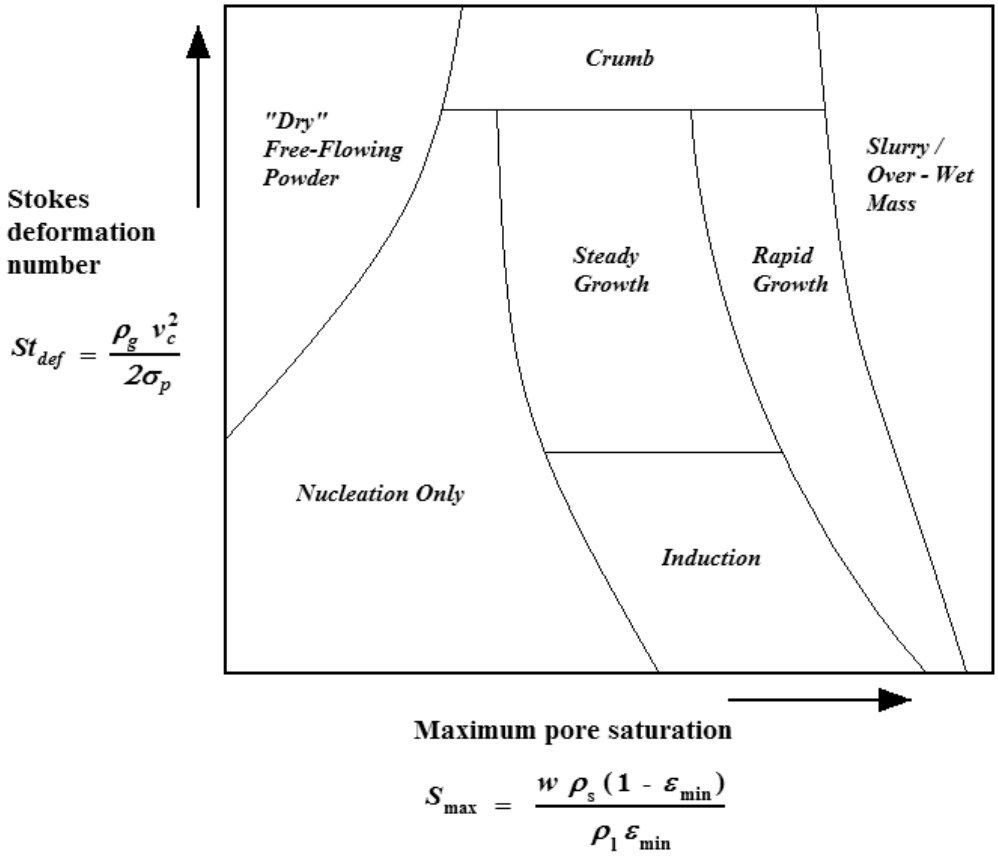

Figure 3.18 *Granule growth regime map (Iveson et al., 2001)*

Maximum granule pore saturation can be used as a measurement of liquid content (Iveson *et al*., 2001; Liu *et al*., 2009).

The Stokes deformation number was therefore estimated for each granulation experiment in Table 3.8. This analysis aims at plotting the granulation system conditions on the growth regime map, in order to identify the state related to granulation experiments with different type of binders. In order to measure the pore saturation, for sake of simplicity ε_{min} is assumed to be the average granule porosity which is determined by the following equation:

$$\varepsilon = 1 - \frac{\rho_b}{\rho_S}, \tag{3.13}$$

in which ρ_b is the bulk density.

The conditions related to the three granulation systems varying the binder compositions are presented in the growth map in Figure 3.19. The comparison in Figure 3.19 can be considered as a first qualitative estimation since some approximations are involved in the calculation of Stokes deformation number and pore saturation. Nonetheless a considerable difference can be noted between conditions related to granulation with the most concentrated binder solutions (i.e. 85.7 wt.% and 90 wt.% potassium or sodium silicate). Regardless the powder blends studied, for these binder solutions the Stokes deformation number (St_{def}) is lower than the critical value of 0.04 then during collisions granules remain intact and granule breakage will not occur. If St_{def} is greater than 0.04 crumb behaviour occur as the formulation/binder system are too weak to form permanent granules.

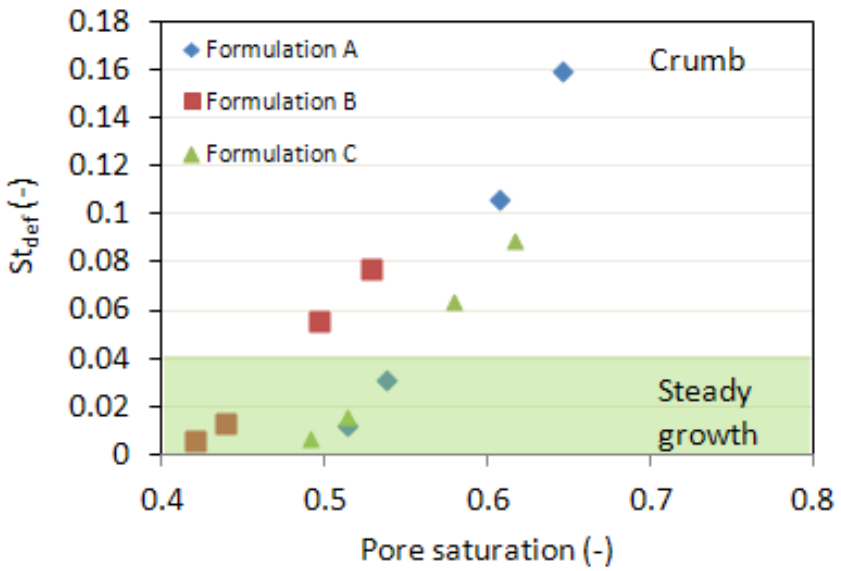

Figure 3.19 *Growth regime map with points related to the three different formulations varying liquid binders*

In Figure 3.19 we can also observe that increasing the pore saturation the growth regime shifts from steady growth to crumb behaviour. This experimental trend is not expected

since the granule strength increases with the increase of pore saturation (Rumpf, 1962). In an attempt to explain the previously discussed results the different states of saturation of liquid-bond granules should be considered. In Figure 3.20 the static yield strength of wet agglomerates versus pore saturation is proposed. We can see that granules can exist in a number of different states of liquid saturation. In the pendular state particles are held together by single bridges at their contact points. In the funicular state partially filling occurs. The capillary state occurs when a granule is nearly complete saturated: all the voids are filled with binder. This state is followed by droplet formation and loss of static strength. In the granulation experiments the calculated pore saturation shifts from funicular to capillary state as the silicate content in binder solution decreases (S = 0.4 ÷ 0.65). Therefore this approach confirms that static strength of granules formed is not high enough to prevent crumb behaviour but it does not explain why increasing granules pore saturation the Stokes deformation number increases.

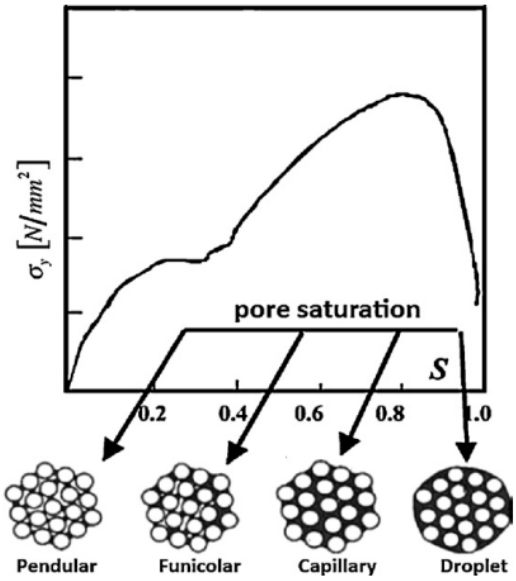

Figure 3.20 *Static yield strength of granules versus pore saturation (Rumpf, 1962)*

Figure 3.21 shows the calculated Stokes deformation numbers as a function of the silicate composition of binder solution. It is clear that an increase in the silicate amount (i.e an increase in binder viscosity) results in stronger granules and a decreasing Stokes deformation numbers.

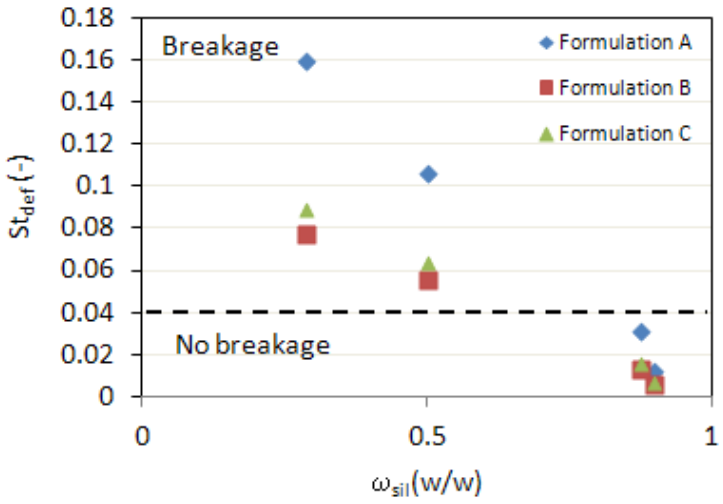

Figure 3.21 *Relation between the Stokes deformation numbers and the amount of silicate in binder solutions*

At a certain value of viscosity the critical Stokes number is reached and a shift in breakage behaviour occurs.

3.11 Conclusions

A study of the agglomeration behaviour of mineral and metallic blends is reported. The effects of both the binder physicochemical properties and the operating conditions have been investigated. Different binder/powder formulations systems were studied and agglomeration experiments were carried out in a low shear pilot plant.

The experimental results point out that concerning the physical properties of aqueous binder solutions the silicate concentrations have a large influence on the granule growth and breakage. Regardless the powder formulation tested, the fraction of fine particles with diameter less than 150 μm decreases with the increase of the amount of silicate in the binder aqueous solutions. Moreover for values of silicate amount greater than 0.4 (w/w) the dry granule strength increases as the silicate introduced is enough to form solid bridge and create granules.

Concerning the process parameters the impeller rotational speed has no significant effect on the binder dispersion when chopper is on. From a granule growth standpoint we observed that the increase of impeller speed leads to a reduction of the mean particle size

When chopper is kept off, to assure an effective mixing of liquid binder high values of impeller speed are required.

The use of the capillary viscous number allowed us to define the boundaries for which granule growth occurs. For a capillary number, *Ca,* greater than 1 growth is controlled by viscous dissipation force. The condition of coalescence between granules was investigated by evaluating the values of Stokes viscous number, $St_{,vis}$. It was found that

for St_{vis}> 7 viscous dissipation in the bridge is not sufficient to absorb the elastic rebound energy of the collision, while for $St_{vis} \leq 7$ the initial kinetic energy is dissipated through viscous friction in the liquid layer during the collision and granule growth occurs. Finally the moderate growth of the granules (the size of the granules is roughly doubled with respect to the largest primary particles during the agglomeration process) was explained in terms of St_{def} number and granule saturation S through the use of granule growth regime maps.

3.12 References

Benali, M., Gerbaud, V., Hemati, M., 2008. Effect of operating conditions and physico-chemical properties on the wet granulation kinetics in high shear mixer, Powder Technology 190, pp. 160-169.

Cheng, H.J., Hsiau, S.S., 2010. The study of granular agglomeration mechanism, Powder Technology 199, pp. 272-283.

Ennis, B.J., Tardos, G., Pfeffer, P., 1991. A microlevel-based characterization of granulation phenomena. Powder Technology 65, pp. 257-272.

Ennis, B.J., Li, J., Tardos, G., Pfeffer, P., 1990. The influence of viscosity on strength o fan axially strained pendular liquid bridge, Chemical Engineering Science 45, pp. 3081-3088.

Ennis, B.J., Litster, J.D., 1997. Particles size enlargement, in: R. Perry, D. Green (Eds.), Perry's Chemical Engineers Handbook, 7th edn., McGraw-Hill, New York.

Ennis, B.J., 2005. Theory of granulation: an engineering perspective, in: D.M. Parikh (Eds.), Handbook of Pharmaceutical Granulation Technology, 2th edn, Taylor and Francis Group, New York.

Hapgood, K.P., Khanmohammadi, B., 2009. Granulation of hydrophobic powders, Powder Technology 189, pp. 253-262.

Iveson, S.M., Litster, J.D., Ennis, B.J., 1996. Fundamental studies of granule consolidation Part 1: Effect of binder content and binder viscosity, Powder Technology 88, pp. 15-20.

Iveson, S.M., Litster, J.D., Ennis, B.J., 1998. Fundamental studies of granule consolidation Part 2: Quantifying the effects of particle and binder properties, Powder Technology 99, pp. 243-250.

Iveson, S.M., Litster, J.D., Hapgood, K., Ennis, B.J.,2001. Nucleation, growth and breakage phenomena in agitated wet granulation processes: a review, Powder Technology 117, pp. 3-39.

Johansen, A., Schaefer, T., 2001. Effects of physical properties of powder particles on binder liquid requirement and agglomeration growth mechanisms in a high shear mixer, European Journal of Pharmaceutical Sciences 14, pp.135-147.

Knight, P.C., Instone, T., Pearson, J.M.K., Hounslow, M.J., 1998. An investigation into kinetics of liquid distribution and growth in high shear mixer agglomeration, Powder Technology 97, pp. 247-258.

Knight, P.C., 2004. Challenges in granulation technology, Powder Technology 140, pp. 156-162.

Kenningley, S.T., Knight, P.C., Marson, A.D., 1997. An investigation into the effects of binder viscosity on agglomeration behaviour, Powder Technology 91, pp. 95-103.

Litster, J.D., Ennis, B.J., 2004. The science and engineering of granulation process, Kluwer academic publishers, Dordrecht, The Netherlands.

Liu, L.X., Smith, R., Litster, J.D., 2009. Wet granule breakage in a breakage only high-shear mixer: Effect of formulation properties on breakage behaviour, Powder Technology 189, pp. 158-164.

Parikh, D.M., 2005. Handbook of pharmaceutical granulation technology, 2th edn., Taylor and Francis Informa Publications, pp. 191–228.

Pietsch, W., 1991. Size enlargement by agglomeration. Wiley; Aarau; Salle and Sauerländer, Chichester.

Rajniak, P., Mancinelli, C., Chern, R.T., Stepanek, F., Farber, L., Hill, B.T., 2007. Experimental study of wet granulation in fluidized bed: Impact of the binder properties on the granule morphology, International Journal of Pharmaceutics 334, pp. 92-102.

Rumpf, H., 1962. The strength of granules and agglomerates, in: Agglomeration, W.A. Knepper, ed. Interscience, New York, pp. 379-414.

Susana, L., Cavinato, M., Franceschinis, E., Realdon, N., Canu, P., Santomaso, A.C., On the characterization of powder wettability by drop penetration observations, Presented in 6th Word Congress on Particle Technology i.e. WCPT6 2010, Article 0116, Nuremberg (Germany), 26-29 April 2010.

Tardos, G.I., Khan, I.M., Mort, P.R., 1997. Critical parameters and limiting conditions in binder granulation of fine powders, Powder Technology 94, pp. 245-258.

Van den Dries, K., Vromans, H., 2002. Relationship between inhomogeneity phenomena and granule growth mechanisms in high shear mixer, International Journal of Pharmaceutics 247, pp. 167-177.

Van den Dries, K., Vromans, H., 2009. Quantitative proof of liquid penetration-involved granule formation in a high shear mixer, Powder Technology 189, pp. 165-171.

Waldie, B., 1991. Growth mechanism and the dependence of granule size on drop size in fluidized-bed granulation. Chemical Engineering Science 46, pp. 2781-2785.

Yang, W.L., Hsiau, S.S., 2006. The effect of liquid viscosity on sheared granular flows, Chemical Engineering Science 61, pp. 6085 – 6095.

Chapter 4

Discrete Element Modelling of Seeded Granulation in high shear granulator

4.1 Summary

A particular type of agglomeration called seeded granulation is simulated by the Discrete Element Method (DEM) inside a 5 litre high shear granulator. Different impeller rotational speeds were considered: 150, 200, 287 and 345 rpm. It has been observed that the seeded granules form by a continuous reduction and growth in size during the granulation process. Quantitative analysis shows that in general a higher number of seeded granules form at low impeller rotational speeds; however it was found that for all the seeded granules the seed surface coverage by fines is from 5% to 60%. Further analysis revealed that seeded granules with the seed surface coverage higher than 50% are more frequently formed at high impeller rotational speeds.

Moreover a comparison of seeded granulation of pharmaceutical powders with agglomeration of mineral and metallic powders which is described in Chapter 3 is proposed. It was found a clear correlation between simulation results and experimental findings in terms of nuclei structure: SEM images of metallic agglomerates illustrate a layering structure similar to seeded granules formed by using DEM simulations. Regime maps proposed by Rahmanian *et al*. (2010, 2011) for seeded granules of calcium carbonate in high shear granulator have been successfully applied to predict seeded granules growth of metallic powders. Furthermore experimental results suggest that regime maps can be also generalized for low shear granulation.

4.2 Introduction

Granulation of fine powders is carried out in many industrial sectors, for example food, detergents, pharmaceuticals and agrochemicals to improve physical and material properties of powders such as size, structure, dissolution rate, flow behaviour and reduce the problems associated with segregation and dust formation.

Accepted in:
Hassanpour A., Susana L., Pasha M.., Rahmanian N., Santomaso A.C., Ghadiri M., Discrete element modelling of seeded granulation in high shear granulator, Powder Technology.

the granulation processes (Ennis and Litster, 2007; Litster and Ennis, 2004; Hapgood *et al*., 2007; Salman *et al*., 2007). However, little attention has been paid so far to the properties of the granules, and in particular to their internal structure and the mechanisms leading to the formation of different internal granule structures.

The internal structure of a granule is an important property that affects macroscopic characteristics such as bulk density, mechanical strength, dissolution and dispersion behaviour. In a recently-concluded research work, Rahmanian *et al*. (2011) described a novel method for manufacturing granules with a large particle of the feed at their cores, referred to seeded granules. It was found that the formation of seeded granules strongly dependent on the impeller tip speed and primary particle size distribution. In the seeding mechanism, partially wetted primary particles and larger seed particles adhere to each other to form granules composed of a large particle surrounded by fines (see Figure 4.1). Therefore seeded mechanism is akin to coating, however the mechanism at single particle level is unclear.

Properties of granules depended not only on their external morphology and size, but more importantly depended on their internal microstructure. Granule microstructure is the most important property that eventually dictates macroscopic and bulk behaviour of the product. This can be such as bulk density, granule strength, flowability, and dissolution rate. Therefore, if microstructure at the single granule level can be controlled, the bulk properties of the granules will be predictable. This is of the great importance for industries involved in the production of granules such as chemical and pharmaceutical companies. The objective of seeded granulation is to produce granules with controlled structure leads to control of granule properties such as strength, size, density and porosity. It has already been tried experimentally to find an operational window for production of seeded granules using calcium carbonate (Durcal) powder and aqueous polyethylene glycol. Seeded granulation was identified using a simple regime map under certain conditions for calcium carbonate (Rahmanian *et al*., 2011). So far it is unknown if the regime map can be generalised for materials with different physical and mechanical properties than that of calcium carbonate especially for those which are produced for pharmaceutical applications. The boundaries proposed in the regime map has not yet been firmed up and tested for various types of powders. An attempt was made to generalise the proposed regime map. For this, the Stokes deformation number introduced by Tardos *et al*. (1997, 2004) was found a suitable criterion. It is found, using an experimental model, that Stokes deformation number of about 0.1 is favoured to produce substantial amount of seeded granules of calcium carbonate in the range of 500-600 μm. This criterion was found a very helpful tool as it can predict amount of seeded granules. However, there are still uncertainties in the mechanism of the process at single particle/granule level and responsible mechanism for seeded granulation is not solidified. The uncertainties are

including but may not be limited to the effect of shape and type of primary particles, effect of residence time, effect of input energy, geometry of the impellers, type of granulators (batch or continuous) (Rahmanian and Ghadiri, 2010). All of these parameters can affect on optimum shearing conditions and hence internal microstructure of granules and formation of seeded granules. To our knowledge, it is almost impossible to discover experimentally mechanism of seeding at single granule level using current available technologies. Therefore, it has been decided to use simulation techniques based on DEM to explore and have an insights to the process at the particle level. Apart from the reasons stated at the previous paragraph, this is another justification which causes motivation of this work. DEM in fact gives full information of particle trajectory, hence it is the best method for this particular purpose. Later on, based on findings from DEM, it is possible to run limited experiments to validate the model. The Distinct Element Method (DEM) modelling is used to analyse the bulk behaviour of particles, such as particle flow patterns during the granulation process and the microscopic and macroscopic granulation mechanisms (Hassanpour *et al*., 2011). An attempt is made to investigate the process conditions which lead to formation and breakage of seeded granules. The subject of the work is a 5l Cyclomix granulator, manufactured by Hosokawa Micron B.V.

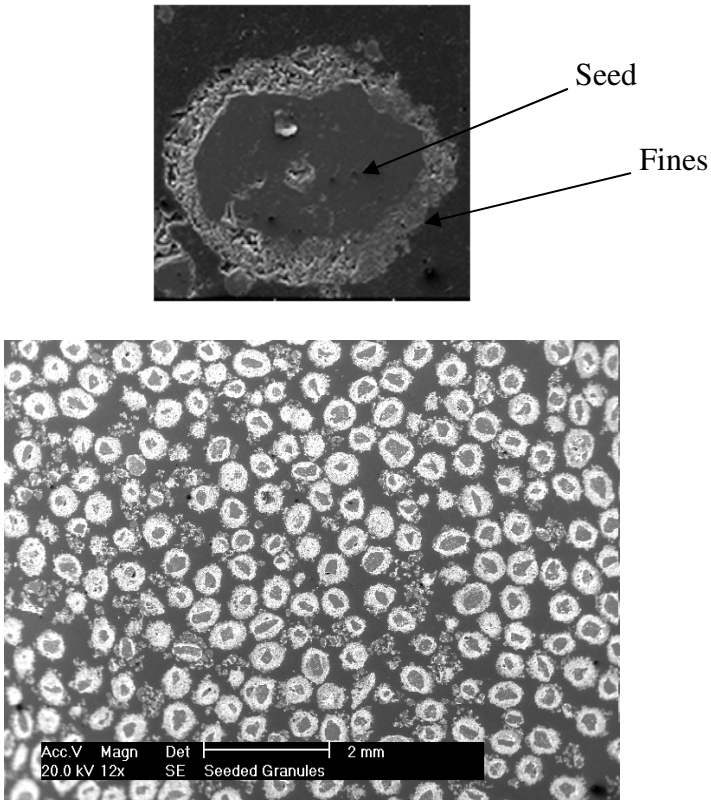

Figure 4.1 *SEM image of the internal structure of a seeded granule (Rahmanian et al., 2011)*

4.3 Methodology

DEM simulations of the granulation process were conducted using EDEM® software provided by DEM Solutions. The Hertz-Mindlin contact model was used for the elastic behaviour of the particles. Based on this model, the normal contact force between two elastic spheres in contact is given by (Thorton and Ning, 1998):

$$F = \frac{4}{3} E^* R^{*\frac{1}{2}} \alpha^{\frac{3}{2}} \tag{4.1}$$

where α is the normal overlap, E^* and R^* are respectively the equivalent Young's modulus and the equivalent radius which are given by the following equations:

$$E^* = \left(\frac{1-\upsilon_1^2}{E_1} + \frac{1-\nu_2^2}{E_2} \right)^{-1}; \tag{4.2}$$

$$R^* = \left(\frac{1}{R_1} + \frac{1}{R_2} \right)^{-1}. \tag{4.3}$$

A linear cohesion model was used to simulate the cohesion force, F_c, between the particles based on the following equation:

$$F_C = kA, \tag{4.4}$$

where A is the contact area between the particles and k is the cohesion energy density with the unit Jm^{-3}. In the present work the energy density k was related to its equivalent JKR interface energy (Johnson *et al.*, 1971). The material properties used in the simulations are summarised in Table 4.1.

Table 4.1 Material properties used in the simulations

Property	Particles	Geometry
Density (kg/m^3)	800	7800
Poisson's Ratio (-)	0.2	0.29
Young's Modulus (GPa)	0.24	200
Interface Energy (J/m^2)	1.5	-

The particle system for the simulation includes 1460 seeds with 8 mm in diameter and 146000 fine particles with 2 mm in diameter. The size ratio between the seeds and fine particles is selected according the minimum size ratio from the regime map suggested by

Rahmanian *et al.* (2011) an it was fixed at 4. The interactional properties used in the simulations are summarised in Table 4.2. In these simulations it is assumed that all particles are cohesive resembling the case where the binder is uniformly distributed among seeds as well as fine particles.

Table 4.2. Interactional properties used in the simulations.

Property ➔ **🡻Interaction**	**Coefficient of Restitution** **(-)**	**Coefficient of Static Friction** **(-)**	**Coefficient of Rolling Friction** **(-)**
Particle-Particle	0.2	0.5	0.1
Particle-Wall	0.2	0.3	0.1

The 3D CAD geometry of a 5 litre Cyclomix high-shear mixer granulator, manufactured by Hosokawa Micron B.V., it is imported into the DEM software as shown in Figure 4.2.

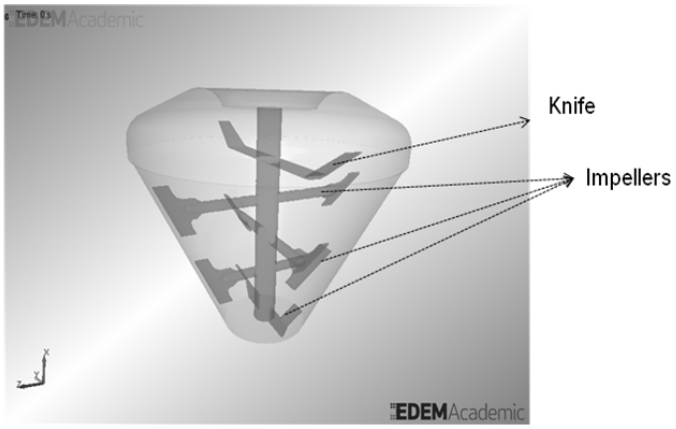

Figure 4.2 *Imported geometry of Cyclomix granulator*

The granulator consists of a centre impeller with four sets of blades and a pair of knives on top. The impeller is enclosed in a bowl shaped in a frustum of a cone. The granulator has a blade (knife) at the top of the bowl to cut/break the loose granules formed in the granulator.

4.3 Results and discussion

The particulate system was created by introducing a random mixture of seed and fine particles from a surface above the knives. The particles were then let to settle under the gravitational forces. The filling was carried out while the impellers were stationary. The simulation was then carried out for 10 s of real time at four different impeller rotational speeds: 150, 200, 287, 345 rpm.

Figure 4.3 shows a snapshot of the velocity field inside the granulator for a representative rotational speed (287 rpm). The figure shows a relatively high shear region near the top impeller. This is in agreement with a previous work (Hassanpour *et al*., 2011). It should also be noted that the concentration of particles at the bottom of the granulator is lower than that of upper part.

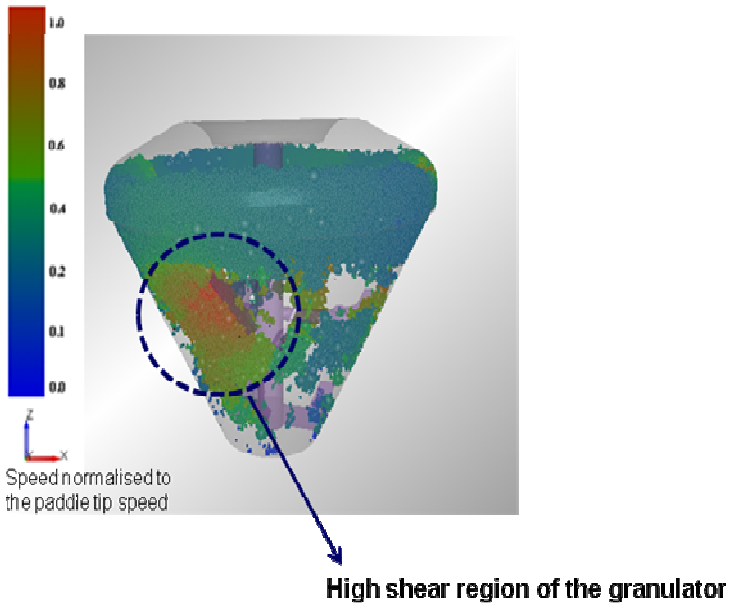

Figure 4.3 *The schematic flow field inside the granulator simulated by DEM, colours correspond to particle normalised velocity*

During the agitation the motion of particles and in particular those of the seeds affects the particle concentration in various regions of the granulator.

The concentration of the seeds in different regions of the granulator (see Figure 4.4) for different impeller rotational speeds is shown in Figure 4.5.

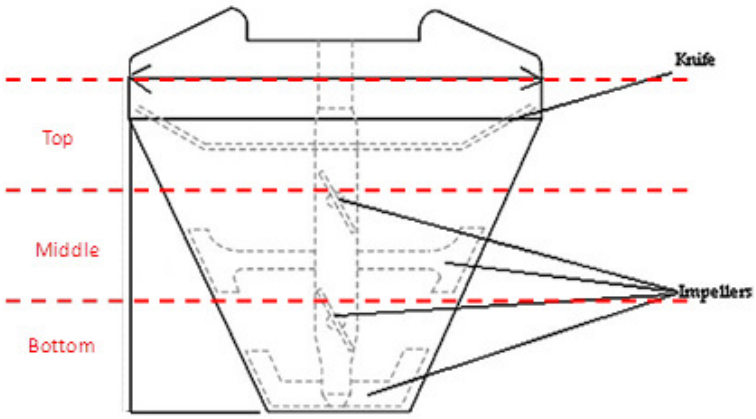

Figure 4.4 *Measurement regions considered for analysis*

It can be seen that as the rotational speeds is increased, the concentration of seeds increases at the top part of the granulator. It can also be seen that the seed concentration at the bottom for the rotational speeds of 287 and 345 rpm is lower than those of 150 and 200 rpm.

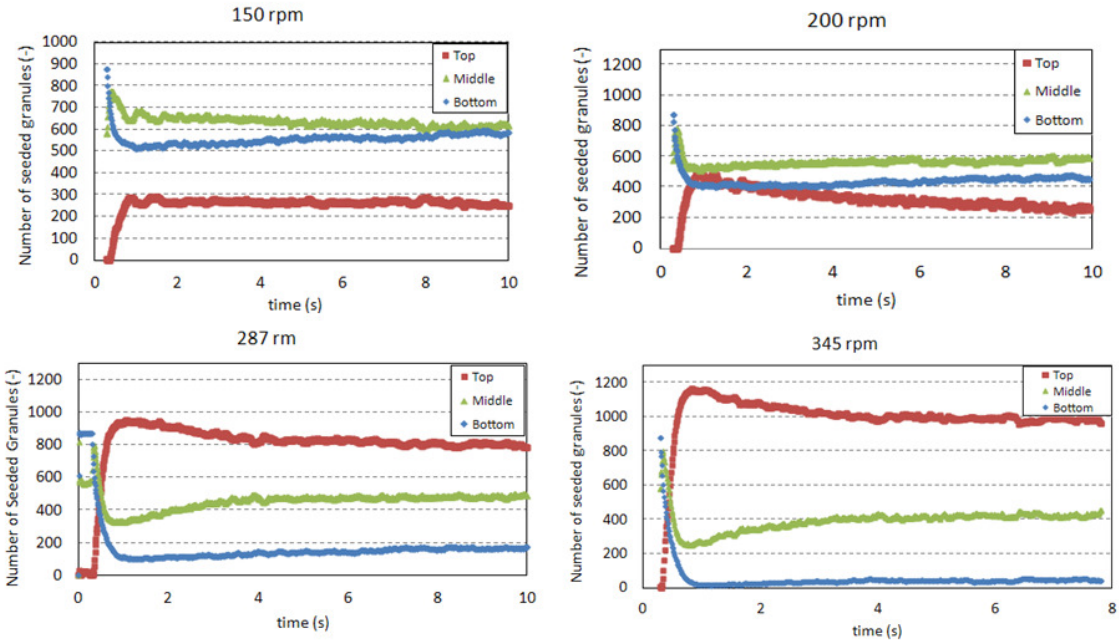

Figure 4.5 *Concentration of seeds at various regions of the granulator at different speeds*

A snapshot of the internal view from the granulator is shown in Figure 4.6, where the formation of agglomerates can be observed qualitatively. It can be seen that the

agglomerates have formed in both seeded and non-seeded forms. A closer observation reveals that the formation of seeded granules involves continuous reduction and growth in size (Figure 4.7, this is best viewed by video observations). Figure 4.7 shows four representative seeded granules (other particles are not displayed for clarity) at different sequential times. The seeded granules in Figure 4.7a grow in size as granulation proceeds to the stage in Figure 4.7d. As it can be seen from Figure 4.7f these granules are now breaking. This phenomenon goes on continuously during the granulation process and causes the seeded granules to grow by adhesion forces and to reduce in size by breaking under shear deformation, giving rise to different sizes and coordination numbers.

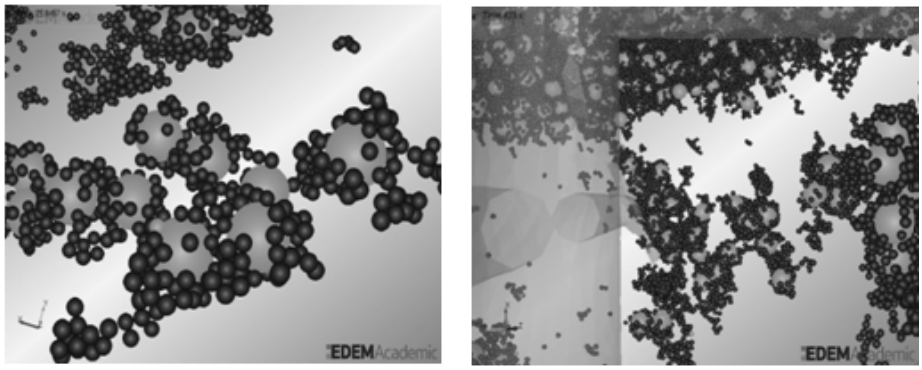

Figure 4.6 *An internal view from simulated granulator showing seeded and non-seeded granules*

The formation of seeded granules are quantitatively analysed at different impeller rotational speeds. Figure 4.8 shows the number of produced seeded granules in the granulator for all rotational speeds.

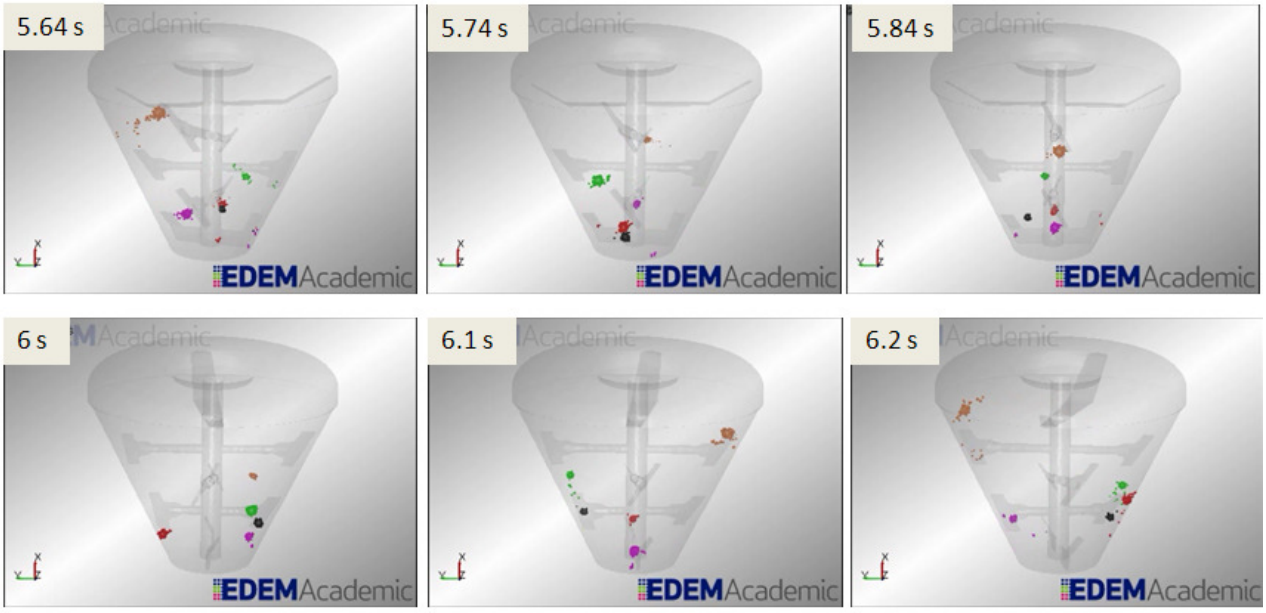

Figure 4.7 *Simulation of reduction and growth of seeded granules at different sequential times*

It can be seen that a significantly higher number of seeded granules are produced at 150 and 200 rpm as compared to those of 287 and 345 rpm. The results in Figure 4.8 are not in agreement with the findings from Rahmanian *et al.* (2011), who have shown seeded granule are formed with a higher probability at higher rotational speeds under specific operation conditions. It should be noted that the seeded granules are identified as those seed particles which are only bonded with fines. This means that a seeded granule could be identified by the computer algorithm when a seed is in contact with fine particles, regardless of its surface coverage of fine particles and coordination number. Therefore further refinement of the results in Figure 4.8 is required.

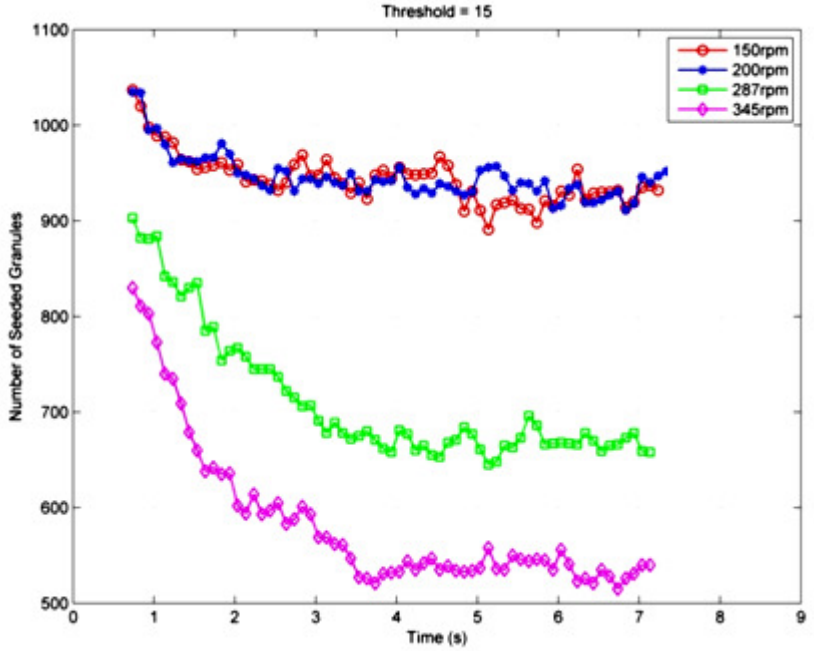

Figure 4.8 *Seeded granules at different impeller rotational speed*

Theoretically, a complete seeded granule should have the seed fully covered with a minimum one layer of fines. Based on the seed to fine size ratio of 4 in this work, a seed should be in contact with approximately 50 fine particles to get full coverage. However, additional quantitative analysis shows that seeded granules in Figure 4.8 are formed with a seed surface coverage ranging from 5% to a maximum of 60% of full coverage. This was also qualitatively observed in Figure 4.6, where no seeded granule could be seen with the full seed coverage. Further quantitative analysis in Figure 4.9 shows the number of seeded granules with a minimum 40% of surface coverage at different impeller rotational speeds. As it can be seen, the results are closer at different impeller rotational speeds as compared to Figure 4.6. However, Figure 4.10 shows that those seeded granules formed with a minimum of 50% coverage are more frequently seen at higher rotational speeds, i.e. 345 and 287 rpm. It should be noted that the work reported by Rahmanian *et al.*

(2011) showed all analysed seeded granules have their seeds fully covered by the fines. Few possible reasons could contribute to the discrepancies in surface coverage observed between the simulations and previous experimental work. One reason could be due to the fact that the granulation experiments are carried out for a few minutes, while the current simulations are only carried out for 10 s of real time due to the computing limitation.

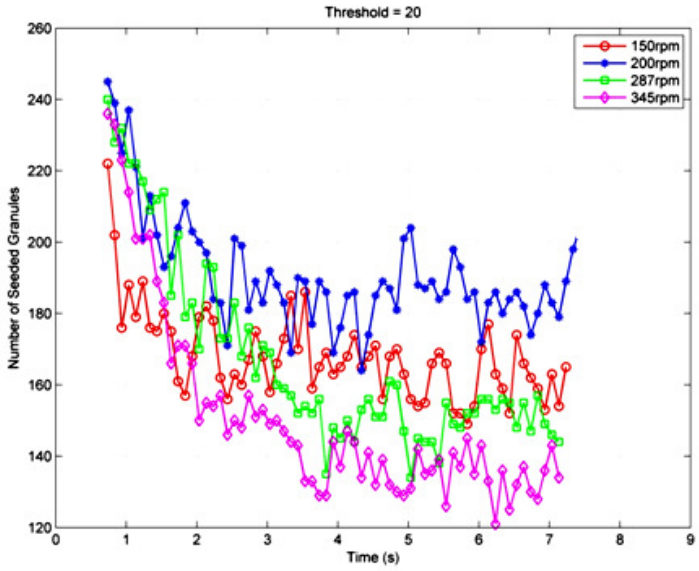

Figure 4.9 *Seeded granules (minimum 40% of the seed surface covered) at different impeller speeds*

Another reason could be due to the differences in the particle shape and size distribution between the simulations and experiments.

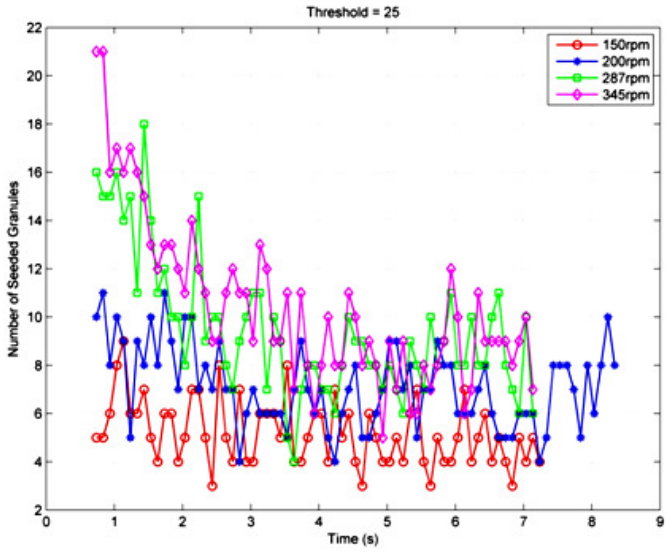

Figure 4.10 *Seeded granules (minimum 50% of the seed surface covered) at different impeller speeds*

4.4 Comparison to agglomeration of mineral powders

In his recent experimental work, Rahmanian *et al*. (2011) observed that seeded structure is strongly dependent on the impeller speed and the primary particle size, particularly the ratio between seeds and fine particles. The regime map developed for production of seeded granules shows that for the Stokes number of around 0.1 the formation of seeded structures is favourable. Moreover for St > 0.1, the percentage of seeded granules is increased drastically (see Figure 4.11).

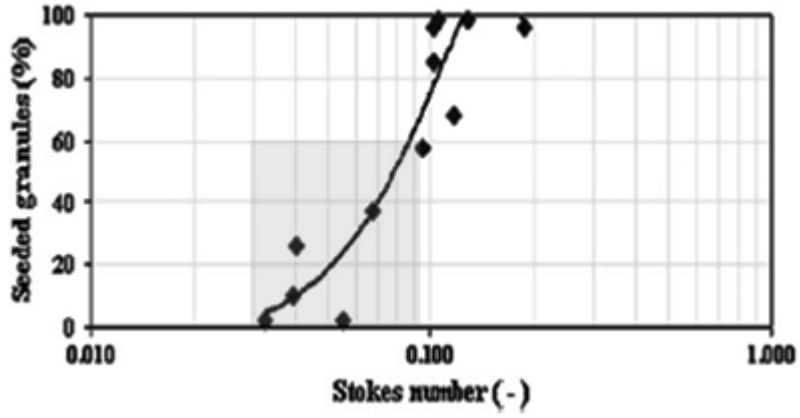

Figure 4.11 *The trend of percentage of seeded granules versus Stokes number (Rahmanian et al., 2011))*

It was also found that if the impeller speed is less than 3.5 m/s seeded granules cannot be formed. Moreover regardless of impeller speed for size ratio less than 2 granule structure is not seeded (see Figure 4.12).

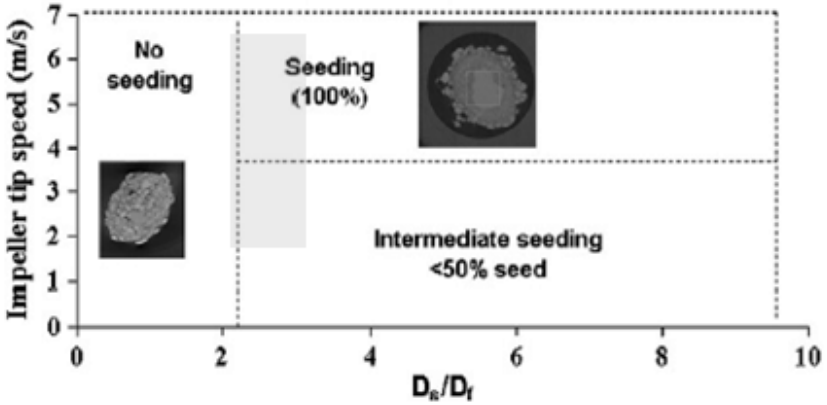

Figure 4.12 *The regime map for the production of seeded structures presented by Rahmanian et al., 2011*

In this analysis we attempt to compare seeded granulation with wet agglomeration in laboratory low shear mixer presented in Chapter 3. Figures 4.11 and 4.12 illustrate the operation window in terms of Stokes number and operating conditions for the granulation

trials carried out in the pilot plant using mineral and metallic powders as starting materials (grey areas). We can observe that at lower Stokes number between 0.03 and 0.07, a low percentage of seeded granules can be formed. Moreover the range of impeller speeds (2 ÷ 6 m/s) and the ratio between seed and fine particles employed in the experimental trials confirm this trend. The evidence for this was granule characterisation by using scanning electron microscopy (SEM) to a few granules formed in the pilot plant trials at constant tip speed of 5.8 m/s proposed in Figure 4.13.

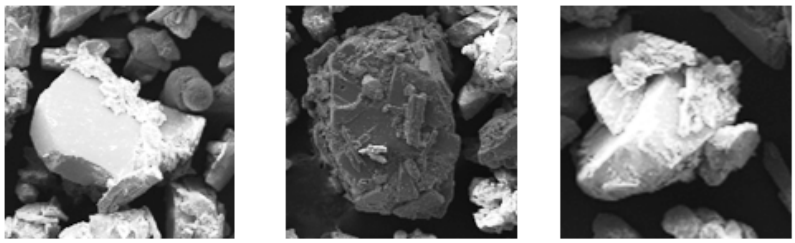

Figure 4.13 *SEM images of the structure of granules made at constant tip speed of 5.8 m/s*

SEM images show a structure akin to seeded nuclei under these operating conditions: fines particles adhere to a larger nuclei particle to form a particular layering structure. Therefore this work here clearly shows that the regime map proposed by Rahmanian and his co-workers (2010) can be generalised for materials with different physical and mechanical properties than that of calcium carbonate. Moreover high shearing is not required for the production of seeded structure. A low shear mixer also allow to start seeded granulation.

4.5 Conclusions

The process of seeded granulation inside a 5 litre Cyclomix high shear granulator has been simulated by DEM. The results show that during granulation process the seeded granule formation involves a continuous growth and reduction in size. The simulation results show that all formed seeded granules have 5 to 60% surface coverage of the seeds. Further quantitative analysis shows that the seeded granules with high surface coverage are present more frequently at high rotational speeds.

A comparison of seeded granulation with the agglomeration of mineral and metallic powders is also discussed. The Stoke criterion was found very helpful to predict the formation of seeded granules also for materials with different physical and mechanical properties than that of pharmaceutical powders. Particularly we tested for three different formulations of mineral and metallic powders the boundaries proposed in the regime map by Rahmanian *et al*. (2010). According to the values of Stokes number and impeller

speeds, SEM images of mineral and metallic granules indicate that in these operating conditions seeded granulation can start.

4.6 References

Ennis, B., Litster, J.D., 1997. Principles of size enlargement. In Perry's Chemical Engineers, Green, D., Perry, R. (Eds.), Handbook-7th Edition, Mc Graw Hill, New York.

Johnson, K.L., Kendall, K., Roberts, A.D., 1971. Surface Energy and the Contact of Elastic Solids, Proc. R. Soc. London, A324, pp.301-313.

Litster, J.D., Ennis, B., 2004. The Science and Engineering of Granulation Process, Kluwer academic publishers, Dordrecht, The Netherlands.

Hapgood, K.P., Iveson, S.M., Litster, J.D., Liu, L.X., 2007. Granulation Rate Processes. In: Salman, A.D., Hounslow, M.W., Seville, J.P.K. (Eds.), Chapter 20 in Handbook of Powder Technology, vol. 11, Granulation, Elsevier, Amsterdam.

Hassanpour, A., Tan, H., Bayly, A., Gopalkrishnan, P., Ng, B., Ghadiri, M., 2011, Analysis of Particle Motion in a Paddle Mixer using Discrete Element Method (DEM), Powder Technology 206, 1-2, pp. 189-194.

Rahmanian, N., Ghadiri, M. 2010. Seeded granulation, batch and continuous granulation processes, 6th World Congress on Particle Technology i.e. WCPT 6, Article 0213, Nuremberg, Germany, 26-29 April 2010.

Rahmanian, N., Ghadiri, M., Jia, X., 2011. Seeded Granulation, Powder Technology 206, 1 – 2, pp. 53-62.

Rahmanian, N., Naji, A. and Ghadiri, M., 2011. Effect of process parameters on the granule properties made in a high shear granulator. Chemical Engineering Research and Design, 89(5), pp. 512-518.

Salman, A.D., Reynolds, G.K., Tan, H.S., Gabbott, I., Hounslow, M.J., 2007. Breakage in Granulation. In: Salman, A.D., Hounslow, M.W., Seville, J.P.K. (Eds.), Chapter 21 in Handbook of Powder Technology, vol. 11, Granulation, Elsevier, Amsterdam.

Chapter 5

Development and characterization of a new thief sampling device for cohesive powders

5.1 Summary

Segregation of multi-component mixtures during agglomeration processes is a common problem, which is of particular interest to those industries where homogeneity is a critical requirement (Iveson *et al*., 2001).

For evaluating the composition of final granules and to evidence segregation samples have been taken in different positions inside the granulator. Thief probes are the most popular sampling method in the industry even if there are many drawbacks to their use. Particularly thief probes may not provide with representative samples of the actual content uniformity and they may modify the structure of the original bed of powder during sampling operation.

For these reasons new sampling probes and methods for cohesive powders are conceived, designed and characterized. Probes are made of two metallic shells (a slide and a cover) which need to be inserted sequentially into the bed of powder in order to extract representative samples. Because of the thin profile of the shells and of the particular insertion procedure, stresses on the powder are minimized reducing both the invasiveness and the dragging of material through the bed. Probes of similar design with different shape and size have been tested on synthetically stratified beds of cohesive powders of different colors. Sampling performances are quantitatively compared among different probes (for size and shape) and also with literature data, indicating that the new sampling devices effectively improve sampling efficiency, reliability and possibilities. The simple construction and use suggest they can be viable and effective alternatives to traditional probes for cohesive mixtures. These new devices are used to collect granules which were produced in the batch wet granulation carried out in the pilot plant.

Published in:
Susana L., Canu P., Santomaso A.C., Development and characterization of a new thief sampling device for cohesive powders. International Journal of Pharmaceutics 416 (2011), 260-267.

5.2 Introduction

The need for sampling a mixture of powders for analytical purposes naturally arises during intentional mixing or handling that might lead to unwanted segregation. Mixing of powders is a common and delicate unit operation in solids processing (Bridgwater, 1976; Harnby, 2000). Methods for a precise characterization of the mixture must be available both for routine process control and to sustain the development of predictive models, to support equipment design and to plan mixing strategies (Santomaso *et al*., 2005). The purpose of sampling is that of collecting a predetermined quantity of powder (typically some grams) expected to be representative of the whole solid mixture under examination. It requires the highest level of accuracy to guarantee significance to the following quantitative analyses. Mixture characterization imply the quantitative assessment of both chemical (i.e. composition) and physical homogeneity (e.g. particle size).

An effective mixing requires preventing or minimizing segregation. Free-flowing powders containing particles with different physical properties (particle size, density, shape) are known to segregate (Bridgwater, 1976; Zik *et al*., 1994; Santomaso *et al*., 2004). Specifically, any induced flow causes particles to move differently and to accumulate selectively into different et al regions of the mixer (Santomaso *et al*. 2004). Experience suggests that free-flowing dry powders with size larger than 75-100 μm are prone to segregate while reducing size below 75 μm minimizes segregation at large scale of scrutiny because of the increased cohesion (Harnby, 1992). However, while gross segregation is reduced with cohesive powders, it can still occur at smaller scale because of the development of stable microstructure of small aggregates with composition different from the surrounding mixture. Depending on the nature and strength of interparticulate forces, agglomerates can dominate the flow characteristics and transform the cohesive mixture in a system of free-flowing aggregates (Harnby, 1992). Ultimately, both free-flowing and cohesive powders may experience segregation. Also ingredients in very low quantity jeopardize mixture homogeneity since it exists a critical scale of scrutiny at which content uniformity of such ingredients can be excessively poor (Danckwerts, 1953). In every industrial activity where a thorough mixture homogeneity is essential, such as in the pharmaceutical one, reliable sampling and characterization methods of solid mixtures are critical operations. In this context, thief probes are traditionally used to sample the mixture and to check if the products meet specifications.

Notwithstanding traditional thief sampling technique presents some severe limitation (Muzzio *et al*., 1997) and alternative in-line analytical technologies have been developed as implementation of Process Analytical Technology (PAT) solutions such as light-induced fluorescence, light reflectance, effusivity and near-infrared spectroscopy (Benedetti *et al*., 2007), thief sampling remains the routine procedure in many pharmaceutical companies to validate large scale powder mixing operation (Mendez *et*

al., 2010). Representative sampling involves two distinct aspects: the distribution of sampling events both in space and time and the actual collection of material from the mixture. While the former issue is mainly a statistical problem, already discussed (Muzzio, 1997) and considered in the Draft Guidance addressing the issue of unit sampling and assessment (U.S. Food and Drug Administration, 2003), the latter is fundamental to any further speculation. It requires the availability of suitable probes and operating methods. Muzzio *et al*. (1999, 2003) thoroughly demonstrates that traditional thief probes used in the pharmaceutical industry may not yield representative samples of the actual mixing degree and proves that they are particularly invasive, since they modify the structure of the original bed of powder, thus biasing the collected sample.

They are typically made of two concentric cylinders, in which the inner cylinder has one or more cavities that can be opened and closed by rotating the outer one, acting as cover. This type of probe allows taking samples from the mixture when the holes of the outer cylinder are aligned with the cavities of the inner one. Thief probes are called side- or end-sampling probes, depending on the location of the cavities, i.e. several on the side or a single one at the lower extremity. In both cases, the probe is introduced into the powder bed with its cavities closed. Once insertion is complete, the rotation of the outer cylinder opens the cavities allowing the powder to flow inside. The cavities are then closed before withdrawal of the probe. The aforementioned published studies highlight the invasive nature of this kind of probes. Specifically, Muzzio *et al*. (2003) compares three different types of traditional thief samplers with a new probe called Core Sampler (CS). It is an end-sampling probe which simply consists of a cylindrical tube, one end of which is tapered to a sharp angle (see Figure 5.1).

Figure 5.1 *Picture of a Core Sampler (CS)*

The sample is collected by inserting the CS into the powder bed to a predetermined depth, thus isolating a cylindrical core of powder in the tube. The core is then extracted by the action of a piston inserted into the tube. The final extraction operation requires a dedicated apparatus to be properly performed since it may need the application of large forces to push out the sample from the sampling tube. Despite its simplicity, the CS

results to be the best probe among those examined since it minimizes the drag of powder on the outer side of the probe; this means it does not cause the disruption of the original structure of the bed of powder it is inserted in. External drag is caused because traditional thief probes are intrinsically intrusive. Since probes occupy a finite volume their insertion determines an equivalent displacement of material and the friction with the walls of the probe allows the transmission of stresses to the surrounding bulk of powder generating shear within it. With CS such powder displacement is minimized. Also internal drag results minimized (Muzzio *et al*., 2003).

Starting from these evidences on the advantages of CS, we deepened the features and applicability of CS-type probes, eventually suggesting a novel probe geometry. We collected evidences that a simple CS probe, even if it reduces drag, can induce relevant deformation of the sampled core thus biasing the measurement. We also explained this experimental evidence through powder mechanics arguments; we experimentally and theoretically demonstrated that CS can significantly compact the powder bed during insertion up to the point that the probe becomes blocked and cannot be completely filled. Consequently, we proposed an alternative probe, called Sliding Cover Sampler (SCS) which was able to overcome these limitations giving better results than the CS.

5.3 Materials and methods

5.3.1 The Sliding Cover Sampler

In order to overcome some of the limitation of traditional sampling probes and to expand further the benefit introduced by the CS, it appeared important to improve the sampling procedure during the probe filling and the sample withdrawal stages. It seemed indeed important to reduce the undesired increase of stresses in the sampled powder, eventually leading to compaction, uncompleted probe filling and drag of material along the inner wall surface. It appeared likewise important to preserve the arching mechanism in the material during extraction, to allow the withdrawal of the probe with its sample without the need of closing the bottom of the probe. Addition of any end closure device would indeed be complicate and intrusive. All these motivation led to design thief probes made of two parts, to be used at different times to reduce the stresses on the powder during the probe insertion stage. It was made of a slide and a cover which needed to be inserted sequentially into the bed of powder in order to gather the sample. Also the extraction of the sample from the probe for subsequent analysis resulted much simpler, faster and more reliable.

The concept is illustrated in Figure 5.2, showing one of the possible geometries for the SCS.

a) b)

Figure 5.2 *Picture of the SCS (a) and sketch of the components and operation (b)*

This new thief probe can be considered as an evolution of the former CS. With respect to traditional probes, the underlying idea in CS and SCS is reversing the filling mechanism: it is not the powder that moves, entering into the probe cavities, but it is the probe that moves, enveloping a static portion of the powder bed, eventually isolating the sample from the bulk. Dealing with a static portion of powder has the advantage of eliminating segregation typical of flow conditions. The procedure of using a SCS consists in inserting first the slide into the powder bed until it reaches the predetermined sampling depth and then closing the probe with the sliding cover to isolate the core from the bulk. Once extracted, the probe provides the whole composition profile along the sampled bed with a single sampling operation. Differently from the CS sampling procedure, the sequential insertion of two independent parts dramatically reduces radial and axial stresses on the sample thus reducing further drag and compaction as will be clearer in the following.

Prototypes of the SCS were made with aluminum sheets (0.6 mm thin) but other materials would fit the scope such as stainless steel or rigid polymers, including Teflon-coated metals , with the purpose of tuning both the mechanical strength and the surface properties. Two different shapes were tested, triangular and semi-circular cross-section (see Figure 5.3). In the triangular SCS the probe once closed has a triangular cross-section; slide and covers are indicated in Figure 5.3a.

Three sizes of the triangular SCS have been tested, with L = 10, 15 and 20 mm.

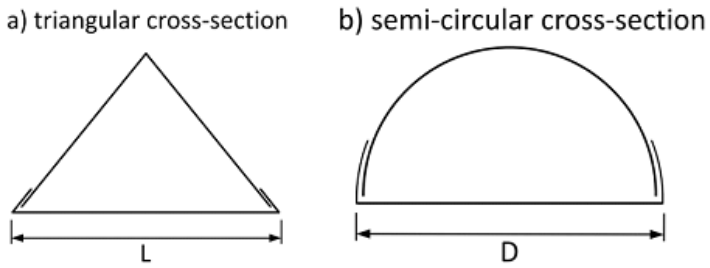

Figure 5.3 *Sketches of the SCS cross-sections used in this work, with their characteristic dimension. The slide is always the lower part, and the cover above*

The semi-circular SCS is similar to the former excepted for the cover which is replaced by a semi-circular shell (Figure 5.3b) in order to eliminate one angle and increase up to 90° the two acute angles on the side of the triangular SCS slide. This geometry was used to assess the effect of corners on powder drag. Corners are required to couple the two parts, but reproduce locally a narrow confinement amenable to stresses build up. Two semi-circular SCSs have been designed, with D= 8 and 10 mm.

Once the mixture was sampled the extraction of the sample from the probe was much simpler, faster and more reliable with the SCSs than with the CS. As shown in Figure 5.4, the probe was placed horizontally and the slide removed.

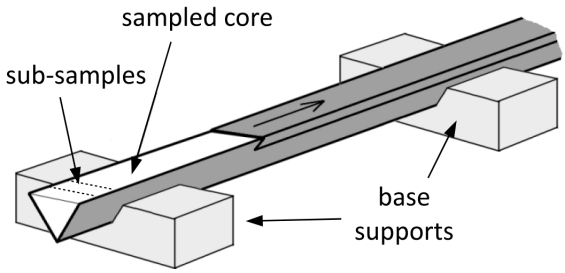

Figure 5.4 *Schematic of the procedure for unloading the SCS*

In order to detach the sampled core from the slide before removal, thus preventing further drag and eliminating residual stresses, the slide was gently tapped. During this operation the sample did not move therefore preserving its structure. The sampled core then could be further sub-sampled by slicing it at the desired depth and with the desired size. This very simple procedure circumvented completely the limitations of extracting the sampled core by pushing it with a piston as required by CS.

5.4 The sampling efficiency

In order to characterize and compare the performances of the different probes a measure of sampling efficiency was proposed. It quantifies the compaction resulting from the insertion of the probe into the bed of powder. The efficiency was simply given by the ratio between the powder volume withdrawn by the probe, V_e, and the volume that could be theoretically withdrawn in the absence of friction and compaction, V_t. Because of the constant section of the probes, the efficiency reduced to the ratio between the length of the sampled core, h_e, and the depth of insertion, h_t:

$$\zeta = h_e/h_t. \tag{5.1}$$

It was evaluated for any type and size of probes with lactose monohydrate (d_{90} = 72 µm) in a 150 mm deep bed. Larger bed thickness could be sampled with CS and SCS, however this depth was sufficient to highlight the differences in performance between the two probes. To minimize the powder compaction level prior to any sampling test, the bed of powder was realized by pouring lactose through a sieve (Santomaso *et al*., 2003).

5.5 The drag test

The drag of material along the wall of the probe is caused by friction, which determines some shear in the neighboring material. If large, it can affect the significance of the sampled material. It is a disturbance very relevant for traditional probes and still present for both CS and SCS, although greatly reduced by the SCS strategy. To investigate the phenomenon, a powder bed with a depth of 80 mm was realized. It was made of materials with clearly contrasting colours, i.e. two layers of lactose monohydrate (white) separated by a layer of cocoa (dark) powders (d_{90} = 100 µm). The thickness of the upper layer was 20 mm and it was 30 mm for the others. To measure the magnitude of internal drag after insertion, a solidification technique was applied to the whole bed of powder with the probe inserted. Details of the technique can be found in Dal Grande *et al*. (2008). Shortly, the technique requires wetting the powder with a liquefied mixture of hydrocarbons (Createc® Gmbh, Weiler Bremenried, Germany) at 80°C (the melting point of the gel is 68°C). The powders were impregnated by the gel both outside and inside the probe. After cooling at ambient temperature the bed of powder and the sample within the probe were solidified. The probe was then removed and opened and the solidified core was transversally sectioned in slices 2 mm thick. This procedure gave therefore a spatial resolution of 2 mm which is higher than that of previous published works (order of 1 cm) and allowed to quantify the drag of the dark cocoa on the white lactose by image analysis. A Matlab routine for image analysis was used to determine the average composition from

digital images of each cross sectional slice. The composition was defined as the ratio between the number of dark pixels and the number of pixels of the total cross-sectional area. It was assumed that the cross-section with a cocoa composition equal to 50% could denote the initial interface between white lactose and dark cocoa powders. Composition values of the dragged material were measured up to an axial distance of 40 mm, that is, the value corresponding to the thickness of lactose layer. Each sampling experiment was replicated three times. The freezing procedure was used only in the drag test just to measure the spatial composition by image analysis and it is not necessary during normal sampling operations.

5.6 Results and discussion

Since SCS is expected to be an improvement of CS, the latter has been characterized first. In order to understand the major limitation of the CS, i.e. possibility to withdraw non-representative samples, a brief description of the sampling procedure under the light of powder mechanics is required.

5.6.1 Powder Mechanism

Three critical stages can be found during the sampling procedure with the CS: a) probe filling during the insertion into the bed of powder, b) probe withdrawal from the bed of powder and c) probe emptying with the extraction of the sampled material. The first and the last stages are critical because of the high consolidation stresses which may develop in the material and will be examined in details. The main physical assumptions and the underlying mathematics are similar to that of Janssen's original analysis of stresses in cylindrical bins and belong to classical results of powder mechanics (Nedderman, 1992; Schulze, 2008). As in Janssen's original analysis the following assumption have been made:

1. the material was assumed to be cohesionless. Cohesion would just complicate the analysis without giving further physical insight on stresses transmission;
2. the stresses were assumed to act uniformly across any axial section of the material;
3. the axial and radial stresses were assumed to be principal stresses. This means that no shear stresses act axially and radially inside the material. In this case the relationship between the principal stresses is: $\sigma_{rr} = K\sigma_{zz}$ where σ_{rr} and σ_{zz} are the radial (or normal) and axial stresses respectively, K is a material constant also called Rankine coefficient or Janssen coefficient.
4. The bulk density was considered constant.

Differently from Janssen's analysis we made two further assumptions:

5. the gravity was neglected. Sample are small and gravitational contribution is negligible with respect to the frictional contribution developed by the walls of the probe. Moreover this assumption is compatible with the fact that sampling does not depend on the direction of probe insertion; the probe can be inserted in any direction (also horizontally) into the bed of powder;
6. the shear stress at the wall depends both on friction and adhesion so that the wall yield criterion follows a Coulomb-type relationship: $\tau_W = \mu_W \sigma_{rr} + a_W$ where τ_W is the shear stress at the wall, μ_W is the wall friction coefficient and a_W is the adhesion stress between the powder and the wall, which is present also in the absence of normal stresses σ_{rr}.

Similarly to Janssen's model, we do not consider the cohesion within the material (at particle-particle contacts), but we introduce cohesion between powder and wall through the adhesion term.

Core sampler filling

While inserting a cylindrical CS probe into a static bed of powder, the material inside the tube is 1) pushed inward by the new material entering at the bottom and 2) is constrained by wall friction.

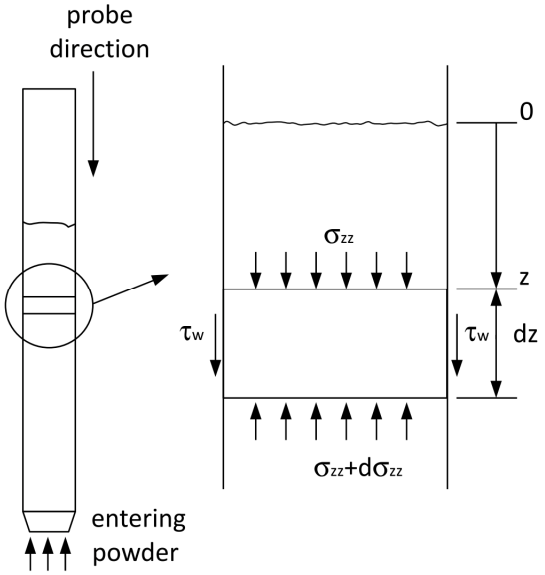

Figure 5.5 *Schematic of the Core Sampler with stresses on a differential element of powder during filling*

The following force balance on a differential slice of material inside the tube (Figure 5.5) holds:

$$\sigma_{ZZ} A + \tau_W P dz + (\sigma_{ZZ} + d\sigma_{ZZ}) A \tag{5.2}$$

where A (= $\pi D^2/4$) and P(= πD) are the internal cross sectional area and the perimeter of the probe respectively. τ_w is the only external stress acting on the material since gravity has been discarded, hypothesis (4), and its direction is reversed with respect to that of Janssen's analysis since powder is moving in opposite direction with respect to the wall displacement, in this case. The following simple equation results:

$$\frac{d\sigma_{zz}}{dz} = \frac{4}{D}\tau_W \tag{5.3}$$

which gives the following simple first order non-homogeneous differential equation, considering hypotheses (3) and (6):

$$\frac{d\sigma_{zz}}{dz} - \frac{4}{D}\mu_W K\sigma_{zz} = \frac{4}{D}a_W \tag{5.4}$$

Integrated with the boundary condition $\sigma_{zz} = 0$ at z = 0, (5.4) gives:

$$\sigma_{zz} = \frac{a_W}{\mu_W K}(e^{(4\mu_W K/D)z} - 1) \tag{5.5}$$

Eq. (5.5) shows that the axial stress that must be overcome to keep filling the probe grows exponentially with its filling level, z. For a given final length of the sample H inside the probe, the consolidation stress at the inlet is:

$$\sigma_{zz}(H) = \frac{a_W}{\mu_W K}(e^{(4\mu_W K/D)z} - 1) \tag{5.6}$$

The stress developed does not depend on gravity but on the adhesive and frictional property of the wall (a_w, μ_w). Predictions of $\sigma_{zz}(z)$ are reported in Figure 5.6 as a function of probe diameter, given μ_w, and the reverse. According to hypotheses (3) and (6) also radial and shear stresses at the walls increase with the same exponential trend. Stress profiles suggest that increasing drag at the walls (due to radial stresses, σ_{rr}) and powder compression (due axial stresses, σ_{zz}) have to be expected as a consequence of the progressive insertion (i.e filling) of the probe.

The level of drag and of consolidation should be maximum at the inlet and decreases along the probe, up to total extinction.

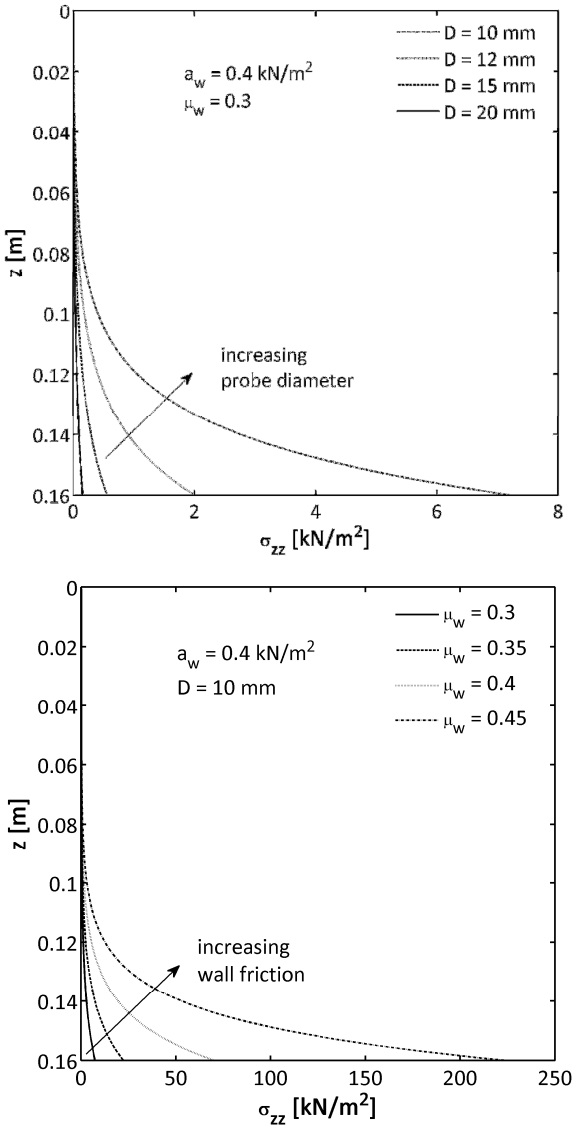

Figure 5.6 *Increase of vertical stress at the inlet of the Core Sampler as a function of the level of filling of the probe. a) effect of probe diameter and b) of wall friction. K is assumed to be 0.4*

Figure 5.6 shows also that combinations of probe size and surface finishing (or construction material), i.e. D and μ_w (typically small D and high μ_w), can easily increase stresses by one or two orders of magnitude. Consequently, each combination of probe diameter and surface finishing can lead to a critical amount of powder that can enter into the probe, before plugging it completely, so that no additional powder can be sampled.

According to original Janssen's analysis (Nedderman, 1992) the asymptotic (maximum) stress developed because of gravitational force would be (5.7):

$$\sigma_{ZZ}^{\infty} = \frac{\rho g D}{4 \mu_W K} \tag{5.7}$$

Assuming $K = 0.4$; $\mu_w = 0.4$, $D = 10^{-2}$ m and $\rho = 400$ kgm^{-3} (lactose), σ_{zz}^{∞} is 0.061 kNm^{-2}, much smaller than stresses developed by frictional forces at the wall (see Figure 5.6) and therefore fully justify hypothesis (5).

Core sampler extraction

After the filling of the CS probe the powder remains consolidated and most of the stresses leading to the formation of the plug cannot be recovered unless the powder is sheared. While this allows the safe removal of the sample, without closing the probe extremity, complication arise to recover the sampled powder, since consolidation prevents any motion of the material and a piston is required to push out the plugged material (Muzzio, 1999; 2003).

Sample withdrawal from the CS

The use of a piston for sample extraction results in a uniaxial compression of a preconsolidated material. It can be treated within the same mathematical framework, but the direction of z is reversed with respect to the probe wall, since the material moves in the opposite direction and the boundary condition at the probe extremity is different.

The force balance gives the same result expressed (5.2).

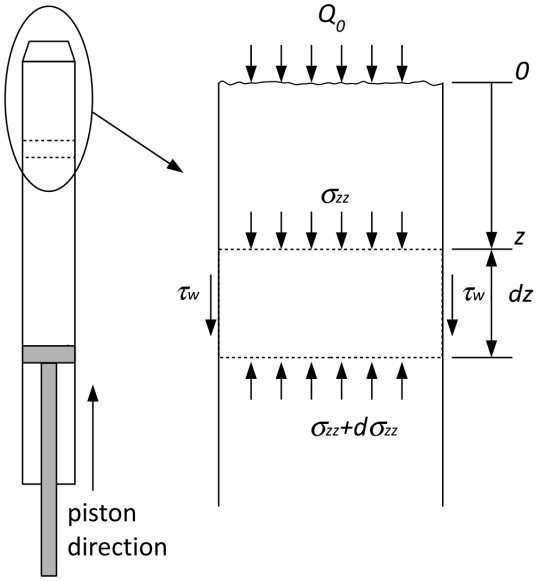

Figure 5.7 *Schematic of the Core Sampler with stresses on a differential element of powder during sample extraction with a piston*

The pressure required to push out the sampled powder needs to overcome the stresses developed at the walls by the consolidated material. If it is assumed that the maximum consolidation stress gained during the filling stage, $\sigma_{zz}(H)$, persists during the withdrawal stage, it can be modeled as an overload, $Q_0 = \sigma_{zz}(H)$, acting on the surface and opposing the action of the piston (Figure 5.7).

The overload acting at the probe extremity is given by (5.5). Therefore using it as a new boundary condition:

$$\sigma_{zz}(H) = Q_0 = \frac{a_W}{\mu_W K}(e^{(4\mu_W K/D)H} - 1) \text{ at } z = 0 \tag{5.8}$$

Integration of (5.2) gives:

$$\sigma_{zz} = \frac{a_W}{\mu_W K}(e^{(4\mu_W K/D)(z+H)} - 1) \tag{5.9}$$

Since the height z of the plug to be pushed out is identically H, the axial stress which has to be transferred through the piston to push the plug results in an exponent which is double with respect to that of Q_0 in (5.5). This means that stresses during sample withdrawal can increase of many order of magnitude with respect to those developed during probe filling. This obviously would compact further the sample, generating strong

shear stresses at the wall, according to hypotheses (3) and (6), and forcing to set-up an unpractical procedure to withdraw the sample (Muzzio, 1999).

5.7 Experiments

To highlight the important effects of the stress distribution inside the probe and to visualize the extent of compaction of the materials inside the CS, before illustrating the advantages of SCS probes, we carried out a simple preliminary experiment. A bed of powder with a total depth of 150 mm, was prepared with four layers of equal thickness, of monohydrate lactose and cocoa powders (dark), as shown in Figure 5.8.

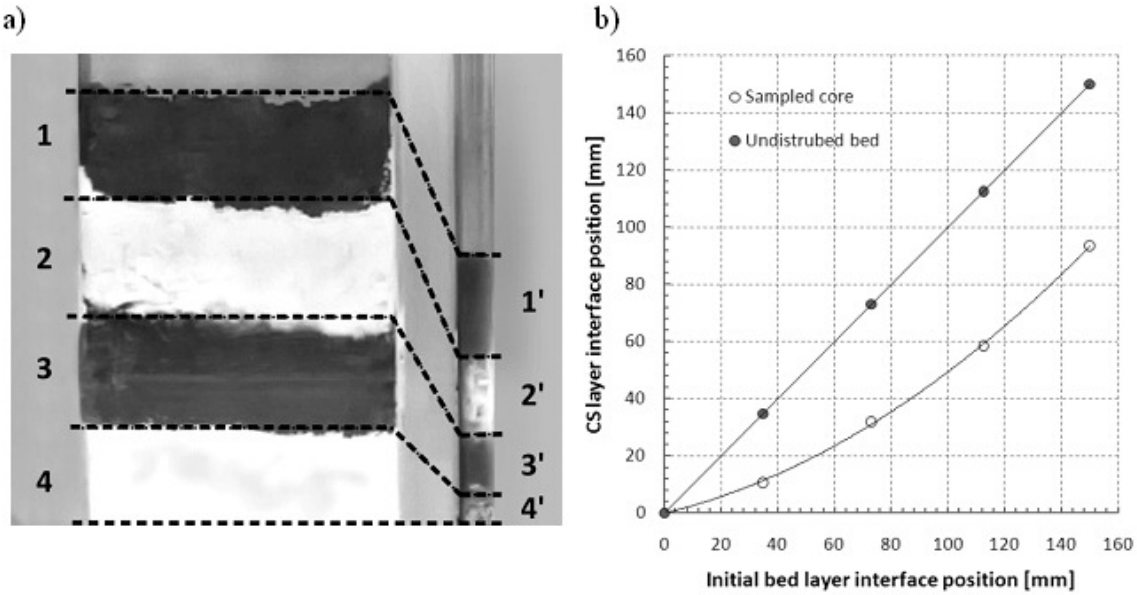

Figure 5.8 *Qualitative (a) and quantitative (b) comparison of bed structure before and after sampling with a glass Core Sampler*

The CS is in this case a transparent glass tube (i.d. 15 mm and o.d. 18 mm) which was vertically introduced into the stratified bed. The structure of the sample withdrawn by the glass probe was then compared to the structure of the original bed. Figure 5.8a clearly shows drag increase with the level of compaction (in particular with radial stresses at the walls).

5.8 The sampling efficiency measurements

Table 5.1 shows the sampling efficiency obtained by the SCSs on the 150 mm thick lactose bed. Results are the average of three tests for each thief probe.

The efficiency of the glass CS is also reported, for comparison.

Table 5.1 *Measured sampling efficiency*

Type of SCS	ζ (%)	***Std. dev. (-)***
Core Sampler, D = 15 mm	60	1.67
Triangular, L = 10 mm	85	0.77
Triangular, L = 15 mm	86	1.76
Triangular, L = 20 mm	87	0.77
Semi-circular, D = 8 mm	89	1.02
Semi-circular, D = 10 mm	95	0.67
Triangular, L = 15 mm (CaF_2)	86	0.87
Triangular, L = 15 mm (TiO_2)	82	0.96

As expected, efficiency increases significantly with the new SCS probes, the most efficient being the largest semi-cylindrical. Results confirm that the new probes cause a lower powder consolidation when inserted into the bed, thus preventing the formation of the plug. To quantify the extent of compaction of the materials inside the SCSs, the variation of bulk density of the material contained into the probe has been measured by weighting subsamples of given volume. Experiments were carried out on powder beds of monohydrate lactose, 150 mm deep.

In Table 5.1 the sampling efficiency obtained by the triangular SCS (L = 15 mm) on fluorspar and rutile powder bed of 10 mm deep is shown. These experiments have been carried out before using the triangular SCS to collect granules formed in granulation experiments. Sampling efficiency results show that these thief probes are good devices to assess the bulk solid composition during the granulation process in order to investigate segregation nucleation/growth mechanisms.

After sampling with the SCSs, the core collected was transversally sectioned with a resolution of 10 mm along the probe; each portion of the core was weighted and the bulk density calculated.

The axial profile of density inside each probe is shown in Figure 5.9. A comparison with the calculated density inside the CS is also shown. The density for CS was estimated using the information from Figure 5.8 on the level of sample compression.

The differences of levels between the interfaces lactose-cocoa allowed to estimate the degree of compression of the sample and therefore the increase in bulk density. So only four average data, estimated from the thickness of the four alternated layers were available.

It is clear that the material is much more consolidated in the case of the CS as a consequence of the exponential increase of the consolidation stresses and that for the SCSs wider probe correspond to lower compaction according to the model predictions. At comparable size, the semi-cylindrical probes yield the lowest bulk densities confirming the above results on sampling efficiency.

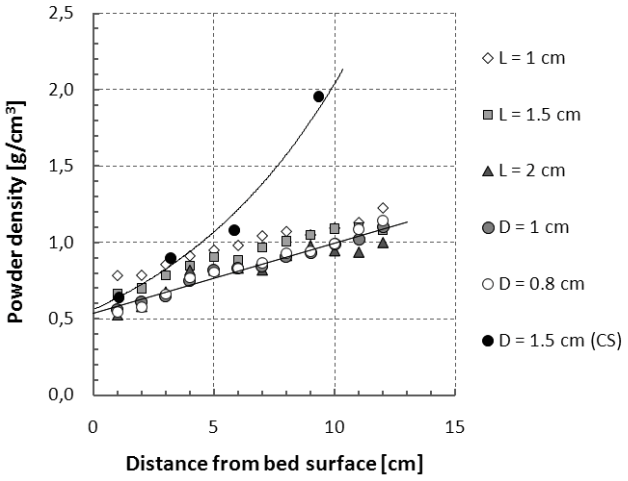

Figure 5.9 *Axial bulk density trends in SCS and CS after sampling*

5.9 The drag characterization

We compared the two SCS shapes for determining the intensity of material drag during insertion. We used a sharp material interface and the solidification and slicing technique described above.

Figure 5.10 shows typical results, with three cross-sections extracted from the solidified core of a triangular (L = 20 mm) and a semi-cylindrical (D = 10 mm) SCS. Sections are progressively farther from the cocoa (dark) – lactose (white) interface, illustrating the carryover of dark powder in the white region.

We immediately perceive that the semi-cylindrical probe reduces drag with respect to the triangular probe, being lower the amount of dark powder dragged to the lactose area . Repeated experiments confirmed that drag in the triangular probe is more intense at the corners, as apparent form Figure 5.10. Friction in narrower confinements (acute angle corners) is higher presumably because of a larger local stress, eventually leading to significant drag. On the contrary, the semi-cylindrical construction reduces narrow angles and thus the material drag, suggesting that an even better SCS would be obtained by two semi-cylindrical parts, suitably coupled.

The same freezing and slicing technique followed by image analysis allows to investigate quantitatively the penetration of contamination across a sharp composition interface, due to material drag.

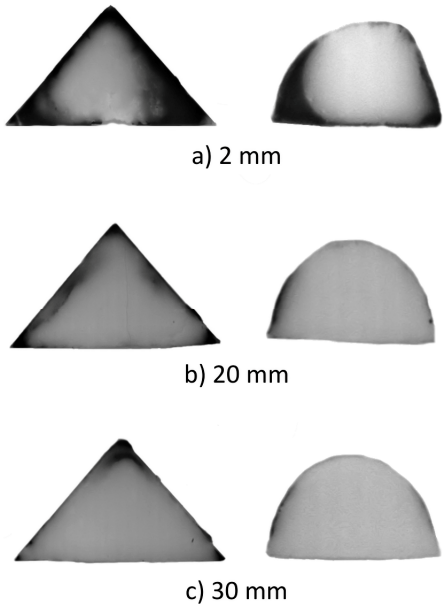

Figure 5.10 *Cross-sectional view at 3 different distances (2, 20, 30 mm) below the cocoa-lactose interface for a triangular (L = 20 mm) and a semi-cylindrical (D = 10 mm) probe. Sections are not represented at the same scale*

The experimental composition profile expressed as fraction of top material (cocoa powder) vs. the depth relative to the interface between the two materials is shown in Figure 5.11 for a triangular SCS (L = 15mm). An interpolation curve is superimposed, to allow an easier comparison among several data.

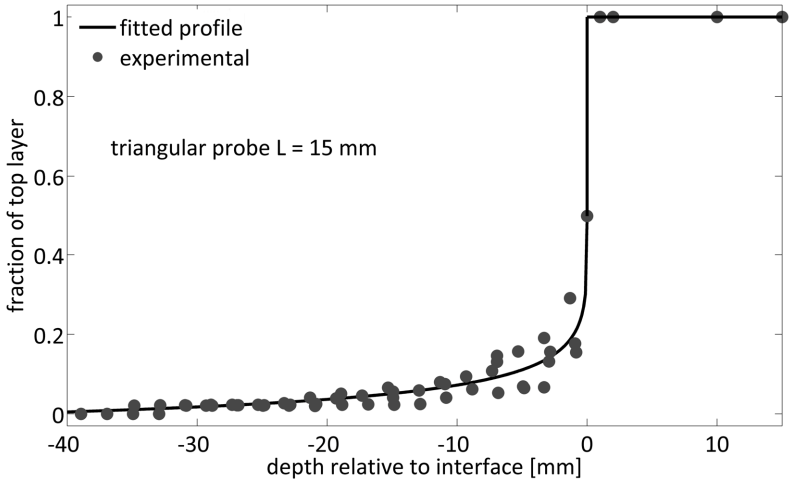

Figure 5.11 *Composition profile of cocoa powder (top layer) as a function of distance from the cocoa-lactose interface*

Figure 5.11 shows that the amount of top material dragged below the interface drops rapidly, while there is no mutual contamination of the two powders above the interface, because of the direction of insertion. The extraction procedure for the SCS does not require the powder to move further, since we simply access the core by removing the slide. Consequently, no additional upwards contaminations by drag are possible and the composition profile above the interface coincides with the expected.

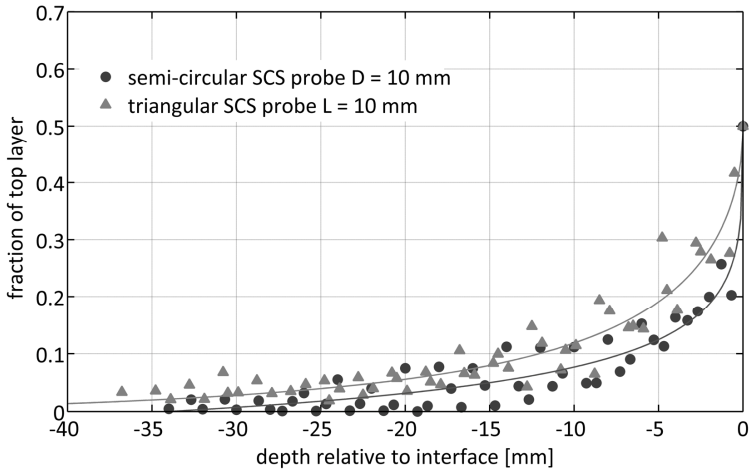

Figure 5.12 *Composition profile of cocoa powder (top layer) as a function of distance from the cocoa-lactose interface, comparing two geometries: semi-circular and triangular cross section*

To compare the effect of the two different geometries (semi-circular and triangular cross section) two probes with the same width (i.e. those with the slide 10 mm wide) have been compared. Similar to Figure 5.11, Figure 5.12 compares the composition profiles of a triangular and a semi-circular probe below the lactose-cocoa interface. The two probes behave similarly, though the semi-circular ones shows a faster decay of powder concentration from the top layer (i.e. less powder drag after insertion) with respect to the triangular one. That was expected because of the reduction of narrow corners. Table 5.2 compares the contamination due to material drag at the walls for all the probe.

The SCS results are also compared with available Literature data for other thief probes in terms of fraction of top material at a distance of 10 mm below the interface.

Table 5.2 *Drag efficiency as % of material above the interface found 10mm below it*

Type of sampler	References	Composition (%)
SCS (L=10mm)	Present work	12
SCS (L=15mm)	Present work	6
SCS (L=20mm)	Present work	6
SCS (D=8mm)	Present work	6
SCS (D=10mm)	Present work	8
Core Sampler	1, 2	<10
Slug (end-sampler)	1	45
Side sampler	1, 2	90

[1]Muzzio et al. (1999); [2]Muzzio et al. (2003)

On the whole the our data for SCS are comparable, frequently better, than CS, according to the literature measurements, with exception of a very narrow (10 mm wide) triangular probe. Further SCS and CS performances are clearly superior to other thief probes, including commercial ones. It is worth observing that the comparison between concentration at a given distance below the surface is also negatively biased by the high level of consolidation (and therefore compression) of the sample in the CS case. Moreover the core withdrawal procedure required by the CS may introduce additional errors, in the form of reverse drag. Contamination of the upper layer by materials in the lower ones can be generated by the inversion of the material translation within the probe, required by CS for core extraction. Such biases are not present in the procedure for SCS core extraction.

5.10 Conclusions

We conceived, designed and characterized novel thief probes for cohesive powders, that we called the Sliding Cover Samplers (SCS). They consist of two thin metallic shells to be inserted sequentially into the bed of powder in order to extract a representative core. Because of the thin profile of the shells and of the particular insertion procedure, stresses on the powder are minimized reducing both the invasiveness on the bed and the dragging of material in the sample. The extremity of the probe does not require to be closed since cohesion prevents the outflow of material from the probe during the extraction. The advantage of this sampling probes is that powder does not move to enter the probe but it

is the probe that envelope a static portion of material. Also the final withdrawal of the core from the probe does not require the powder to move since it is the probe that is opened, exposing the sampled core. This procedure reduces therefore the possibility of segregation (which is associated to flow conditions) and minimize the possibility of contaminating the sample with material dragged from the upper levels, as quantitatively proved in this work. SCSs of different shapes and sizes have been tested and compared with other kind of thief probes (commercial and not). Results showed that SCSs are more efficient than traditional devices since they reduce significantly both the consolidation and the drag of the powder. SCSs probes are not limited to any sampling depth, differently from CS. SCSs probes also allow in a single operation to determine a composition profile along the whole powder bed depth. Considering that SCSs simplify the probe design and use, they can be considered a viable alternative to commercial thief probes when dealing with cohesive powders.

5.11 References

Benedetti C., Abatzoglou N., Simard J.-S., McDermott L., Léonard G., Cartilier L., 2007. Cohesive, multicomponent, dense powder flow characterization by NIR. International Journal of Pharmaceutics, 336, pp. 292–301.

Bridgwater, J., 1976. Fundamental powder mixing mechanisms. Powder Technology, 15, pp. 215-236.

Brown, R. C., & Richards, J. C. (1970). Principles of powder mechanics. Pergamon.

Dal Grande, F., Santomaso, A., Canu, P. 2008. Improving local composition measurements of binary mixtures by image analysis. Powder Technology, 187, pp. 205–213.

Danckwerts, P.V., 1953. Theory of mixtures and mixing. Chem. Eng. Res. 6, pp. 355.

Harnby, N. The mixing of cohesive powders. In: Mixing in the process industry.

Harnby, N., Edwards, M.F., Nienow, A.W. eds., Butterworth-Heinemann, Oxford, 1992.

Harnby, N., 2000. An engineering view of pharmaceutical powder mixing. Pharmaceutical Science & Technology Today, 3, pp. 303.

Mendez A.S.L., de Carli G., Garcia C.V., 2010. Evaluation of powder mixing operation during batch production: Application to operational qualification procedure in the pharmaceutical industry. Powder Technology, 198, pp. 310-313.

Muzzio, F.J., Goodridge, C.L., Alexander, A., Arratia, P., Yang, H., Sudah, O., Mergen, G., 2003. Sampling and characterization of pharmaceutical powders and granular blends. International Journal of Pharmaceutics, 250, pp. 51-64.

Muzzio, F.J., Robinson, P., Wightman, C., Brone, D., 1997. Sampling practices in powder blending. International Journal of Pharmaceutics 155, pp. 153 - 178.

Muzzio, F.J., Roddy, M., Brone, D., Alexander, A., Sudah, O., 1999. An improved powder-sampling tool. Pharmaceutical Technology, April, pp. 92 - 100.

Nedderman, R.M. Statics and kinematics of granular materials. Cambridge University Press, Cambridge, 1992.
Santomaso A., Lazzaro P., Canu P, 2003. Powder flowability and density ratios: the impact of granules packing. Chemical Engineering Science 58, pp. 2857–2874.

Santomaso A., Olivi M., Canu P., 2004. Mechanisms of mixing of granular materials in drum mixers under rolling regime. Chemical. Engineering. Science 59, pp. 3269–3280.

Santomaso A., Olivi M., Canu P., 2005. Mixing kinetics of granular materials in drums operated in rolling and cataracting regime. Powder Technology 152, pp. 41-51.

Schulze, D. Powders and Bulk Solids: Behaviour, Characterization, Storage and Flow, Springer-Verlag, Berlin, 2008, pp. 259-265.

U.S. Food and Drug Administration, 2003. Guidance for Industry, Powder Blends and Finished Dosage Units—Stratified In-Process Dosage. Unit Sampling and Assessment, Draft Guidance, Pharmaceutical CGMPs.

Vargas, W.L., Hajra, S.K., Shi, D., McCarthy, J.J., 2008. Suppressing the Segregation of Granular Mixtures in Rotating Tumblers, AIChE Journal 54, pp. 3124-3132.

Zik O., Levine D., Lipson S.G., Shtrikman S., Stavans J., 1994. Rotationally induced segregation of granular materials. Physical Review Letters,73(5), pp. 644-647.

Chapter 6

Conclusions and future perspectives

This research was mainly concerned with the study of the wet agglomeration of mineral and metallic powders carried out in low shear mixers. Particularly this work is a practical framework of binder granulation which takes place in the process of manufacturing of welding rods.

The purpose of this study was to investigate the effect of primary particle properties and process parameters on the finale granule characteristics in order to minimize segregation mechanisms.

The research activity can be summarized in three main points:

1. Wettability study of mineral and metallic powders by using two different techniques: sessile drop and Washburn's method. This experimental work has allowed us to suggest a general method for characterizing wettability of mineral and metallic powders.
2. An in-depth study of agglomeration of mineral and metallic powders with particular attention to the understanding of nucleation and growth regimes of granules by using dimensionless numbers approach; this study was carried out both experimentally in low shear pilot plant and by means of numerical simulations (DEM, Discrete Element Modelling);
3. Development and characterization of sampling tools to collect cohesive powders in order to assess chemical composition and degree of segregation of granules formed.

Concerning the wettability measurements, it was found that the main weakness in the sessile drop method is to get reproducible data. The drop penetration behaviour is quite complex and highly dependent on the structure of powder bed, particularly for a non-ideal surfaces such as mineral and metallic powders. Drop penetration results are affected by powder compaction and the porosity at the surface. Furthermore it has been very difficult to identify the correct instant when the drop penetration starts and this aspect can also affect the measurements of penetration time and rate.

Concerning Washburn's experiments, the choice of the best wetting liquid remains a critical step. This work showed that for mineral and metallic powders the reference liquids so far most commonly used in the literature (alkanes) were not suitable. The experimental data demonstrated that a surfactant solution containing fluorinated ethers

was the most appropriate total wetting liquid for mineral and metallic powders. By using this surfactant solution, it has been possible to calculate the value of cosθ for all the powders tested.

Therefore we can conclude that Washburn's method perform much better then sessile drop method for the mineral and metallic powders tested in this work. However in general there is not an universal reference liquid for all the possible powders and the determination of the constant *C* remains a major limitation of Washburn approach.

A further study is therefore advisable in order to develop a new method which does not require a calibration step with a total wetting liquid. It would be better to calculate *C* on the base of basic physical properties of powder packed bed such as porosity, tortuosity and particle size.

For what concerns the granulation experiments it was found that for all the powder blends tested there is a critical ratio of the amount of silicate beyond which granule growth occurs and the means size increases abruptly from about 80 μm to 160 μm. Moreover for the binder solution more concentrated (4.3 ÷ 4.5 wt.%) the fines fraction tents toward zero. Batch grinding tests also showed that a critical silicate amount is requires to enhance granule strength. It was found that for all the formulations for values of silicate composition above 0.5 (w/w) granules are stronger are less sensitive to attrition which can occurs in the subsequent handling during the process.

Concerning the process parameters the impeller rotational speed has no significant effect on the binder dispersion when chopper is on. From a granule growth point we have observed that the increase of impeller speed leads to a reduction of the mean particle size. Experimental results showed that the chopper rotational speed played a major role than the impeller speed in the binder dispersion. It was found that increasing the chopper speed a more uniform liquid distribution and consequently a controlled nucleation were achieved.

Granule nucleation and growth were investigated using three different dimensionless numbers: the modified capillary viscous number, *Ca*, to investigate the effect of physicochemical properties of binder, the viscous stokes number, St_{vis}, as growth criterion and finally the stokes deformation number, St_{def}, as granule growth limitation criterion.

The use of the capillary viscous number allowed us to define the boundaries for which granule growth occurs. The binder viscosity has no significant effect on the granulation process for a capillary number lower than 1. For $Ca \geq 1$, the viscous forces control the granule growth.

For what concerns the condition of coalescence between granules, it was found that for $St_{vis} > 7$ viscous dissipation in the bridge is not sufficient to absorb the elastic rebound energy of the collision and agglomeration growth is promoted for $St_{vis} \leq 7$. In this case the initial kinetic energy is dissipated through viscous friction in the liquid layer during the

collision and granule growth occurs. In an attempt to explain why the values of kinetic constant were so low (granule mean sizes were just double compared with raw materials) Stokes deformation number approach was applied. Results showed that with the most concentrated binder solutions (i.e. 85.7 wt.% and 90 wt.% potassium or sodium silicate), regardless the powder blends studied, St_{def} was lower than the critical value of 0.04 then during collisions granules remained intact and granule breakage did not occur. For St_{def} > 0.04 crumb behaviour took place as the formulation/binder system was too weak to form permanent solid bridge.

Fortunately in the industrial process for manufacturing of welding rods, powder agglomeration is carried out with the most concentrated binder solutions, therefore granule breakage is controlled.

DEM simulations of seeded granulation allowed us to compare this kind of agglomeration with mineral and metallic granulation. It was found a clear correlation between simulation results and experimental findings in terms of nuclei structure: mineral and metallic granules showed a structure akin to seeded granules. Moreover regime maps proposed by Rahmanian *et al*. (2010, 2011) for pharmaceutical application in high shear granulator have been successfully applied for metallic powders in a low shear mixer. Therefore experimental results suggest that regime maps can be generalized for other materials and for low shear granulation as well. A further analysis is required in order to firm up and test the boundaries proposed in the regime map for other types of powders.

Finally a new sampling probe which we called the Sliding Cover Sampler (SCS) was developed and characterized in terms of efficiency and drag. Results showed that this thief was suitable for colleting cohesive powders. SCS can sample powder more accurately and efficiently and it allowed to minimize the invasiveness on the granular bed during the insertion. Therefore by using SCSs it was possible to overcome the main limitations of the sampling devices so far used. Among SCSs the thief that produced the most accurate and reliable results was the semi-cylindrical one because it caused a minor drag and minor degree of consolidation. Moreover ease of use and design make SCS a good sampling technique for industrial applications, particularly to assess the bulk solid composition during the granulation process in order to find evidence of segregation and investigate binder spreading homogeneity and nucleation/growth mechanisms.

List of Publications and Presentations

International Journal

Published:

- Susana L., Canu P. and Santomaso A.C., Development and characterization of a new thief sampling device for cohesive powders, International Journal of Pharmaceutics 416 (2011), 260-267

Submitted:

- Susana L., Campaci F., Santomaso A.C., Wettability of mineral and metallic powder: applicability and limitations of sessile drop method and Washburn's technique, Powder Technology;
- Hassanpour A., Susana L., Pasha M., Rahmanian N., Santomaso A.C., Ghadiri M., Discrete element modelling of seeded granulation in high shear granulator, Powder Technology (accepted).

To be submitted:

- Susana L., Campaci F., Santomaso A.C., Experimental study of wet granulation of mineral and metallic powder in low shear mixer, Powder Technology;

International Conferences

Susana L., Canu P. and Santomaso A.C., Development and characterization of new sampling devices for cohesive powders. Podium presentation.
In Proceedings of Word Congress on Particle Technology (WCPT6), Nuremberg (Germany), April 26-29, 2010.

Susana L., Cavinato M., Franceschinis E., Realdon N., Canu P. and Santomaso A.C., On the characterization of powder wettability by drop penetration observations.
In Proceedings of Word Congress on Particle Technology (WCPT6),
Nuremberg (Germany), April 26-29, 2010.

Susana L., Canu P. and Santomaso A.C., The Sliding Cover Sampler. Poster presentation
In Proceedings of IFPRI AGM 2010, Ph.D. Particle Technology Research Day,
University of Liegi (Belgium), June 30, 2010.

Hassanpour A., Susana L., Pasha M., Santomaso A.C. and Ghadiri M., Discrete element modeling of granulation in high shear granulators. Podium presentation.
In Proceedings of 5th International Granulation Workshop, Lausanne (Switzerland), June 20-22, 2011. University of Liegi (Belgium), June 30, 2010.